PATTERN ANALYSIS OF A VERTICAL SPINNING DISK NOZZLE

By

REZA ALIMARDANI

Bachelor of Science in

Agricultural Engineering

Oklahoma State University

Stillwater, Oklahoma

1983

Submitted to the Faculty of the
Graduate College of the
Oklahoma State University
in partial fulfillment of
the requirements for
the Degree of
MASTER OF SCIENCE
May, 1985

PATTERN ANALYSIS OF A VERTICAL

SPINNING DISK NOZZLE

Thesis Approved:

John B Solie

Thesis adviser

James D Summers

David G Batchelder

Norman N Durham

Dean of the Graduate College

ACKNOWLEDGMENTS

I wish to express my sincere gratitude to my major adviser Dr. John B. Solie for his intelligent guidance, concern, and invaluable assistance during the course of the entire project. Appreciation is also expressed to the other committee members; Professor David G. Batchelder and Dr. James D. Summers for their assistance and suggestions in preparation of this thesis.

I am grateful to the Agricultural Engineering Department for supplying research assistance and financial support for the research and myself through a research assistanship.

I wish to express my attitude and grace to my parents, my wife, our daughter, Fatemeh, and our son, Hajji Mahdi for their understanding, encouragement, and many sacrifices during the period of this study.

TABLE OF CONTENTS

LIST OF TABLES

LIST OF FIGURES

Figure Page

Figure Page

Figure Page

Figure Page

Figure Page

CHAPTER I

INTRODUCTION

Background

In recent years, pesticide application has been an important activity in agriculture. For 1985, a total predicted amount of 500-540 million pounds of farm pesticide is reported (USDA, 1984). Because of the economic considerations, use of low-cost, accurate pesticide applicators have attracted the public interest. An increase in pesticide application rate of material will increase the cost of application when a large area of land is sprayed.

Uniformity of spray pattern and amount of material reaching the intended target are the two most important factors to be considered whenever pesticide application equipment is selected. Efficient, effective, and precise pesticide application equipment is needed to overcome the non-uniformity of pesticide applications.

The application of agricultural chemicals has presented many problems including pesticide drift, spray pattern shift from wind, and non-uniform pattern. The drift of agricultural chemicals during application is one of the major problems confronting aerial and ground applications. This problem has been an important topic and will likely remain

so, partly because of the increased application of chemicals to control weeds, insects, and other diseases in field crops and also the public demand for reduction in spray drift.

A continuing effort is being made by researchers to reduce or eliminate drift from agricultural sprayers. Previous studies show that spray drift is affected by three factors: meteorological conditions, pesticide formulation, and operational parameters. In presence of these factors, the spray drift has been reduced, but because of the un-controllable meteorological factors, the spray drift has not been eliminated.

Uniformity of spray pattern and amount of material deposited on targets beyond the swath are also affected by wind and sprayer motion. Droplet size distribution affects both the effectiveness of chemicals in contacting and controlling the pest and the drift of portions of the spray away from the intended target.

The horizontal spinning disk nozzles are designed to produce relatively uniform droplets of proper size for application at low volumes. Droplet size is directly related to speed of the disk. However, spray patterns of these nozzles can be shifted large distances by wind. A vertical spinning disk nozzle (the Tecnoma Girojet) has the potential of reducing the drift due to wind or sprayer motion since the vertical disk allows the droplets to spun off with a vertical component of velocity at great speeds which ensures a vertical penetration into the foliage and reduces the time required for droplets to reach the ground.

Operating parameters of the Girojet: nozzle height, nozzle spacing, disk speed, flow rate, and disk angle are not well defined and there is no information available comparing the vertical and horizontal spinning disk nozzles for low volume application.

In this study, theory is developed to predict the performance of the vertical spinning disk nozzle. The vertical spinning disk nozzle is compared with two horizontal spinning disk nozzles and a regular flat fan nozzle. To accomplish this task, the following objectives must be met:

Objectives

1. Determine the optimum operating parameters for the vertical spinning disk nozzle (Girojet).

2. Develop a simulation model to predict the spray pattern of the Girojet, under both wind and no-wind conditions.

3. Evaluate the effects of operating parameters and meteorological conditions on spray pattern characteristics of the vertical and horizontal spinning disk nozzles and to compare the performance of the these nozzles with the regular flat fan nozzle.

CHAPTER II

REVIEW OF LITERATURE

The idea of a spinning disk nozzle for agricultural pesticide application is not new. Differently designed types of spinning disk nozzles have been used by farmers. These nozzles are classified as horizontal and vertical spinning disk nozzles. Limited published information is available for the horizontal spinning disk nozzles, but no information is available for the vertical spinning disk nozzles. Researchers have studied the characteristics of hydraulic spray nozzles both theoretically and experimentally.

Theoretical Investigations

An alternative method of studying spray drift and spray droplet dynamics is through mathematical modeling and computer simulation. This method has been limited to focusing on trajectory of a single droplet (Marchant, 1977), droplet size distributions (Goering and Smith, 1978), and dynamics of an evaporating spray droplets (Smith, 1970; Williamson and Threadgill, 1974; and Goering et al., 1972). Computer simulation can be used to evaluate the effectiveness of application for a large number of targets and application conditions, also interpreting the field results,

designing equipment, and predicting the potential for drift in a given condition.

Upon ejection from the spray vehicle, a droplet may be subjected to a combination of forces which include: (a) gravitational force, (b) aerodynamic force, (c) buoyancy force, and (d) electrical, radiometric, molecular, etc. forces (Williamson and Threadgill, 1974). In their study, only two forces were considered significant: drag (the parallel component of aerodynamic force) and gravitational forces.

A mathematical model was developed to describe the dynamics of a non-evaporating droplet which was ejected from a moving vehicle into the air. Further, a generalized model was developed by considering droplet evaporation. It was assumed that physical properties of the gas in the film are essentially those of air at the film temperature, since the mole fraction of the liquid vapor in the film is sufficiently small.

The governing differential equations for the in-flight motion and mass transfer of an airborne droplet were solved simultaneously for the velocity components and droplet diameter as a function of time, using a Runge-Kutta numerical integration technique. Simpson's Rule was used to calculate the components of displacement from the velocity components. The accuracy and validity of the simulation was verified experimentally by a series of tests in wind tunnel. They concluded that the simulation model accurately

predicted the horizontal and vertical displacement, as well as, the change in droplet diameter.

Barker et al. (1978) developed a set of equations of motion for an evaporating spray droplet approaching a three dimensional object. In their study, all forces except gravitational and drag forces were neglected. The theoretical development in this study was similar to Miles (1972) and Williamson (1972). Evaporation rate and change in droplet diameter were determined by equations developed by Sjenitza (1962) and Williamson (1972). The equations of motion were solved by a Fortran based simulation language. The executive program provided a fourth-order variable step-size Runge-Kutta integration procedure for all state equations.

To verify the simulation, four sets of data from Barker (1977) were chosen for comparison of observed and simulated results. The predicted deposition efficiencies were considerably higher than those observed in the wind tunnel by Barker (1977). They concluded the program did provide a tool to study the deposition on a three dimensional object.

Goering et al. (1972) also developed a mathematical model of spray droplet. They based their model on the analog simulation developed by Smith (1970). In their study, the gravitational, buoyancy, and drag forces were considered significant. Also evaporation of the droplets was included in the model. The governing equations for acceleration and theoretical equations for rate of diameter change were combined to comprise the model. These equations

were programmed on a digital computer. A simulation routine developed by Goering et al. (1969) was used to program the model.

Experimental data published by Roth and Porterfield (1965) were used for partial verification of the model. The differences between the predicted and measured results were examined. The most probable reason for differences appeared to be that of substantial spray-induced air currents that were present during experimental tests. Incorporation of such air currents into the model led to good agreement between predicted and measured results.

Experimental Investigations

The effect of equipment, operational parameters, and environmental conditions on spray drift have been studied by researchers. The most common method used to study the characteristics of spray pattern and drift problems was fluorescent tracer technique. This technique was used by researchers to study the spray pattern uniformity, deposition, and drift of aerial and ground applicators.

Yates and Akesson (1963) used the fluorescent tracer technique to measure spray drift characteristics. The experiment was conducted using 1136 liters of spray mixture containing 1.8 kg of Brilliant Sulfo Flavine (BSF) plus at least two common pesticide chemicals for each test. Four replicate Mylar sheets, 15.2 x 45.7 cm x 5 mills, were placed in 6 downwind locations. In addition, four replicate

alfalfa samples of 2.25 to 4.5 kg each were collected at the above sampling locations immediately after the application. A Turner 110 fluorometer was used to measure the fluorescence of BSF samples. They showed a good correlation between BSF on Mylar sheets and pesticide deposited on alfalfa.

Goering and Butler (1975) measured the amount of material drifting beyond the swath using the fluorescent tracer technique. The experiment was conducted using a dual boom technique with the booms 0.3 m apart and constructed so that each boom was equipped with 8 Spraying Systems 8002 flat fan nozzles spaced 0.51 m apart, which resulted in a 4.1 m swath. Two distinctive fluorescent dyes, Rhodamine B and Brilliant Sulfo Flavine were sprayed over the targets at the same time. Fourteen Mylar sheets of 14 x 35.7 cm were used to collect the deposition samples. A sample station was also included to measure the rate of dye degradation. After the test dyes were removed from sample sheets, a small sample was pipetted from each bottle into a cuvette for analysis in a Turner 111 fluorometer. The concentration of each sample dye was determined by comparison with a standard calibration curve. A drift index was devised so that results of an experiment could be expressed in a single number. The following were the results of their study:

1. The fluorescent tracer dyes used degraded, and thus results had to be corrected for degradation.

2. Drift deposits and downwind distance were fitted with a curve having only slight curvature on log-log paper.

3. Lowering nozzle height and pressure reduced drift deposit.

4. Low temperature and high relative humidity caused decreased drift and spray loss.

5. Increasing air turbulence produced greater spray loss but less downwind drift deposits.

6. Increasing horizontal wind velocity produced greater spray loss but produced either greater or smaller drift deposits, depending upon other meteorological factors.

Carlton and Bouse (1981) developed a system to characterize the spray deposition on 35-mm film by use of light transmitted through the film. The diffuse incandescent light was transmitted through a 2 cm^2 aperture of the prepared film. The light was optically spread over a solar cell and quantified. The basis for characterizing the spray deposit came from the high statistical correlation (98%) between aperture light transmission and percentage of spray coverage of the film. The amount of spray deposited was found to be exponentially correlated to light transmitted through film.

Smith et al. (1982) showed the relative importance of pertinent equipment, operational, and meteorological variables on amount of materials deposited downwind. A fluorescent tracer technique was used and 99 test were conducted in their experiment. In the experiment, 64 polyester film targets of 5.1 x 10.2 cm were used. The

targets were placed end to end for the first 11 targets, 20.4 cm center to center for next 14 targets, 40.6 cm for the next 20 targets, and 81.3 cm for the last 19 targets. A single flat fan nozzle was mounted on a boom. Boom height was varied from 0.8 to 1.6 m. The horizontal wind velocity at 3 levels (0.5, 2.5, and 10 m), vertical wind velocity, and wind direction were measured. Temperature difference at 2.5 and 10 m elevations were also recorded. Relative humidity was calculated by measuring the dry and wet bulb temperatures. After extracting the dye (BSF) from targets, the amount of fluorescent dye for each target was measured and recorded.

The nozzle height and horizontal wind velocity were the two most important drift related variables. They further suggested that barometric pressure was not an important factor, and the wind velocity be measured at only one level to obtain the stability ratio (ten times the temperature differences divided by the horizontal wind velocity squared) to make the experiment less costly and easier to conduct.

Bode et al. (1982) studied the spray characteristics of a horizontal spinning disk nozzle (Micromax) over a range of disk speeds, flow rates, disk heights, and mounting angles. The first part of study was conducted in laboratory by using a spray patternator table to measure the spray distribution pattern as affected by the above factors. Results from laboratory tests showed that the uniformity of spray pattern from Micromax could be improved by proper choice of boom spacing and tilt angle. In the second part of the study,

drift from the Micromax was measured in the field and compared with a 8001 flat fan nozzle, using a dual tracer technique. The field test results were as follow:

1. Micromax spray tends to move off the swath and deposit in the first few meters downwind much more than the flat fan nozzle. This result probably was due to the horizontal trajectory of the drops leaving the Micromax cup.

2. The airborne drift from Micromax was less than flat fan nozzle due to the droplet spectra produced by Micromax.

3. Total recovery from Micromax was considerably greater than flat fan, but this may be due to difference in dye degradation.

CHAPTER III

MATERIALS AND METHODS

A simulation model was developed to investigate the effects of meteorological conditions and operating parameters on spray pattern distribution and uniformity of the Tecnoma Girojet vertical spinning disk nozzle (distributed by Wilbur-Ellis Co. in the United States). Experiments were conducted in the laboratory to measure the effects of selected operating parameters on the spray pattern distribution of Girojet. Results of these tests were used to partially verify the simulated spray pattern of a single Girojet nozzle. Information obtained from laboratory tests was used to establish the operational parameters for field tests.

A number of direct comparisons were made from field tests between the Girojet vertical spinning disk nozzle and the two horizontal spinning disk nozzles, the Micromax and the Spraying System Rotojet, versus the regular 8001 flat fan nozzle. The data obtained from field tests was also used to verify the simulation model.

Computer Model

Mathematical modeling is an alternative method of studying spray drift and spray droplet dynamics of a nozzle.

The spray pattern characteristics of a nozzle such as pattern shift and uniformity of coverage can be evaluated using a computer simulation model capable of generating these spray patterns. However, many variables can not be controlled in a field test, it has been difficult to determine the relative importance of the factors such as; droplet evaporation, sprayer speed, wind, and height and orientations of the nozzle. The advantages of simulation are that, even with simplified models, the relative importance and interactions of various factors affecting droplet motion can be determined in a dynamic condition.

Mathematical Equations

The forces which may act on a droplet and control its trajectory are gravitational, aerodynamic, buoyancy, electrical, radiometric, and molecular, etc. According to Newton's second law of motion, a particle acted on by a force moves such that the time rate of change of its linear momentum is defined as:

$$\frac{d(mV)}{dt} = F \qquad (1)$$

where m is the particle mass, V is the vector velocity, and F is the external forces acting on particle. Smith (1970) developed an analog simulation of in-flight evaporation of spray droplets by analyzing the momentum changes as follow:

$$\frac{m(dV)}{(dt)} = F - \frac{Ve(dm)}{(dt)} \qquad (2)$$

where:

m = Mass, Kg

Ve = Velocity of evaporated mass relative to droplet, m/s

t = Time, s.

The term Ve(dm/dt) is an external force acting on the particle due to change of particle mass. According to Smith, because of the momentum change through the control surface surrounding the droplet, the value of Ve cannot be equal to zero, and can be approximated by the velocity of droplet relative to airstream, Vr. Therefore equation (2) can be written as:

$$\frac{m(dV)}{(dt)} = F + \frac{Vr(dm)}{(dt)} \qquad (3)$$

The aerodynamic force can be separated into drag and lift forces. The literature indicates that lift, electrical, radiometric, and molecular forces are small compared to gravitational and drag forces and can be neglected (Barker et al. 1978). Therefore equation (3) can be rewritten as:

$$\frac{m(dV)}{(dt)} = mg + F_d + \frac{Vr(dm)}{(dt)} \qquad (4)$$

where:

g = Gravitational acceleration, m/s^2

F_d = Drag force, N.

A fixed rectangular coordinate system can be used to describe the acceleration, velocity, and force components.

Thus, the positive x is directed to the right, positive y direction is directed out of the page, and positive z direction is downward (Figure 1). Sprayer motion is in the positive x direction and gravitational force is in the positive z direction.

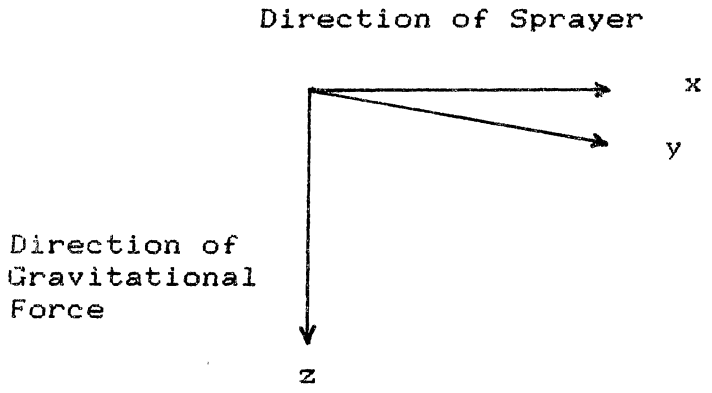

Figure 1. The coordinate system

The relative velocity of particle can be expressed as:

$$Vr = -(Vx-Vwx)i - (Vy-Vwy)j - (Vz-Vwz)k \quad (5)$$

where:

Vx, Vy, and Vz = Components of droplet velocity in the x, y, and z directions, m/s

Vwx, Vwy, and Vwz = Components of wind velocity in x, y, and z directions, m/s.

The first, second, and third terms in the right hand side of

equation (5) are the components of relative velocity; Vrx, Vry, and Vrz in the x, y, and z directions, respectively. Therefore, the magnitude of relative velocity, is calculated as:

$$|Vr| = ((Vrx)^2 + (Vry)^2 + (Vrz)^2)^{0.5} \quad (6)$$

The general form of drag force is described in terms of projected area of the body A in m^2, the relative velocity of the body Vr, the density of air ρ_α in Kg/m^3, and dimensionless drag coefficient C_d as:

$$F_d = 1/2\ (C_d \rho_\alpha A)|Vr|^2 \quad (7)$$

A mathematical expression of standard drag coefficient (C_d) versus Reynolds number (Nre) was determined as a three part expressions by fitting a curve to the drog coefficient and Reynolds number data (Giles, 1962) as follow:

$$C_d = 24/Nre,\ Nre < 0.5 \quad (8a)$$

$$C_d = 0.49 + 26.38(Nre)^{-0.845},\ 0.5 =< Nre < 150 \quad (8b)$$

$$C_d = 7.86\ Nre^{-0.440};\ 150 =< Nre < 1000 \quad (8c)$$

The shape of water droplet falling through the air was studied by Hughes and Gilliland (1952). They concluded that a liquid particle falling in air could be considered to be a sphere. The total surface area of droplet then is:

$$A = \Pi\ D^2 \quad (9)$$

where D is the diameter of droplet in meter. Mass of

particle can be expressed as a function of diameter of particle as follow:

$$m = 1/6(\Pi \rho_\ell D^3) \qquad (10)$$

where ρ_ℓ is the density of water droplet (Kg/m^3). Mass transfer rate then can be written as:

$$\frac{dm}{dt} = \frac{1}{2}(\Pi \rho_\ell D^2 \frac{dD}{dt}) \qquad (11)$$

Goering et al. (1972) derived the following equation for the rate of mass transfer:

$$\frac{dm}{dt} = K_g \; A \; P \; Mv \qquad (12)$$

where:

Mv = Molecular weight of the diffusing vapor, gm

P = Vapor pressure difference, N/m^2

and K_g is the mass transfer coefficient presented in the following form by Marshall (1954):

$$K_g = \left(\frac{Dv \; \rho_\alpha}{Mm \; D \; P_f}\right)(2+0.6Nsc^{1/3}+Nre^{1/2}) \qquad (13)$$

where:

Dv = Diffusivity of water vapor in air, m^2/hr

Mm = Mean molecular weight of gas mixture in transfer path, gm

P_f = Partial pressure of air, N/m^2

Nsc = Dv/v, Schmidt number

v = Kinematic viscosity of air, m^2/hr

Nre = Vr D/v, Reynold's number.

Equations (8), (10), (11), and (12) were combined and simplified by Goering et al. (1972), and the following theoretical equation for the rate of diameter change of an evaporating spray droplet was derived :

$$\frac{dD}{dt} = -2\left(\frac{Mv\ Dv\ P\rho_\alpha}{Mm\ D\ P_f\rho_\ell}\right)(2+0.6Nsc^{1/3}+Nre^{1/2}) \qquad (14)$$

the minus sign indicates a decreasing diameter as evaporation proceeds.

The component equations for drag force were determined by combining equations (5) and (7) as follow:

$$F_{dx} = 1/2\ (C_d\ A\ \rho_\alpha\ )|Vr|\ Vrx \qquad (15a)$$

$$F_{dy} = 1/2\ (C_d\ A\ \rho_\alpha\ )|Vr|\ Vry \qquad (15b)$$

$$F_{dz} = 1/2\ (C_d\ A\ \rho_\alpha\ )|Vr|\ Vrz \qquad (15c)$$

where:

F_{dx} = The drag force in x direction, N

F_{dy} = The drag force in y direction, N

F_{dz} = The drag force in z direction, N.

The equations of motion in the x, y, and z coordinates are calculated by combining equations (4), (5),(6), (14), (15a, b, and c) as follows:

$$m_{ax} = F_{dx} + Vrx\ (dm/dt) \qquad (16a)$$

$$m_{ay} = F_{dy} + Vry\ (dm/dt) \qquad (16b)$$

$$m_{az} = mg + F_{dz} + Vrz\ (dm/dt) \qquad (16c)$$

Solving the above equations for accelerations gives:

$$a_x = -3/4(C_d\ \rho_\alpha / \rho_\ell D)|Vr|Vrx - 3(Vrx/D)dD/dt \qquad (17a)$$

$$a_y = -3/4(C_d\ \rho_\alpha / \rho_\ell D)|Vr|Vry - 3(Vry/D)dD/dt \qquad (17b)$$

$$a_z = g-3/4(C_d\ \rho_\alpha / \rho_\ell D)|Vr|Vrz - 3(Vxz/D)dD/dt \qquad (17c)$$

Integration of equations (16a, b, c) with respect to time yields the component velocities in x, y, and z directions, respectively. The resultant velocity can be calculated as:

$$V=(Vx^2+Vy^2+Vz^2)^{0.5} \qquad (18)$$

and

$$\theta_{xz} = \text{Arctan}\ (Vz/Vx) \qquad (19)$$

$$\theta_{yz} = \text{Arctan}\ (Vz/Vy) \qquad (20)$$

where θ_{xz} and θ_{yz} are the components angle in xz and yz planes, respectively. The displacement equations are obtained by a second integration of the acceleration equations.

Simulation Model

Equations (6), (8a, b, c), (14) through (20) comprise a model which predicts the motion of an evaporating spray droplet. The equations were programmed on an IBM-PC computer for solution. Equations were integrated using a Runge Kutta fourth order algorithm. The input data necessary for the model were entered as follows:

1. Droplet Size[1]- Droplet size distribution of Girojet was plotted versus cumulative number of droplets in percent (Figure 2). The corresponding equation which represents the droplet size as a function of cumulative number is:

$$D = 173 - 3.59\ N + 0.072\ N^2 \qquad (21)$$

where D is the droplet size and N is the cumulative number of droplet in percent. Diameters of spray droplets are randomly generated using the Monte Carlo method.

2. Ejection Angle - The effective spraying angle of Girojet (the lower segment of disk) was measured to be 140 degrees. The point of ejection of droplet is assumed to occur with equal probability at any point within the specified range. The location of point of ejection is determined as:

$$0 = N\ (160 - 20) + 20 \qquad (22)$$

Where 0 is the ejection angle in degrees and N is a random generator number with equal probability between 0 and 1.

3. Initial Velocity - The tangential velocity of droplet leaving the disk assuming no slip, can be calculated from following equation:

$$V = (2\ \ r/60)w \qquad (23)$$

---

[1] The data was supplied by personal communication with Loren E. Bode, Department of Agricultural Engineering, University of Illinois.

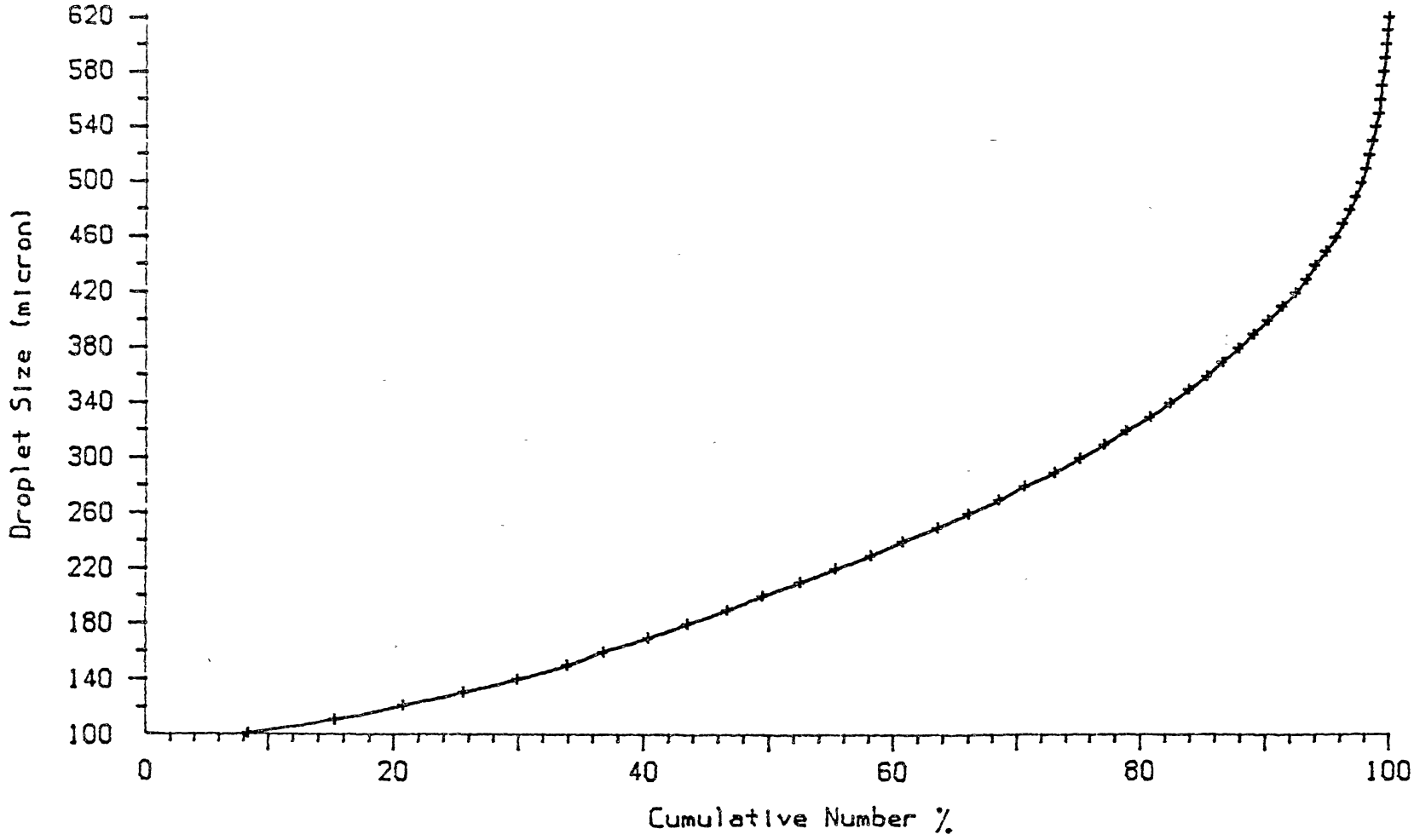

Figure 2. Cumulative Number Distribution of Droplet Versus Droplet Size

where V is the initial velocity of droplet in m/s, r is the radius of disk in meter, and w is disk speed in rpm.

4. Air Velocity - The air velocity in the y direction was determined by the one seventh power-law wind profile model developed by Sabersky and Acosta (1964) as follow:

$$V_{wy} = W_h((h_o - z)/H)^{1/7} \quad (24)$$

where:

V_{wy} = The horizontal wind speed measured in the y direction, m/s.

W_h = Horizontal wind speed measured at the nozzle height (H), m/s.

h_o = Distance above the surface when droplet leaves the disk, cm

z = Vertical component of droplet distance, cm.

H = Nozzle height, cm.

Prediction of Spray Pattern

To generate a complete spray pattern for the Girojet spinning disk nozzle, the following steps are taken. From step 1 to 4, the trajectory of a droplet from the time it leaves the disk to the time it reaches the ground is calculated. Step 5 accumulates the volume of each droplet leaving the disk. In step 6, the initial value of the next generated droplet is calculated.

1) Time step, air velocity, disk speed, nozzle height, application volume, and sprayer speed are entered as input data.

2) The components of resultant velocity and relative velocity are calculated and a time step is selected within the framework of two conflicting requirements. It must be small enough to preserve accuracy and yet not too small so as to give an unacceptably large solution time. Therefore, a varying step size of 0.005 to 0.01 seconds was selected.

3) The integrations are carried out using an Runge Kutta fourth order algorithm which integrates in a step by step fashion.

4) Step 2 and 3 are repeated until the droplet falls a distance equal to nozzle height and then impact location of droplet is calculated.

5) The final evaporated droplet volume is calculated and then, the application rate (ul/cm^2) is accumulated at 2.5 cm intervals of spray pattern width. The volumes of droplets generated before evaporation are accumulated and checked with the given application rate.

6) From step 3, the new components of velocity, Vx, Vy, and Vz are obtained and new ejection angle and relative velocity are calculated.

7) Steps 2 to 5 are repeated until the given application volume is obtained. At this point, the pattern width and the percent of application rate at 2.5 cm intervals are written on a floppy disk for plotting.

The BASIC program was compiled and run on an IBM-PC computer for calculation of droplet trajectories. The time required to generate a profile of spray pattern under no

wind condition was about 5.1 hours, and for the case with the wind speed accounted was 9.2 hours. The list of variables and computer program are listed in Appendix A.

Laboratory Study

Experiments were conducted in the laboratory to measure the spray pattern distribution of the Girojet spinning disk nozzle as a function of flow rate, nozzle height, and disk speed and further to establish operational parameters for precise application of pesticide. The pattern analysis system for ground application equipment developed by Solie and Gerling (1984) was used to measure the spray pattern distribution and further to analyze the spray pattern data.

The experiments were conducted in two parts: first to determine the effect of a single parameter on the uniformity and distribution of the spray pattern and second; and the effect of a combination of parameters was studied to obtain the optimum operating parameters.

Equipment and Procedures

The equipment used to conduct the experiments was essentially the same as used by Solie and Gerling (1984). The pattern analysis system, adapted to ground application equipment, consisted of a Sequoia-Turner 111 fluorometer with modified manual stip scanner (Figure 3). Paper tape, on which fluorescent dye is sprayed, is placed in the feed reel located to the right of the fluorometer. The tape is pulled through the fluorometer by a paper tape drive consisting of

Figure 3. Pattern Analysis System

a rubber faced feed roll and an aluminum pressure roll. The feed roll is driven by a stepper motor. The 200 steps per revolution motor advances the tape 0.0426 cm per step. The take-up reel, located to the left of the fluorometer, is driven by a small DC motor.

The Sequoia-Turner 111 fluorometer, used in these experiments, utilizes an optical bridge to measure light emitted as the material fluoresces. Time to balance this bridge can take as long as 15 s. Fluorescence is measured on a dial graduated from 0 to 100. Fluorescence can be scaled with neutral density filters and by the range selector. The manual stip scanner contains a 2.54 by 1.59 cm aperture with 2.54 cm dimension oriented along the width of the tape. This dimension is the effective tape width. Fluorescence is a measure of the light fluoresced by a section of the paper tape whose dimensions are approximately those of the aperture.

Attached to the top of the fluorometer is an aluminum box containing the transformer, A/D converter, addressable asynchronous transmitter receiver chip, and signal conditioning equipment. The fluorometer is interfaced to a Commodore 64 computer through the serial port. The computer drives the stepper motor, records fluorometer readings, and analyzes data.

A BASIC computer program was written to control the stepper motor, acquire digital output from the fluorometer, calculate percent fluorescence, and record location and

fluorescence on a floppy disk.

The two sampling methods available analyzing the spray pattern data are the continuous and balance methods. In the continuous method, the tape is advanced a predetermined distance, and the fluorescence and location are calculated. Then the data is recorded without waiting for the fluorometer to balance, and the tape is immediately advanced for the next reading. In the balance method, the tape is advanced a predetermined distance and the tape is halted until the fluorometer is balanced. The data is recorded on the disk and the paper is advanced to the next location.

The spray carriage consists of a pressure vessel containing the fluorescent dye, nozzle body, and a solenoid shut off valve mounted on a carriage suspended on rollers from an overhead track (Figure 4). A constant torque motor is used to propel the carriage at velocities ranging from less than 0.7 m/s to 2.5 m/s.

A steel bracket was built for mounting the Girojet on the carriage. The bracket permitted the nozzle to rotate in three directions. The paper tape track, tape feed reel and take-up reel were constructed to collect the spray pattern data. The track consists of a 3.5 cm wide channel constructed of 20 gauge aluminum, 1.5 m in length with the edges folded over 0.3 cm to retain paper tape. Two tracks were connected together by a 0.6 x 3.2 cm piece of aluminum flat stock.

The tape feed reel and take-up reel were attached to the ends of the track. This assembly was located below the

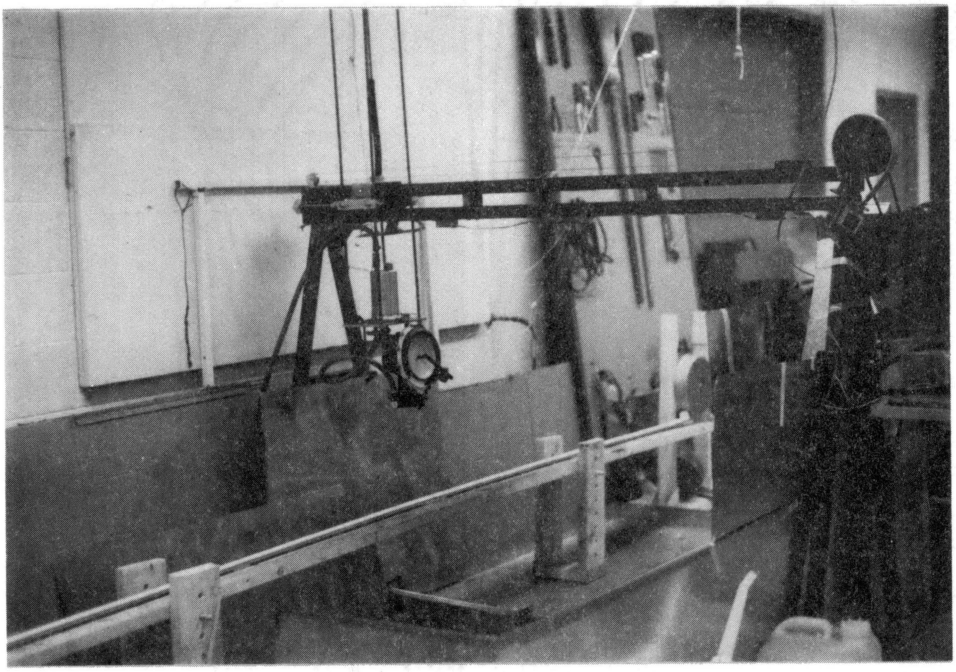

Figure 4. Girojet Nozzle Mounted on the Spray Carriage with Track Assembly

carriage on a 5 by 15 cm board, 5 m long (Figure 4). The board was supported at each end by adjustable stands to select desired nozzle height. An air compressor was connected to the inlet line of 20 liters steel tank by an extension hose, and the outlet line of the tank was connected to the pressure vessel on the carriage. A pressure regulator with a pressure gauge was placed in the inlet line to control the flow rate.

The flow rate was determined volumetrically. Flow rate was controlled by adjusting the pressure in the system, since the flow rate was regulated by a simple orifice only. The fluorescent dye, Rhodamine-B, was applied at a rate of 0.27 g/L through the nozzle in this and subsequent experiments.

The disk speed was adjusted by turning the speed range knob located on the back of Girojet to desired position (Figure 5). The disk speed was calibrated by measuring the speed at different positions of knob by a stroboscope (Type 1531-AB Strobotac). In order to measure the disk rotation, a black spot was marked on the disk and then illuminated by the flashing stroboscope light. The flashing rate of stroboscope was increased or decreased until the stroboscope frequency matched the disk speed (synchronization). The disk speed was determined from the known flashing rate of stroboscope.

A series of tests were conducted to find the best method of obtaining spray pattern data. The tests were

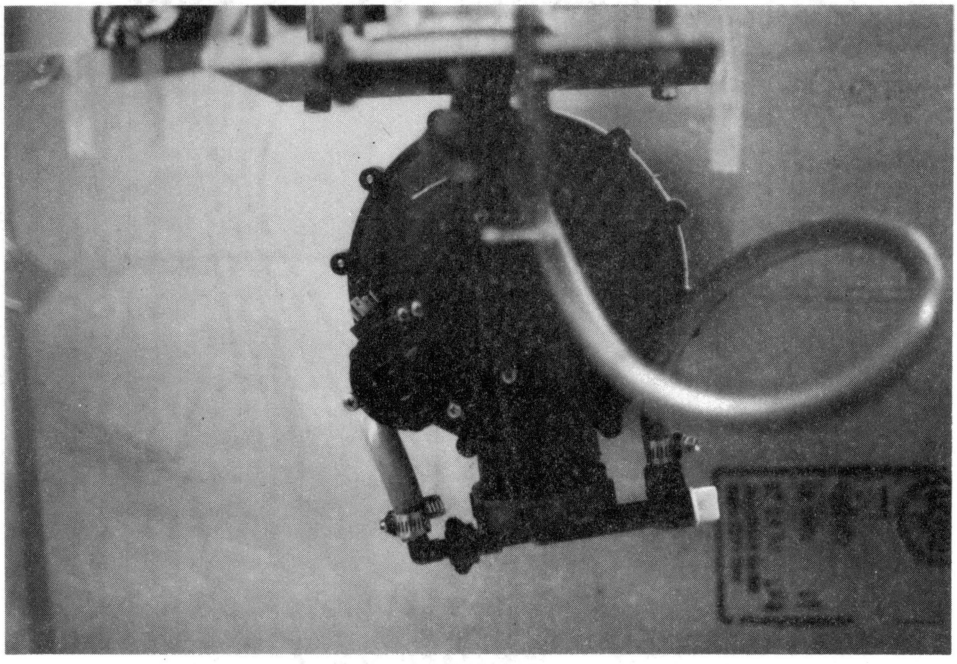

Figure 5. Rear View of Girojet Shown with Speed Range knob Selector

conducted so that there would be as much accuracy as possible in determining the variation in spray pattern distribution as affected by various factors.

Visual inspection of spray patterns led to the following conclusion when the Girojet was operated at 207 kPa, 46 cm height, 2200 rpm of disk speed, 1.34 m/s forward speed, offset 7 degrees vertically (Figure 6a), and rotation angle of 0 degrees (Figure 6b): first, the maximum deposition of spray pattern was observed to be below the center of nozzle and second, the spray pattern was skewed to the left.

To obtain an even distribution of spray pattern, the unit was examined at 0 degrees and with the unit rotated counterclockwise to 3, 6, 9, and 12 degrees in a plane perpendicular to carriage motion (Figure 6b). The average spray pattern profiles (5 replication at each position) were obtained using the spray pattern analysis system.

The results of the above tests showed that an even distribution of spray pattern can be obtained when the unit is rotated counterclockwise 9 degrees in a plane perpendicular to carriage motion. A significant change in total amount of material deposited on paper tape was observed between the replications. This variation was due to the change of liquid level in the nozzle sump (Fig 6b). So after every pass, the injector that controls the flow rate was removed to let the excess liquid to drain out from the nozzle sump.

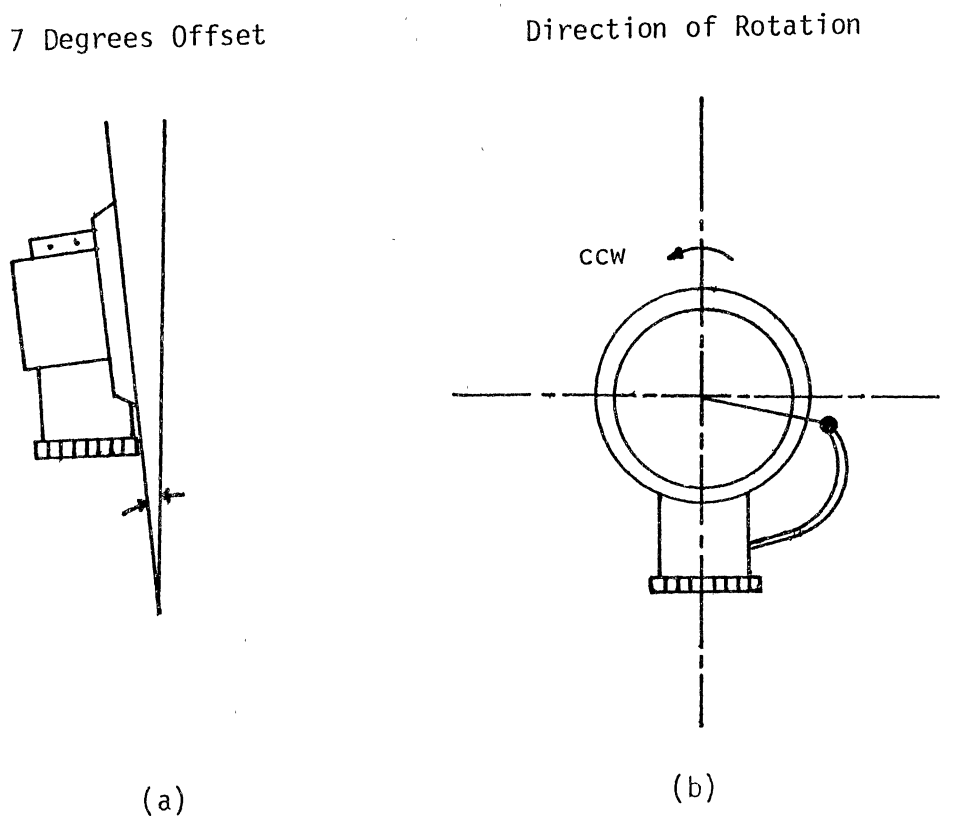

Figure 6. Girojet Mounted at 7 Degrees Offset Angle (a) and Counterclockwise Rotation (b)

The Effect of Nozzle Height, Disk Speed, and Flow Rate

The effect of nozzle height, disk speed, and flow rate on the spray pattern with the Girojet offset 7 degrees and rotated 9 degrees counterclockwise were studied individually as follow:

A. Nozzle Height. The nozzle height tested for the unit ranges from 40 to 72 cm. Therefore the effect of height on the spray pattern distributions was studied at an operating parameters of: 207 kPa, 2200 rpm, and 41, 46, 51, 56, 61, 66, and 71 cm heights.

B. Disk Speed. The disk speed of Girojet ranges from 1000 to 4200 rpm when it is loaded. Therefore, the effect of this factor was studied by applying the dye through the nozzle at: 207 kPa, 46 cm height, and disk speeds of 1400, 1600, 2200, 2700, 3250, and 4000 rpm.

C. Flow Rate. Flow rate was another factor considered to be important. This parameter was studied by conducting the tests at: disk speed of 2200 rpm, 46 cm nozzle height above the paper tape, and flow rates of 0.30, 0.35, 0.40, 0.45, 0.50, 0.55 , 0.60, and 0.65 L/min.

The Effect of Combination of Parameters

Tests were conducted in this part based on the results of studies in the previous part. The Girojet was tested with a combination of factors: a flow rate of 0.50 L/min (276 KPa), two levels of nozzle heights (46 cm and 61 cm), and two level of disk speeds (2200 rpm and 2500 rpm).

The tests were conducted in both parts at a nominal speed of 1.34 m/s and were replicated 5 times. A total of 100 tests were conducted in the first part and 20 tests were run in the second part. The total fluorescence (a measure of total amount of fluorescent dye deposited on paper tapes) were measured and analyzed using the pattern analysis system with the continuous sampling method. The distance and percent of fluorescence of dye applied on the paper tapes were recorded on the floppy disk for plotting.

A BASIC program was written to average the data obtained for 5 replications. The average spray pattern data were plotted using an available plotting program. The pattern width and percent of maximum fluorescence were measured for quantitative comparisons of spray patterns.

Field Study

The field experiments were conducted to study the effect of operational parameters and meteorological conditions on the relative spray pattern shift and uniformity of a veritcal spinning disk nozzle, two horizontal spinning disk nozzles, and regular flat fan nozzle. Tests were divided in two parts. In the first part, the tests were conducted so that the horizontal wind velocity had no effect on the spray pattern distribu- tions. The tests were conducted when the wind velocity was low and wind direction was parallel to the sprayer direction of travel (Figure 7a). In the second part, tests were conducted when the horizontal wind velocity had a significant effect on the

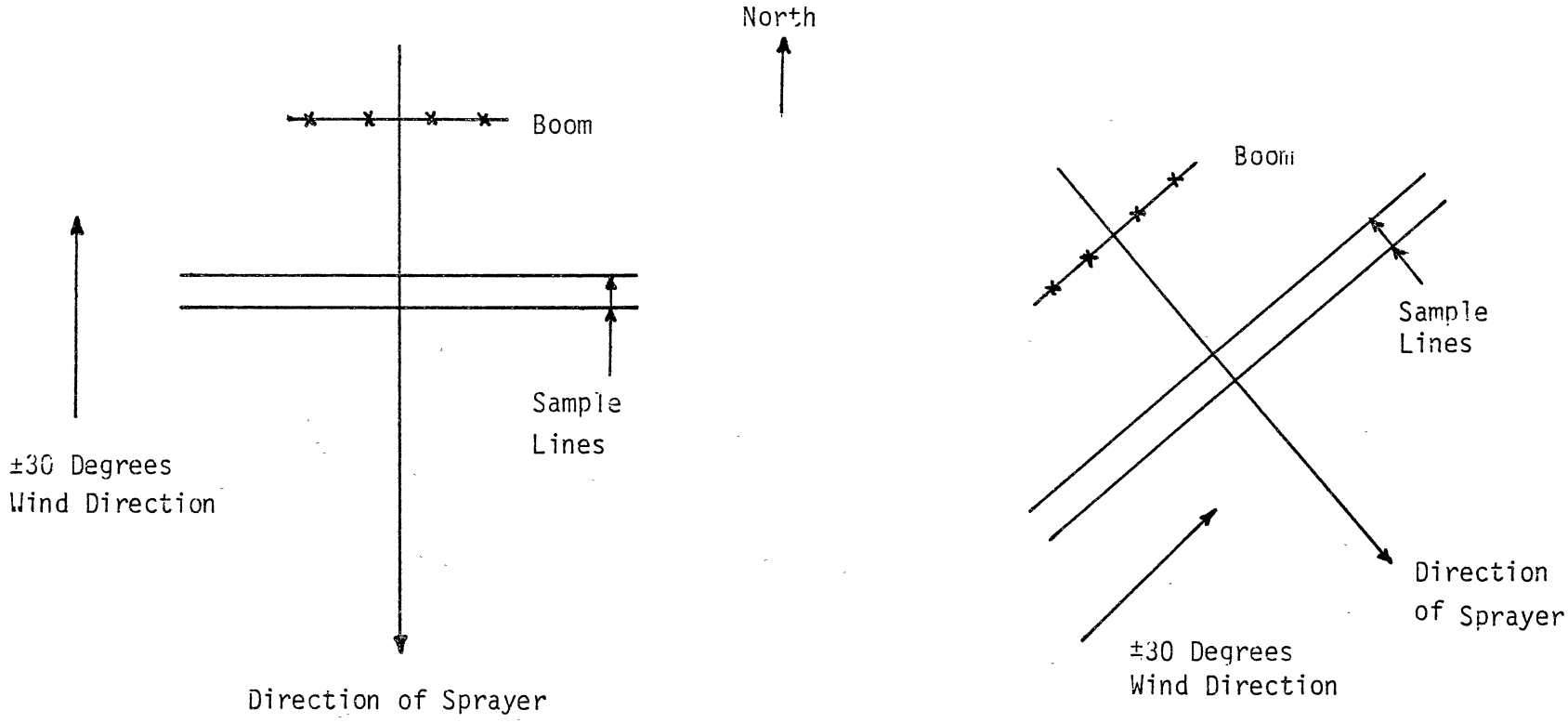

Figure 7. Test Site Configuration

spray pattern. The direction of travel of the sprayer was oriented approximately 90 degree to the wind direction (Figure 7b).

Equipment and Procedures

The equipment used in this part of study consisted of a MF-245 tractor, sprayer system, a ramp board, meteorological instrumentation, and track assembly. The nozzles tested were 4-regular flat fan 8001 TeeJet nozzles (Spraying Systems Co.), 4-Rotojet units (Model AA-900, Spraying Systems Co.), 4 Micromax units (Micron Corp.), and 4 Girojet units. The tests were all run at the Agronomy Farm, Stillwater, OK where a test site of 100 x 100 m was selected.

A ramp board (2 m wide x 2.5 m long x 2 cm thick) was constructed with two gaps, 60 cm apart from center of the board. Two tracks were inserted into these gaps. The ramp board allowed the sprayer to drive over the tracks without damaging the tracks. Ramp height was low enough so that spray could be collected on paper tape inserted in the track without the spray pattern being affected by the ramp board. Tracks used were the same as those used in laboratory study.

For the first part of experiment, where the effect of wind was not significant, 2 sets of tracks, 8 m in length were used. In the second part, the total track lengths were 15 m to collect all the material deposited in the downwind location.

The sprayer system consisted of a pump, spray tanks, 2 solenoid valves, and a variable height boom. A round steel boom was designed to permit mounting 4 regular 8001 flat fan nozzles, the boom was bolted to the sprayer frame. Three booms were constructed for spinning disk nozzles from 3 x 3 cm square steel tubing. Booms were extenede 0.8 m behind the sprayer to prevent the sprayer from interfering with the spray patterns of horizontal spinning disk nozzles. The spinning disk nozzles were mounted on these booms, four units of the same spinning disk nozzles on each boom. The booms were attached to the sprayer frame by two U-shaped brackets with one end of each bracket welded to the boom and the other end pinned to the sprayer frame (Figure 8).

The meteorological equipment consisted of a 2.5 m mast, 2 temperature sensors, one TRS-100 Radio Shack Computer for data collection, 3 anemometers (Figure 9), and a sling psychrometer. The Radio Shack computer was interfaced to the instruments through a custom made board. The mast was constructed to permit mounting the temperature sensors and wind anemometers at two locations.

The horizontal wind velocity was measured at the 0.5 and 2.5 m elevations. The wind velocity and direction at the boom height was measured with a combination cup anemometer and wind vane (Model N 200-SD, WeatherMeasure Corp.) mounted on a vertical axis. At the 2.5 m elevation, a cup anemometer (Model 6102, R. M. Young Co.) was used to measure the horizontal wind velocity, the vertical wind velocity was measured by a Gill propeller anemometer (Model

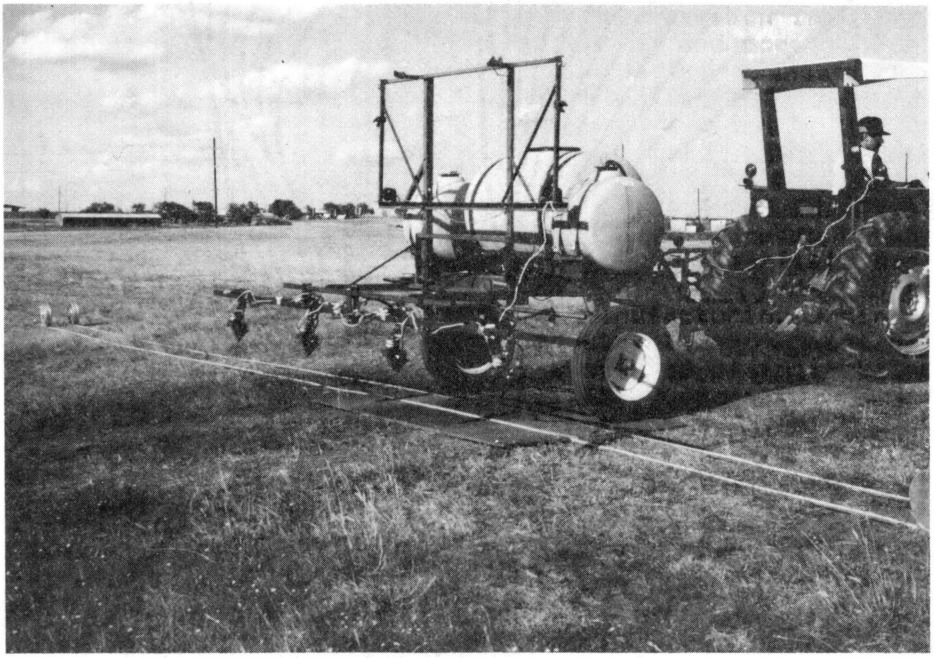

Figure 8. The Paper Tapes Sprayed with the Micromax Mounted on the Sprayer Boom

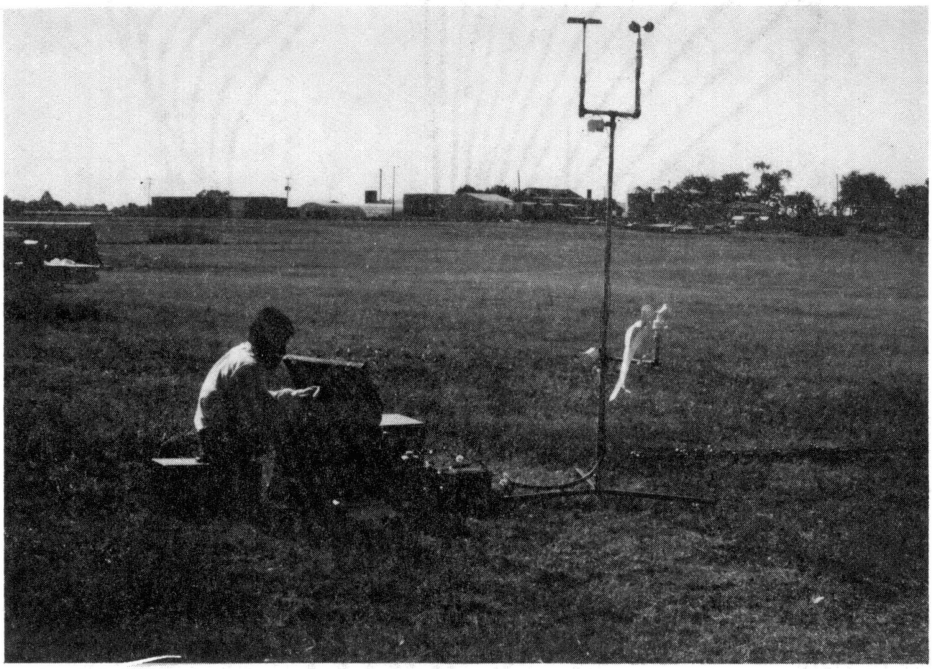

Figure 9. Meteorological Instrumentation

27106, R. M. Young Co.). Instantaneous measurement of wind speed, wind direction, and temperatures were recorded by the TRS-100 computer as the sprayer crossed the tape. The relative humidity was calculated from the wet and dry bulb temperatures measured by a sling psychrometer every two hours.

The application rate of all nozzles was selected to be 42 L/ha for ease of comparison. Since the application rate, spacing, and sprayer speed were known, the flow rate of each nozzle was determined by selection of pressure or orifice size using the following equation:

$$MLPS = (LPH \times MPS \times W)/1000 \qquad (25)$$

where:

MLPS = Flow rate, ml/s

MPS = Sprayer speed, m/s

LPH = Application rate, L/ha

W = Nozzle spacing, cm

1000 = Conversion factor.

The center of sprayer was marked as a referance on the paper tapes. The center of boom on sprayer was aligned with the center of ramp board as a pass was made.

The operating parameters of the nozzles tested are shown in Table I. The operating parameters of 8001 flat fan nozzle were selected as recommended in the Catalog No. 37 (Spraying System Co.), the Micromax operating parameters

were selected from the study conducted by Bode et al. (1982), and the operating parameters for Rotojet were selected from the Spraying System Co. reference manual.

After each pass, the sprayed portion of the tape was identified by nozzle type, pressure, height, and sample pattern. In each pass, two sample patterns were obtained. At the time the tapes were sprayed, the meteorological data were recorded and identified. After identifying the tape and allowing the tape to dry about 3 minutes, the sprayed tapes were wound up on the take up reel. The disk speed and flow rate were checked before conducting each experiment. A completely randomized design was selected as the statistical method to conduct the experiments.

No Cross Wind Experiment

The wind direction was determined to be from the south. Therefore, the sample lines were oriented perpendicular to the wind direction, with the sprayer traveling into the wind. Three passes were made for each set of operating parameters according to Table I. A total of 36 passes were made. Data were not analyzed unless the wind direction was within 20 degrees from sprayer motion line. Two sample patterns were averaged for each pass (replication) and therefore an average was obtained from 3 replications made for each treatment.

Cross Wind Experiment

The sample line location selected in this part was

TABLE I

OPERATING PARAMETERS FOR ALL NOZZLES TESTED

Nozzle	Pressure (KPa)[1]	Nozzle Spacing (cm)	Nozzle Height (cm)	Disk Speed (rpm)	Disk Angle (Deg)[2]
Flat Fan	145	51	46	--	--
	289	76	61	--	--
Girojet	276	104	46	2200	--
	276	104	61	2200	--
Micromax	220	114	46	2000	15
	220	114	46	2000	30
	220	114	61	2000	15
	220	114	61	2000	30
Rotojet	220	102	46	2500	15
	220	102	46	2500	30
	220	102	61	2500	15
	220	102	61	2500	30

1) An application rate of 42 L/ha was selected for all nozzles.
2) Micromax and Rotojet were rotated clockwise in a plane perpendicular to the direction of sprayer.

aligned with the wind direction which was determined to be from the south east. Therefore the direction of sprayer was oriented approximately perpendicular to the wind direction when a pass was made. The data were analyzed only for the wind direction within 30 degree of sample lines. The tests were conducted with the operating parameters shown in Table I. In this part of the experiment, at least 3 passes were made for each nozzle operating condition with the wind magnitude ranging from 0.5 m/s to 1.8 m/s.

The spray pattern data were analyzed the same way as the laboratory data using the O.S.U pattern analysis system. The total fuorescence deposited on the paper tapes were quantified using the continuous sampling method. The average coefficient of variations and centroid of spray pattern profiles of two sample patterns for each replication were calculated as the measure of pattern uniformity and pattern shift for each nozzle.

Centroid Shift

A total of 25 direct comparisons of centroid shift of spray distribution patterns were made of spinning disk nozzles versus a regular flat fan nozzle. The comparisons were made based on a unique set of weather conditions. The pairs selected for comparison had approximately the same wind magnitude and same direction relative to sample lines.

The centroid shift of the spray patterns were calculated for each operating parameters of nozzles by

subtracting the centroid of the spray pattern with no cross wind from the that with cross wind. Comparisons were made at two nozzle heights and two nozzle angles for the horizontal spinning disk and at two level of nozzle heights for the vertical spinning disk and regular flat fan nozzle.

Verification of Model

A series of spray patterns of the Girojet were simulated by the model under the same operating parameters as the experimental data. The simulated spray patterns of a single nozzle were verified using the data obtained from laboratory study, and the simulated spray patterns for the 4 nozzles mounted on the sprayer boom were verified by the field tests data.

The effect of operating parameters were verified by determining the pattern width and the beginning and ending of depositon locations of spray patterns for a single nozzle. The effects of operating parameters and meteorological conditions on spray patterns were verified for the field tests by calculating the centroid of spray patterns for the boom spray nozzles in addition to the pattern width and the beginning and ending of deposition locations.

As a measure of how the variation in the measured spray pattern is explained by the simulated spray pattern of the model, the coefficient of determination, R-square, was calculated for the average of 5 single nozzle spray patterns operated at 46 cm nozzle height, 207 kPa, 2200 rpm, and at 0 and 9 degrees counterclockwise rotation angle.

For the boom spray nozzles, the R-square was calculated for the average of 2 sample spray patterns and 3 replications with no cross wind and for the average of two sample spray patterns with cross wind. The average spray patterns were selected at the operating parameters of 42 L/ha, 2200 rpm, 104 cm nozzle spacing, and 46 cm nozzle heights with no cross wind and 1.48 m/s of cross wind and at 61 cm nozzle height with 1.32 m/s of cross wind to obtain the coorelation between the measured precent fluorescence and the corresponding amount of material applied per square cm on the paper tapes or the swath width.

CHAPTER IV

RESULTS AND DISCUSSION

The effects of operating parameters and meteorological conditions on the spray distribution patterns and uniformity of the Girojet vertical spinning disk nozzle were studied in three parts.

In the first part, the effect of operational parameters of the Girojet was studied in laboratory. From the results of study, the operational parameters of Girojet were established. In the second part, a simulation model was developed for the Girojet. In the third part, based on the results of laboratory study, tests were conducted to study the effects of both operational and meteorological parameters on the boom spray pattern uniformity and relative pattern shift. The comparisons were made of the spinning disk nozzles versus a regular flat fan nozzle.

The simulation model was verified in two parts. In the first part, the simulated spray patterns generated by the model were verified for a single Girojet nozzle using the laboratory data. In the second part, a series of spray patterns were generated under both no cross wind and cross wind conditions. These spray patterns were verified using the data obtained from field tests.

Laboratory test Results

Figures 10 and 11 show the profiles of two spray patterns obtained for the Girojet at 0 degree and 9 degree angles. The profile of spray pattern, when the unit was rotated 9 degrees counterclockwise, is more symmetrical than the profile obtained at the 0 degrees position. The width of the pattern at 0 degrees was measured 213 cm in length, 97 cm to the right and 116 cm to the left of the nozzle. The width of spray pattern at 9 degrees rotation was measured to be 221 cm in length, 110 cm to the right of nozzle center and 111 cm to the left side.

Results of these tests show that orienting the unit 9 degrees counterclockwise (Figure 6b) results in the most symmetrical, evenly distributed spray pattern of any other angles examined (Figures 40 to 44 in Appendix B). Therefore the unit mounted on the spray carriage rotated 9 degrees counterclockwise was used throughout the balance of the experiments.

Nozzle Height

Figures 12 and 13 show the profiles of the spray patterns obtained when the Girojet was operated at 46 cm and 61 cm nozzle heights, respectively. These profiles are the average of 5 replications made at each nozzle height. The nozzle height ranged from 46 cm to 71 cm. The patterns obtained at 51, 56, 66, and 71 cm nozzle heights are shown from Figures 45 to 48 in Appendix B.

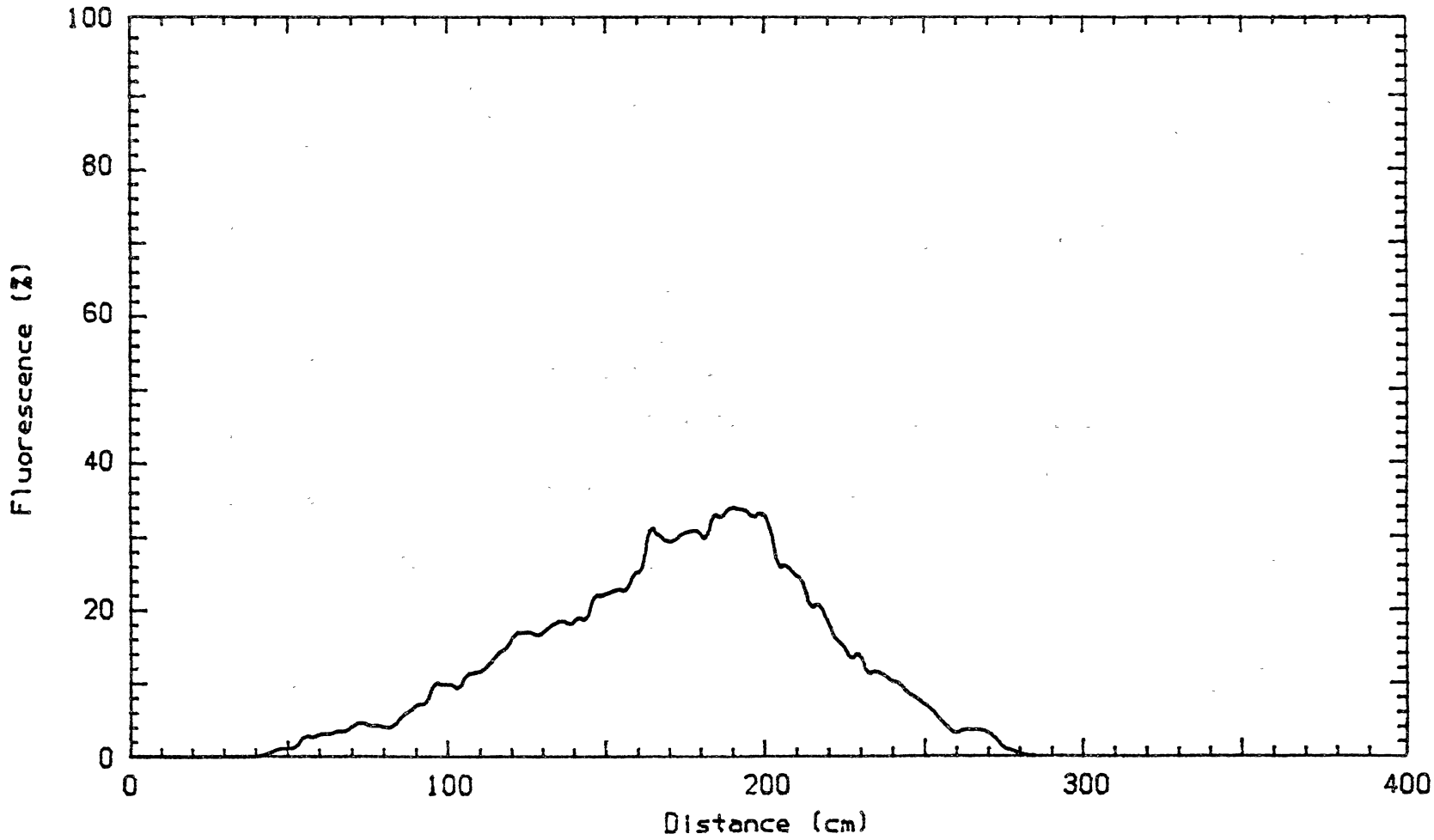

Figure 10. Average Pattern Distribution of Girojet Nozzle Operated at 46 cm Height, 0.45 L/min, 1.34 m/s, and 2200 rpm at 0 Degrees Angle Rotation with center located at 190.5 cm

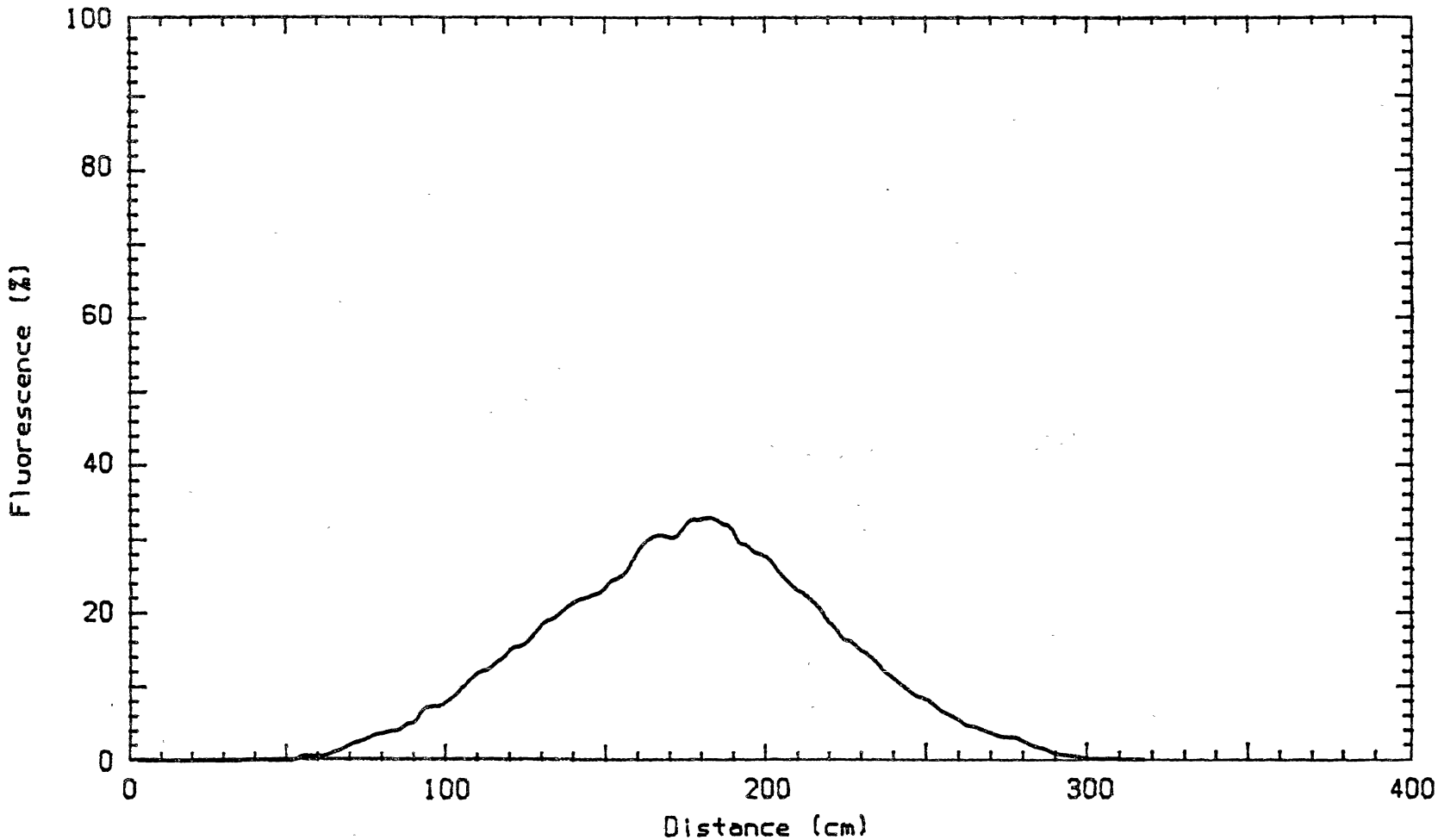

Figure 11. Average Pattern Distribution of Girojet Nozzle Operated at 46 cm Height, 0.45 L/min, 1.34 m/s, and 2200 rpm at 9 Degrees Angle Rotation with center located at 160 cm

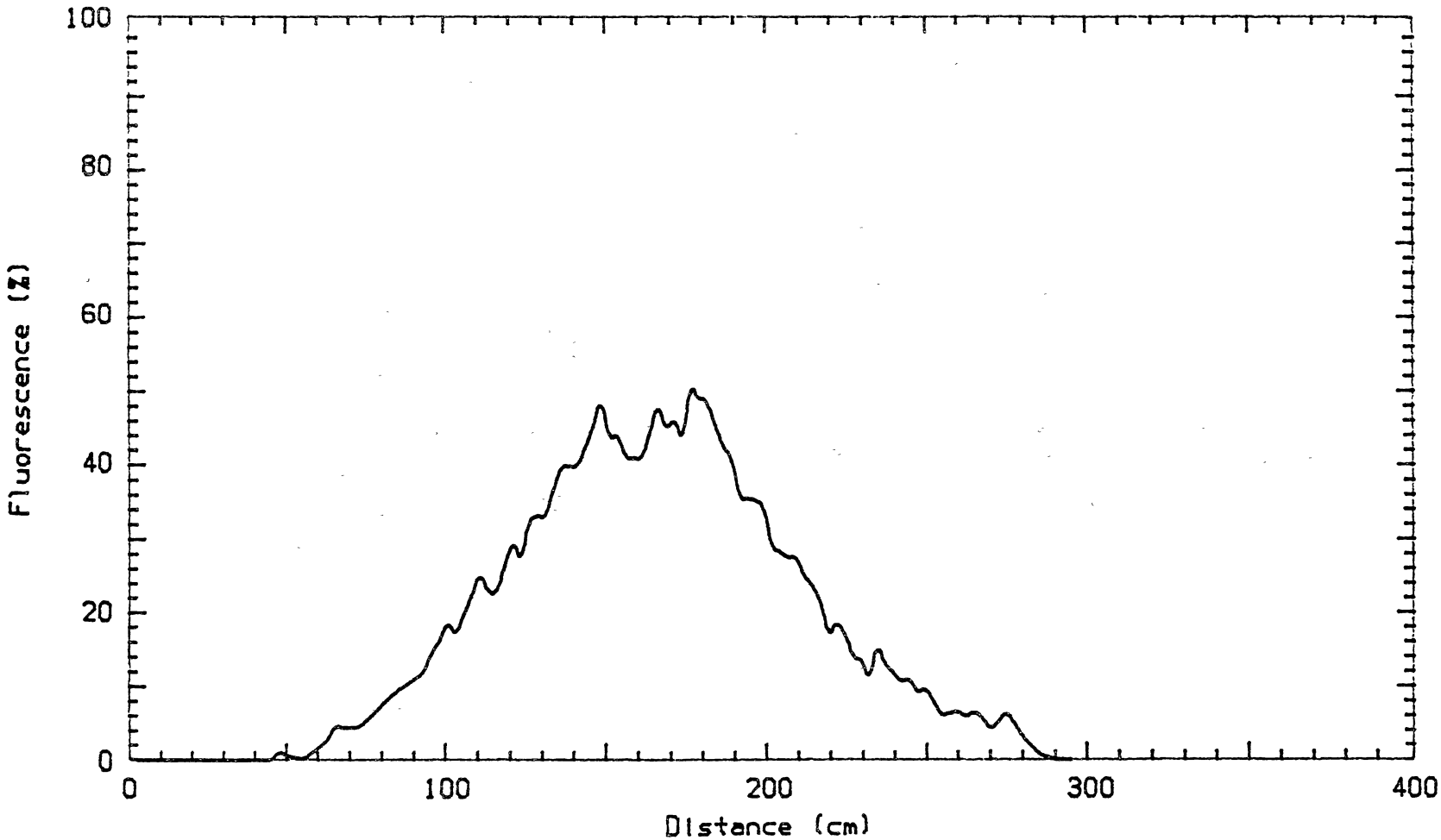

Figure 12. Average Pattern Distribution of Girojet Nozzle Operated at 46 cm Height, 0.45 L/min, 1.34 m/s, and 2200 rpm at 9 Degrees Angle Rotation with center located at 160 cm

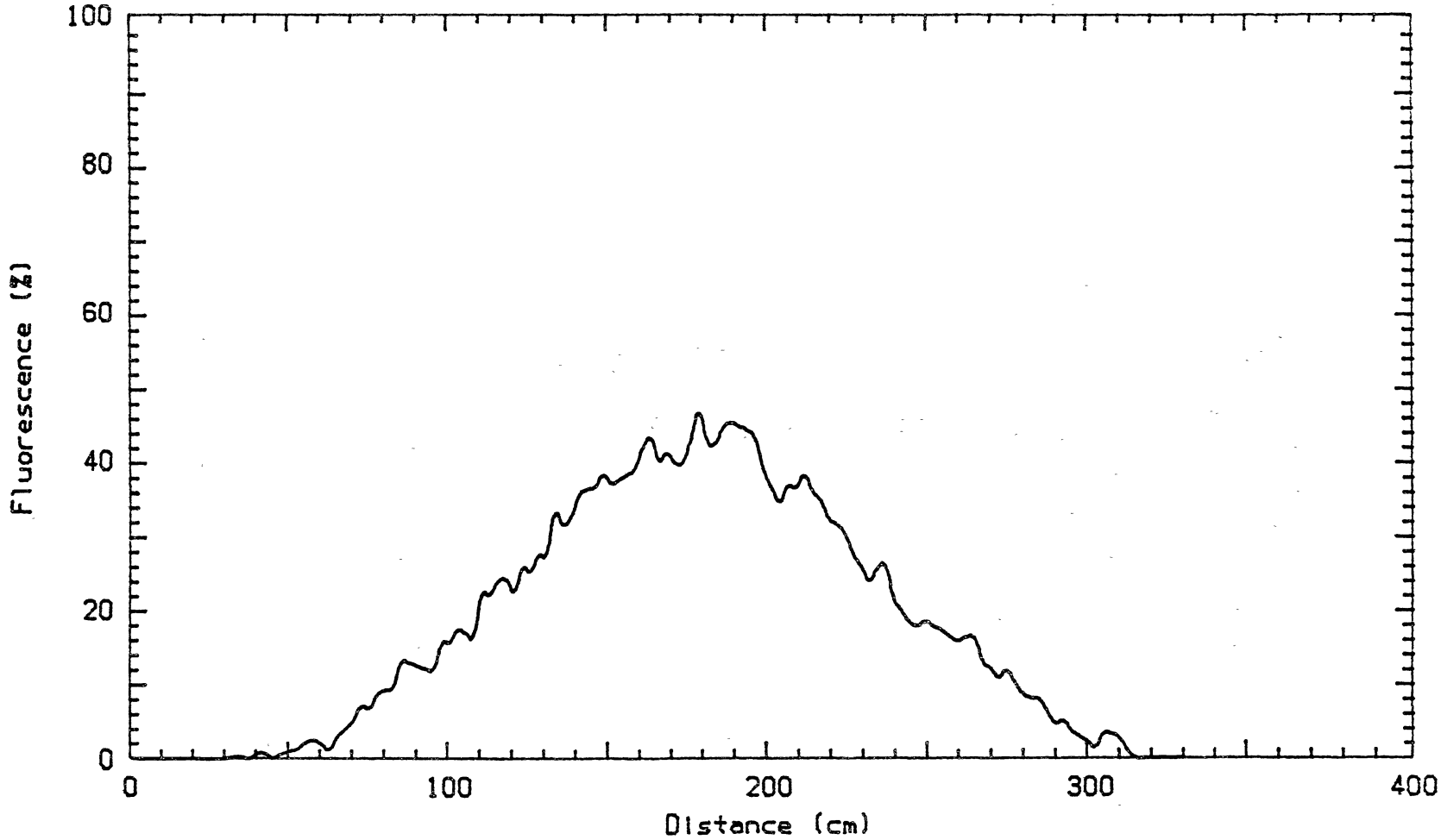

Figure 13. Average Pattern Distribution of Girojet Nozzle Operated at 61 cm Height, 0.45 L/min, 1.34 m/s, and 2200 rpm at 9 Degrees Angle Rotation with center located at 160 cm

The spray pattern width at 46 cm height in Figure 12 was measured to be 220 cm in length, and the maximum fluorescence level (a measure of the amount of fluorescent dye deposited on the paper tape) of 48 percent was observed at this height. A pattern width of 260 cm and the fluorescence level of 42 percent were measured at 61 cm height (Figure 13). Examinations of other profiles show that the spray pattern width tended to increase and the pattern peak (maximum fluorescence level) tended to decrease as the nozzle height was increased.

Disk Speed

Figures 14, 15, and 16 show the profiles of spray patterns at the disk speeds of 2200, 2700, 4000 rpm. The spray pattern profiles at 1400, 1600, and 3250 are shown in Figures 49 to 51 of Appendix B. The pattern width and the maximum fluorescence level were measured to be 230 cm and 30 percent at 2200 rpm, 210 cm and 35 percent at 2700 rpm, and 170 cm and 38 percent at 4000 rpm disk speeds.

An increase in disk speed caused a decrease in pattern width. The maximum fluorescence level at the center of the nozzle tended to increase as the disk speed increased up to 3000 rpm, but increasing the disk speed above 3000 rpm caused the pattern peak to flatten resulting in a pattern where the amount of fluorescence per unit width remained nearly constant about 30 cm from left side of the nozzle center to 30 cm to the right side of the nozzle center.

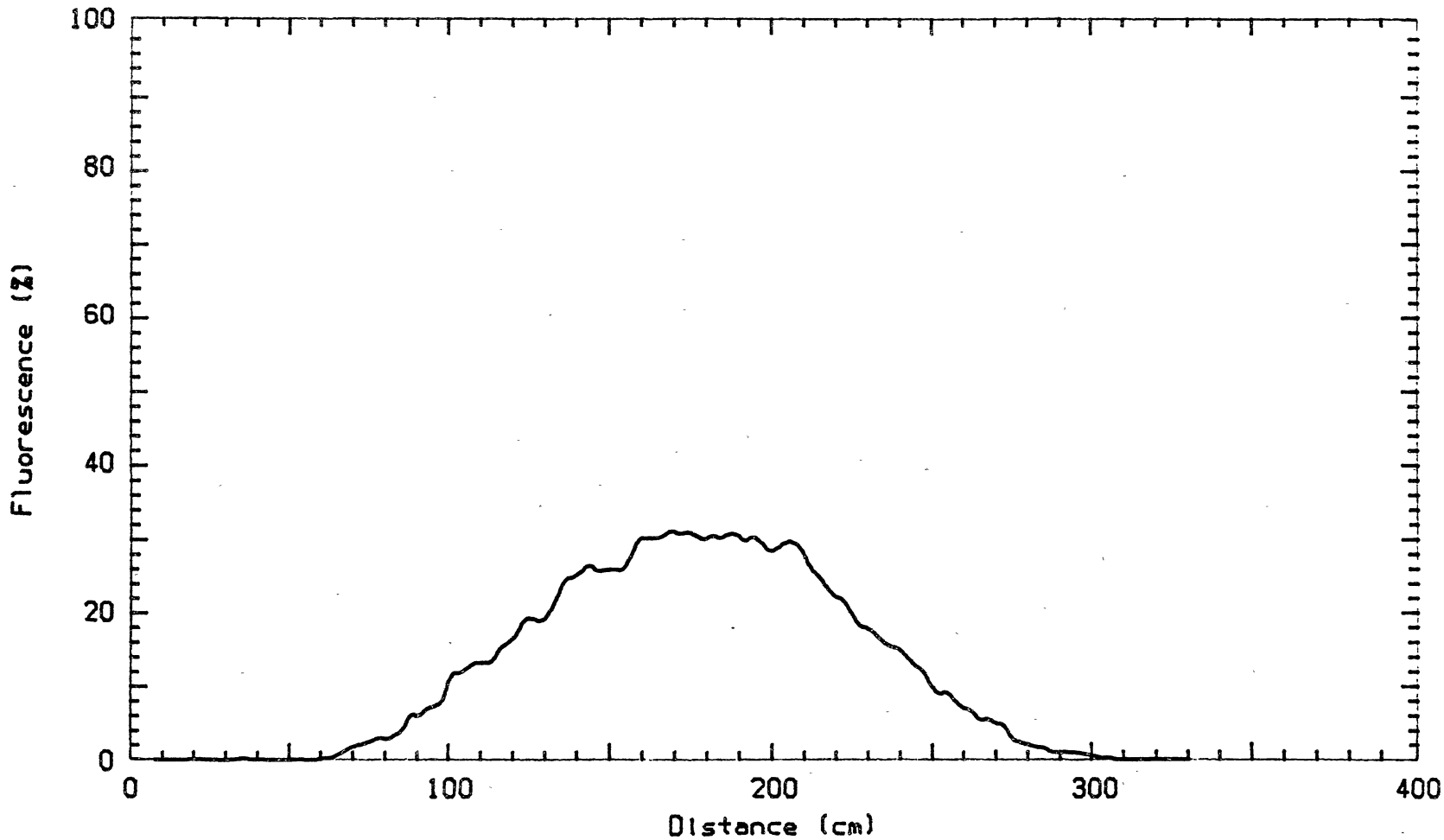

Figure 14. Average Pattern Distribution of Girojet Nozzle Operated at 46 cm Height, 0.45 L/min, 1.34 m/s, and 2200 rpm at 9 Degrees Angle Rotation with center located at 160 cm

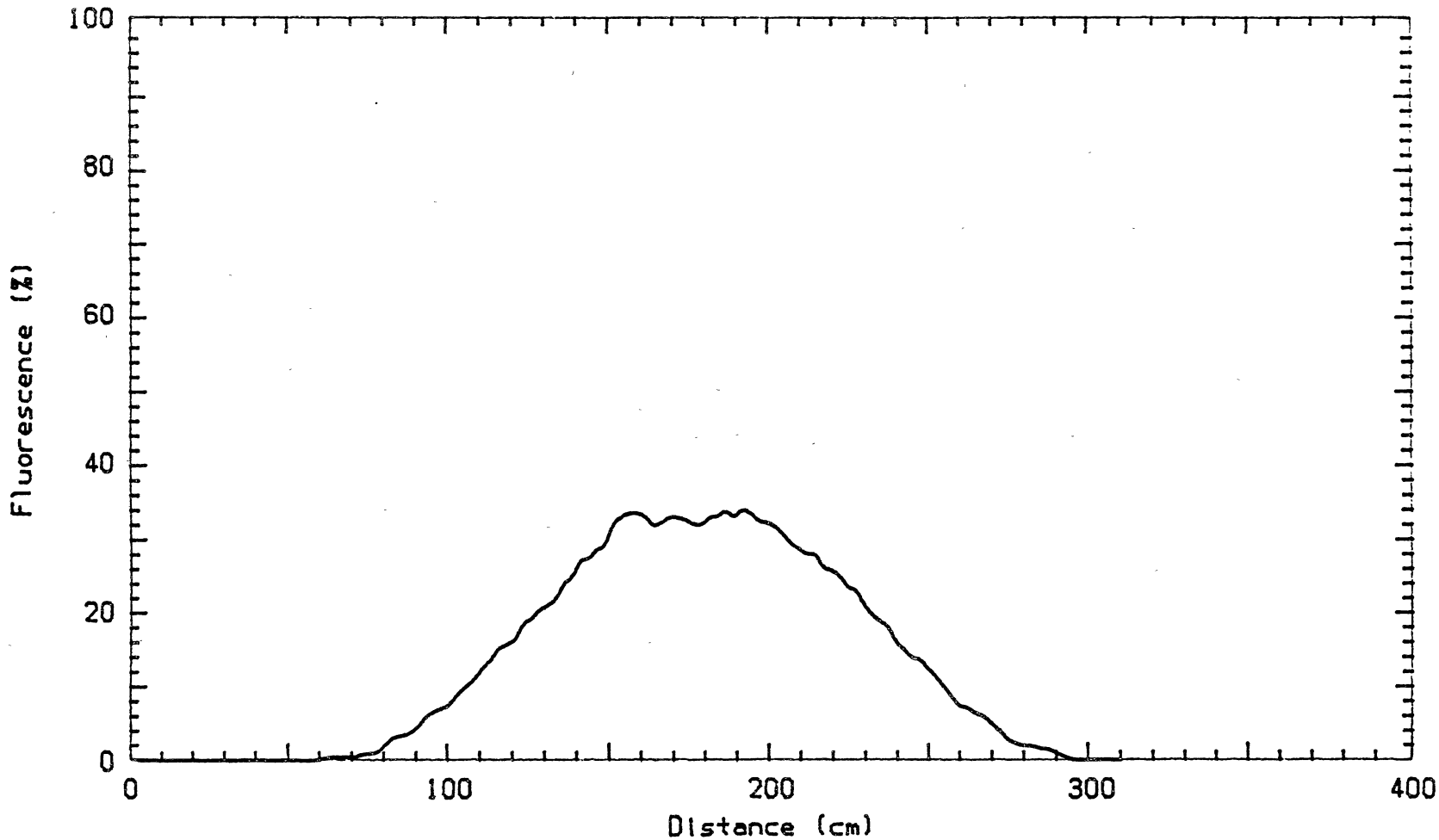

Figure 15. Average Pattern Distribution of Girojet Nozzle Operated at 46 cm Height, 0.45 L/min, 1.34 m/s, and 2700 rpm at 9 Degrees Angle Rotation with center located at 160 cm

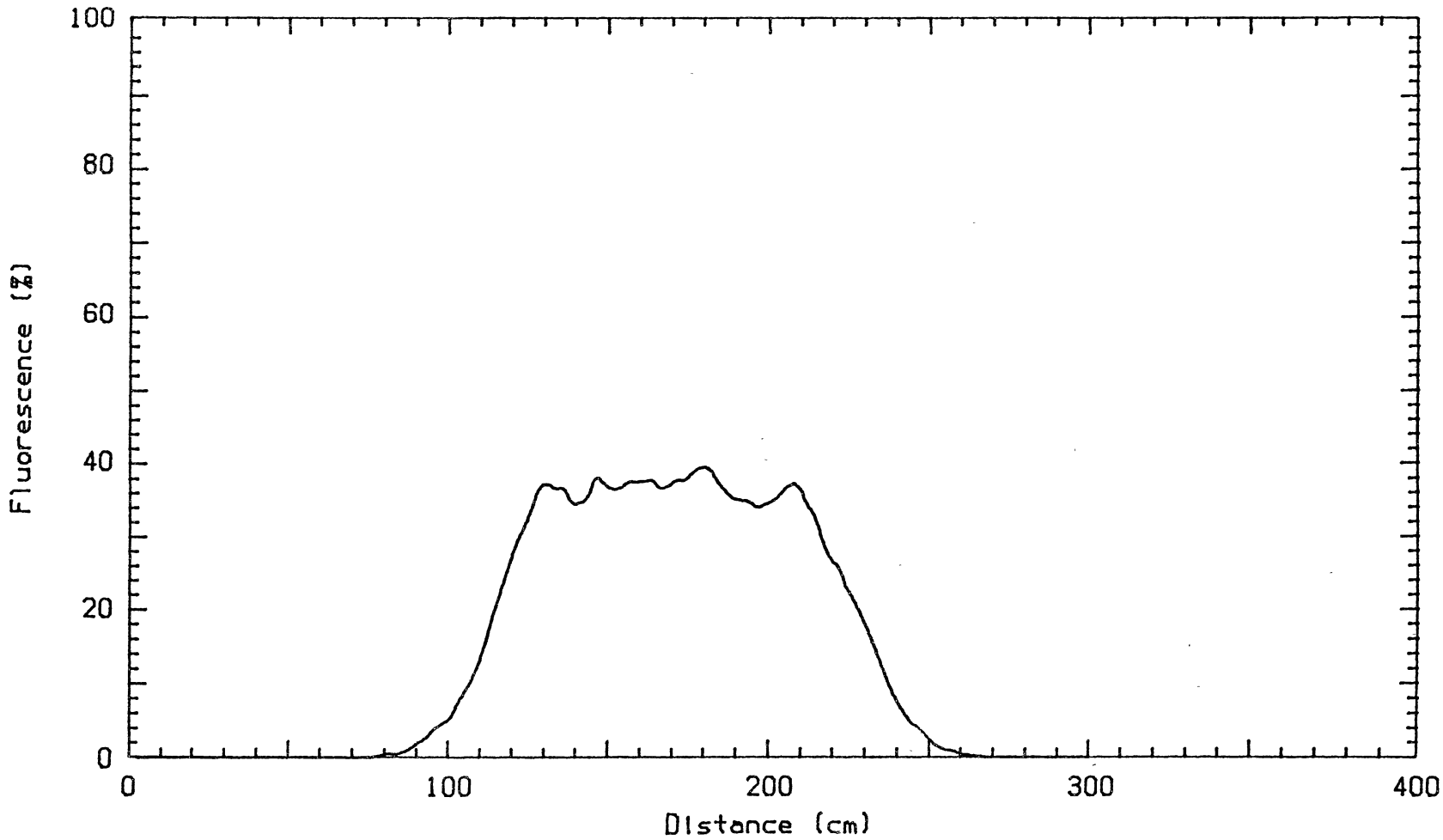

Figure 16. Average Pattern Distribution of Girojet Nozzle Operated at 61 cm Height, 0.45 L/min, 1.34 m/s, and 4000 rpm at 9 Degrees Angle Rotation with center located at 160 cm

Flow Rate

The effect of flow rate was studied in a range of 0.3 L/min to 0.65 L/min. Figure 17, and Figures 52 through 58 in Appendix B show the profiles of the spray pattern for this range. The pattern width and the maximum fluorescence level at the center of nozzle were measured to be 180 cm and 30 percent at 0.30 L/min, 230 cm and 43 percent at 0.50 L/min, 240 cm and 52 percent at 0.60 L/min, and 240 cm and 50 percent at 0.65 L/min flow rate.

It was observed that the flow rate also had a significant effect on the spray pattern width when it was increased from 0.30 L/min to 0.55 L/min, but the pattern width remained nearly the same as the flow rate was increased above 0.55 L/min. The maximum fluorescence level at the center of nozzle tended to increase as the flow rate was increased from 0.3 L/min to 0.55 L/min. The pattern peak tended to flatten as the flow rate was increased above 0.55 L/min.

Combination Effect of Height, Disk Speed, and Flow Rate

Figures 18 through 21 show the spray patterns from the combination tests. The amount of F applied per unit width in Figures 18 and 19 were measured at two locations, 50 cm to either side of the nozzle center. The fluorescence level deposited was 28 percent for the left side and 20 percent for the right side from Figure 18, and the fluorescent level were measured to be 32 percent for the left and 20 percent

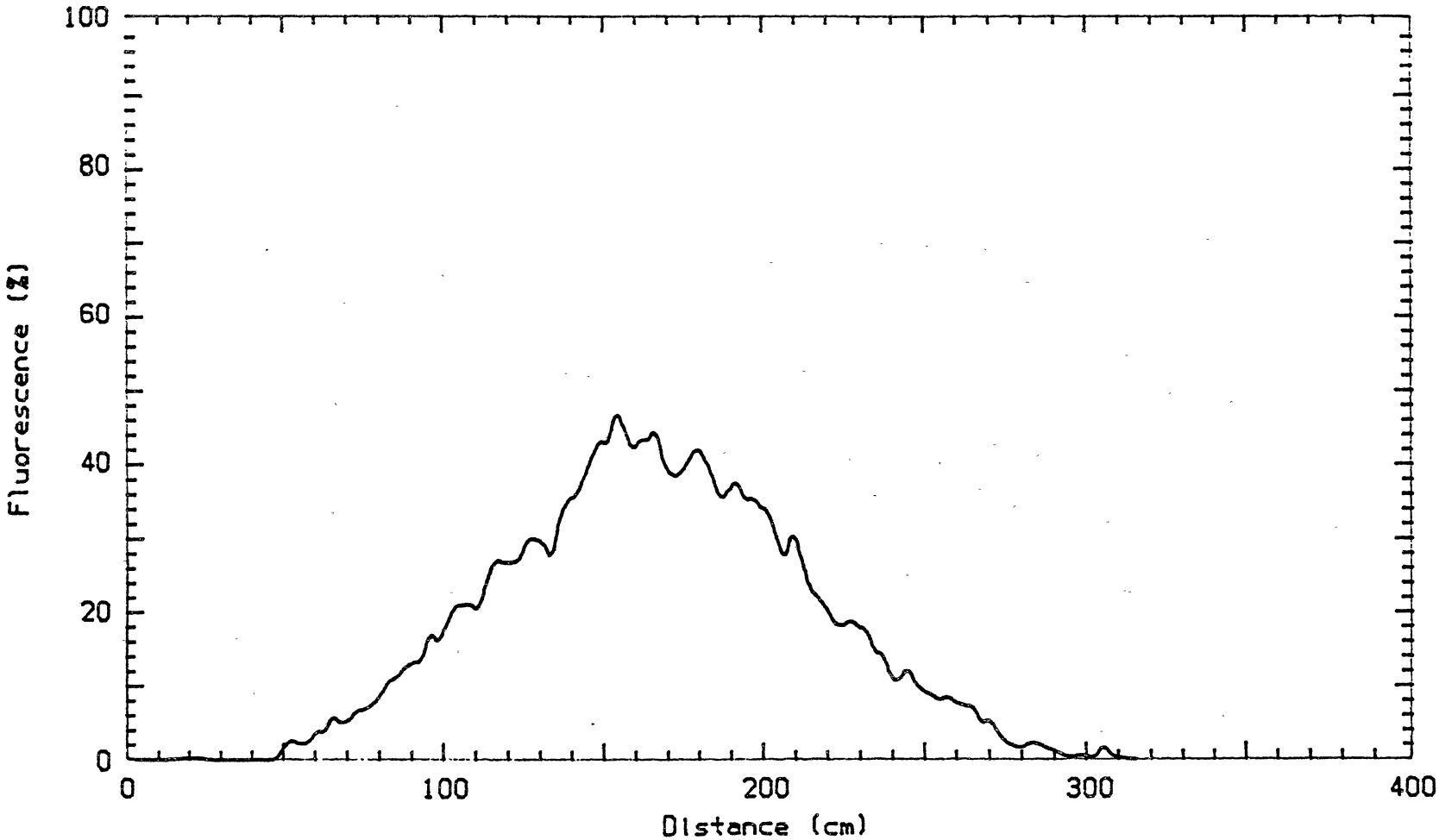

Figure 17. Average Pattern Distribution of Girojet Nozzle Operated at 46 cm Height, 0.50 L/min, 1.34 m/s, and 2200 rpm at 9 Degrees Angle Rotation with center located at 160 cm

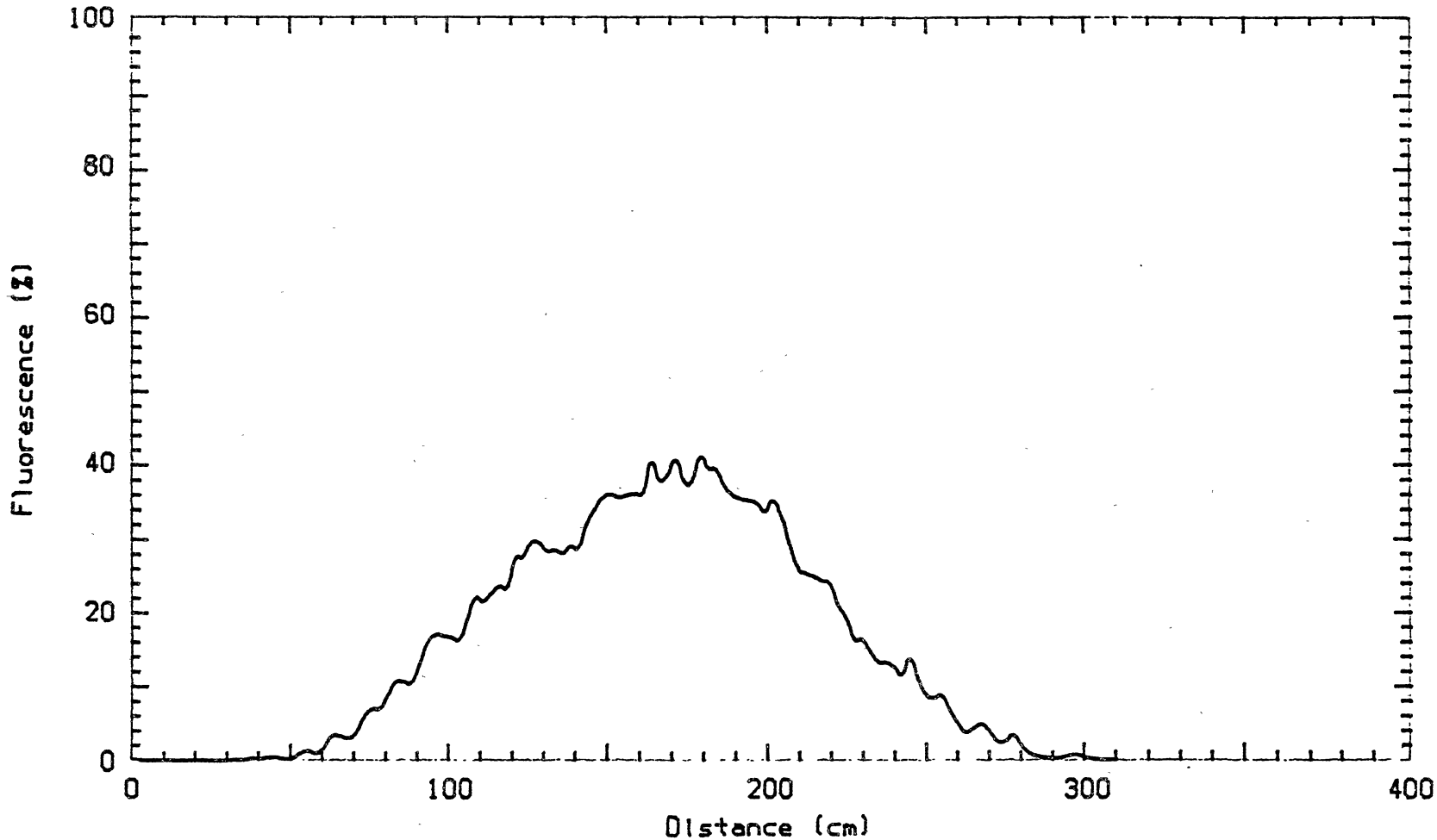

Figure 18. Average Pattern Distribution of Girojet Nozzle Operated at 46 cm Height, 0.50 L/min, 1.34 m/s, and 2500 rpm at 9 Degrees Angle Rotation with center located at 160 cm

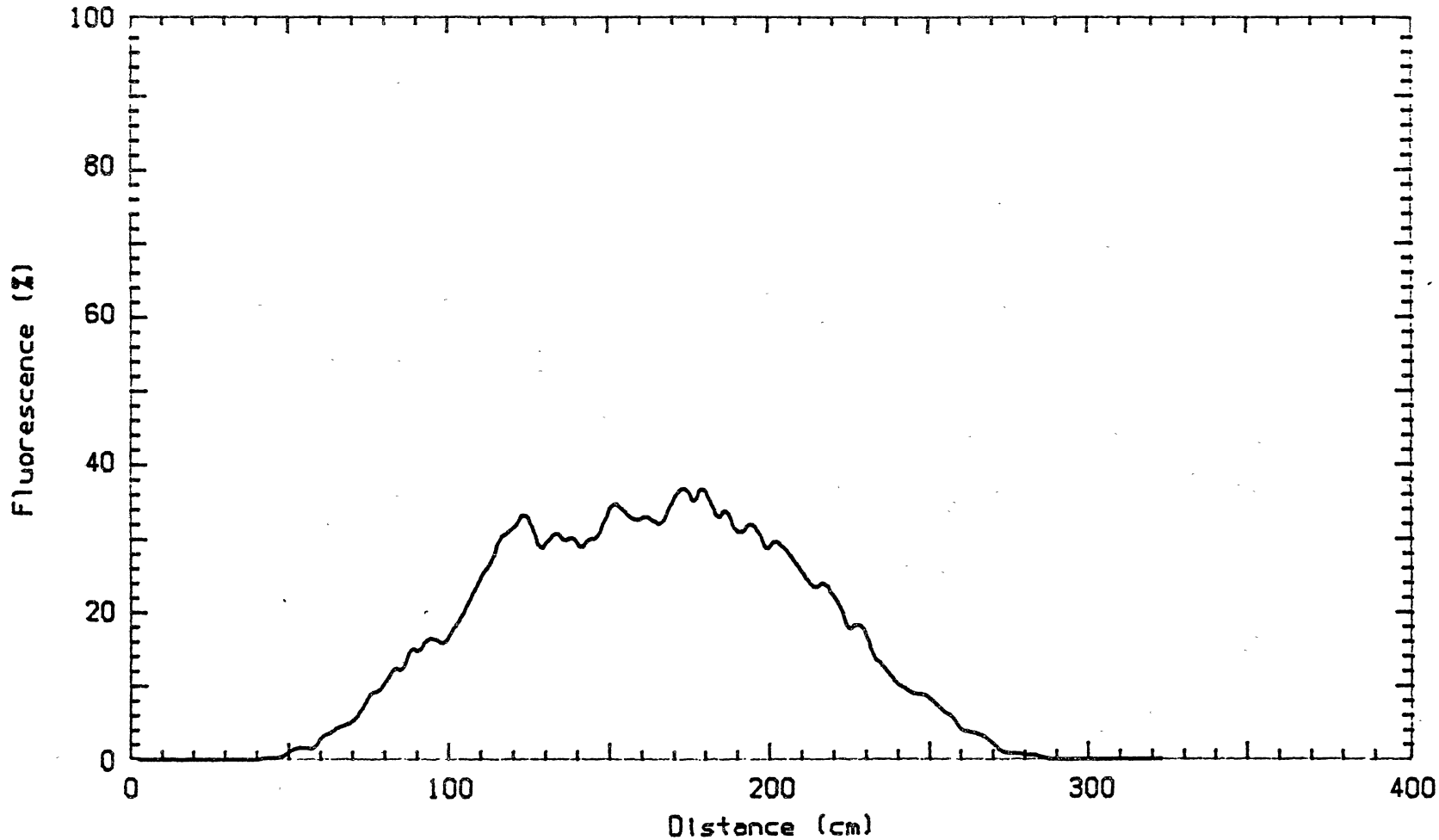

Figure 19. Average Pattern Distribution of Girojet Nozzle Operated at 61 cm Height, 0.50 L/min, 1.34 m/s, and 2500 rpm at 9 Degrees Angle Rotation with center located at 160 cm

for the right side of the nozzle center from Figure 19.

Operating the unit with a flow rate of 0.50 L/min, disk speed of 2500 rpm, and nozzle heights of 46 cm and 61 cm resulted in the patterns with more deposition of material on the left side. This difference was more significant at the 61 cm nozzle height.

When the nozzle was tested at a flow rate of 0.50 L/min, disk speed of 2200 rpm, and at 46 cm and 61 cm nozzle heights (Figures 20 and 21), the fluorescence level was measured to be about 20 percent at 50 cm location on either sides of the nozzle center for the 46 cm nozzle height (Figure 20). For the 61 cm nozzle height, the fluorescence level was measured to be 20 percent at 50 cm location to the left side of the nozzle center and 18 percent at 50 cm to the right side (Figure 21).

Comparing the effect of nozzle height on the maximum fluorescence level deposited at the center of nozzle shows that at the 46 cm nozzle height, the fluorescence level is greater than the 61 cm height (Figures 18 and 20). At 61 cm height, the pattern peak tends to flatten around the center of nozzle (Figures 19 and 21).

As a result of these combination tests, the operating parameters of Figures 18 and 19 were selected to conduct the field tests. The two operating parameters were established to be 0.50 L/min and 2200 rpm at 46 cm and 64 cm nozzle heights. These combinations produced the most symmetrical and uniform patterns.

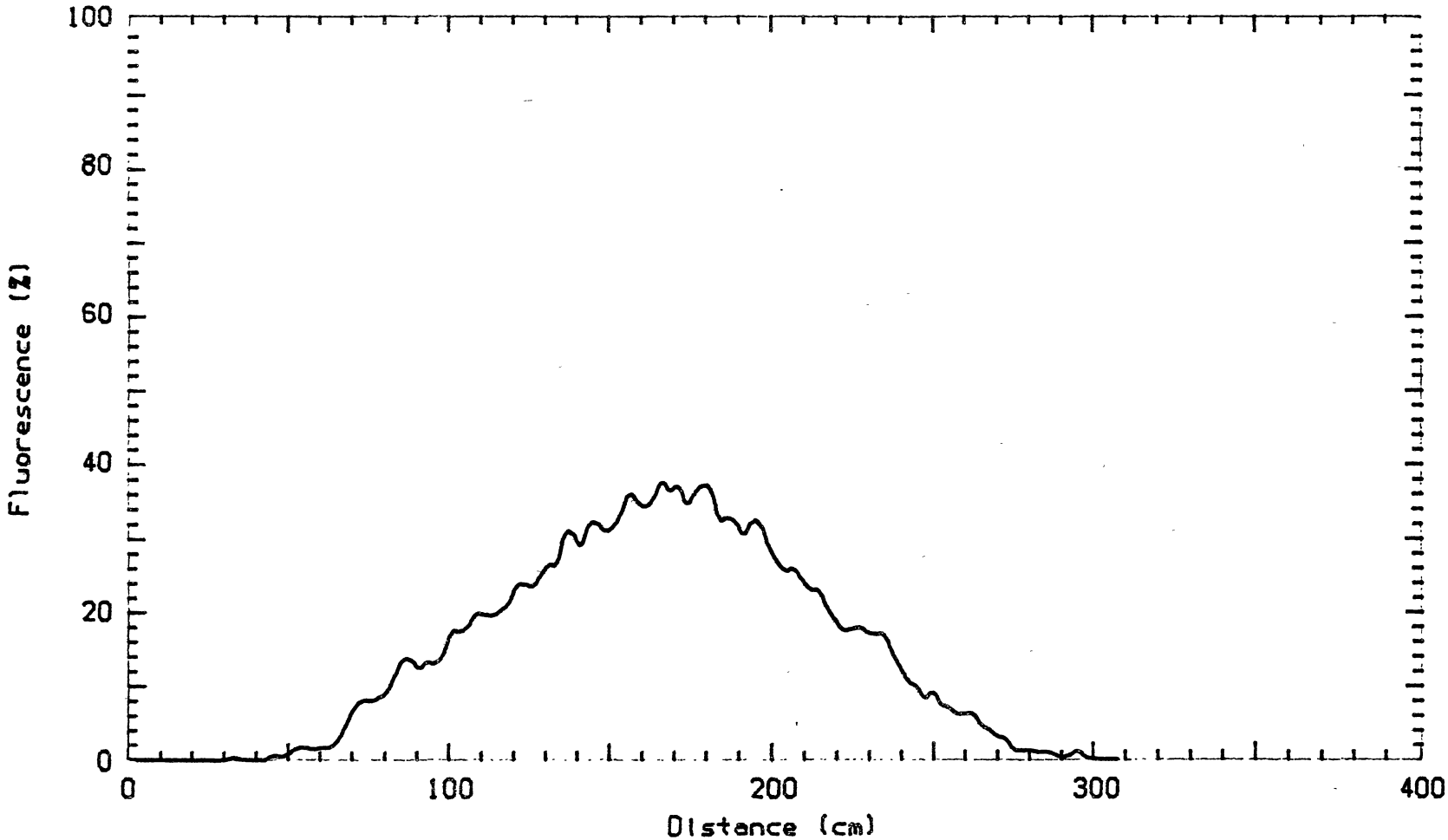

Figure 20. Average Pattern Distribution of Girojet Nozzle Operated at 46 cm Height, 0.50 L/min, 1.34 m/s, and 2200 rpm at 9 Degrees Angle Rotation with center located at 160 cm

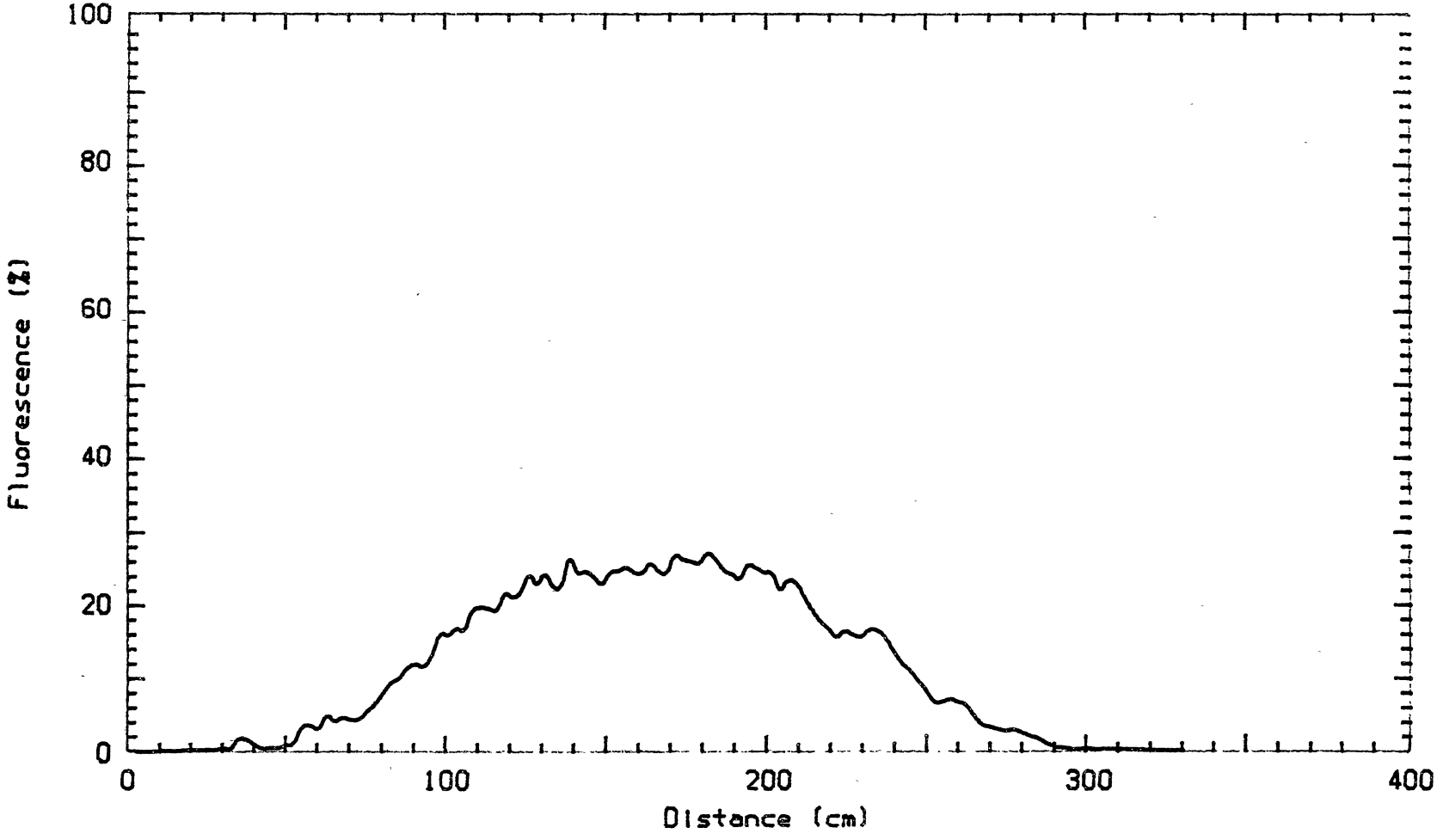

Figure 21. Average Pattern Distribution of Girojet Nozzle Operated at 61 cm Height, 0.50 L/min, 1.34 m/s, and 2200 rpm at 9 Degrees Angle Rotation with center located at 160 cm

Field Test Results

Field experiments were conducted in two parts. In the first part, all the tests were conducted under no cross wind conditions. In the second part, the tests were conducted to study the effect of cross wind on the spray pattern shift and uniformity.

No Cross Wind Tests

Table II shows the average coefficient of variation and centroid of spray patterns (2 sample patterns per pass and 3 passes) for the nozzle spacing and nozzle height tested. The coefficient of variation was calculated from center to center of the outer nozzles. The coefficient of variation and centroid (distance of the spray pattern center from a fixed coordinate) for the average of two sample patterns are shown in Appendix C.

Three passes were made at the 46 cm nozzle height and 3 passes at the 61 cm of nozzle height for the 8001 flat fan nozzle. Figures 59 and 60 in Appendix D show the average profile of the two sample spray patterns and three passes made for the 8001 flat fan nozzle at 46 cm and 61 cm of nozzle height, respectively.

The coefficient of variation of 32.22 percent was obtained for the 46 cm nozzle height, whereas the coefficient of variation for the 61 cm nozzle height was 22.35 percent (Table II). An examination of these figures and coefficient of variation show that the spray pattern at

TABLE II

AVERAGE COEFFICIENT OF VARIATION AND CENTROID OF SPRAY PATTERNS FOR ALL NOZZLES TESTED WITH NO CROSS WIND[1]

Nozzle Height (cm)	Nozzle Spacing (cm)	Disk Angle (deg)	C.V. (%)	Pattern Centroid (cm)
		8001 Flat-Fan		
46	51	--	32.22	208
61	76	--	22.35	220
		Girojet		
46	104	--	26.76	403
61	104	--	21.32	405
		Micromax		
46	114	15	39.10	400
46	114	30	34.27	413
61	114	15	43.22	404
61	114	30	37.82	415
		Rotojet		
46	102	15	29.68	389
46	102	30	27.85	397
61	102	15	33.46	378
61	102	30	31.05	388

1) Flat fan nozzle was operated with 155 KPa and 289 KPa pressure at 46 cm and 61 cm nozzle heights, respectively. Girojet was operated at 276 kPa pressure and 2200 rpm, Micromax at 221 KPa and 2000 rpm, and Rotojet at 221 KPa and 2500 rpm at both nozzle heights. The temperature and relative humidity of 35°C and 64 % were measured, respectively.

61 cm height was more uniform compared to that obtained at the 46 cm height.

Table II also lists the average coefficient of variation and centroid calculated for Girojet. In Figures 61 and 62 of Appendix D, the spray pattern profiles are shown for two different heights. The spray pattern widths were the same (580 cm) for both 46 cm and 61 cm height, but the value of the coefficient of variation was lower at 61 cm height compared to that shown for 46 cm in Table II.

The average coefficient of variation and centroid of the Micromax spinning disk nozzle at two heights and two angles are also listed in Table II. The corresponding spray pattern profiles for the Micromax are shown in Figures 63 through 66 in Appendix D.

The spray pattern width at 46 cm height and 15 degrees tilt angle was observed to be slightly greater than any other combinations examined. The lowest value of coefficient of variation (34.27 %) was found for the Micromax operated at 46 cm height and 30 degrees of tilt angle. No significant difference was observed when the centroid of spray pattern profiles for the Micromax were compared from Table II.

The average coefficient of variation and the centroid of Rotojet with different height-angle combinations are also listed in Table II. In Figures 67 through 70 of Appendix D, the corresponding average spray pattern profiles are shown.

A comparison of coefficient of variation shows that the Rotojet had the lowest value of 27.85 percent for the 46 cm

height and the 30 degrees tilt angle. An increase in nozzle height and tilt angle had no significant effect on the spray pattern centroid.

Analysis of variances at each nozzle height are presented for all nozzles tested in Tables III and IV. At the 5 percent level of significance, the effect of nozzle type and angle on the coefficient of variation was not significant for the 46 cm height, but the effect of nozzle type and angle was significant for the 61 cm height.

Table V shows that the Micromax had the highest average coefficient of variation of any of the nozzles when it was operated with an angle tilted 15 degrees. Tilting the angle to 30 degree had no significant effect on the coefficient of variation of Micromax spray patterns.

Operation of Rotojet at 15 or 30 degrees tilt angle had no significant effect on coefficient of variation compared to Micromax operated at 30 degree tilt angle, but a significant change in coefficient of variation was found for the Rotojet at the 15 or 30 degrees tilt angle when compared to the Micromax operated at 15 degrees. No significant difference was observed between the average coefficient of variation of flat fan and Girojet. According to Table V, Girojet spray pattern had the lowest average coefficient of variation.

Cross Wind Tests

The data obtained in this part are presented in

TABLE III

ANALYSIS OF VARIANCE FOR AVERAGE COEFFICIENT OF VARIATION OF ALL NOZZLE TESTED AT 46 CM HEIGHT WITH NO CROSS WIND

Source	D.F.	M.S.	F-value
Total	17		
Treatments	5	62.915	0.99NS
Passes	2	44.594	
Error	10	58.428	

NS = Not significant.

TABLE IV

ANALYSIS OF VARIANCE FOR AVERAGE COEFFICIENT OF VARIATION OF NOZZLES TESTED AT 61 CM HEIGHT WITH NO CROSS WIND

Source	D.F.	M.S.	F-value
Total	17		
Treatments	5	221.199	15.89*
Passes	2	19.193	
Error	10	13.919	

* Significant at 5 % level.

TABLE V

LEAST SIGNIFICANT DIFFERENCE TEST FOR THE AVERAGE COEFFICIENT OF VARIATION OF ALL NOZZLES TESTED AT 61 CM HEIGHT WITH NO CROSS WIND

Treatments	Pressure (KPa)	Nozzle Height (cm)	Nozzle Spacing (cm)	Disk Angle (Deg)	C.V. (%)[1]
Micromax	221	61	114	15	43.22a
Micromax	221	61	114	30	37.82ab
Rotojet	221	61	102	15	33.47b
Rotojet	221	61	102	30	31.05b
Flat Fan	289	61	76	--	22.35c
Girojet	276	61	104	--	21.32c

1) Means with the same letter are not significantly different at the 5% level according to LSD test.

Appendixes E and F. The average coefficient of variation and centroid of two sample spray patterns, wind speed, and wind direction for all nozzles are shown in Appendix E and spray pattern profiles are shown Appendix F.

The corresponding values for the 8001 flat fan nozzle are listed in the first part of Appendix E. A total of 17 passes were made for flat fan nozzle, 7 passes at 46 cm nozzle height and 10 passes at 61 cm.

In the second part, the average coefficient of variation and the centroid along with the wind speed and direction for the Girojet vertical spinning disk nozzle are listed. The average coefficient of variation and centroid calculated for the Micromax spinning disk nozzle at two different height-angle combinations with the corresponding wind speed and direction are also shown in the third part of Appendix E.

In the last part, the average coefficient of variation, the centroid, and corresponding wind speed and direction for the Rotojet spinning disk nozzle are summarized. A total of 8 passes were made at two levels of height and tilt angle.

Centroid Shift study

A total of 25 direct comparisons of pattern shift made of spinning disk nozzles versus a regular flat fan nozzle are listed in Appendix G. A study of results of pattern shift showed that spray pattern of Girojet and flat fan nozzles were not as greatly affected by wind as the horizontal spinning disk nozzles.

Comparison of pattern shift of the horizontal spinning nozzles to the flat fan nozzle showed that the effect of wind was significant in general, on the pattern shift of these horizontal spinning disk.

Table VI shows the results of the t-test comparisons made between the spinning disk nozzles and the flat fan nozzle at two levels of nozzle height for the Girojet and the 8001 flat fan nozzles and two different angles were included in the comparisons for the Micromax and Rotojet nozzles with the 8001 flat fan nozzle.

The centroid shift of the spray pattern of Girojet nozzle was not significantly greater than the flat fan nozzle. However, except for the Micromax operated with 15 degrees tilt angle at 61 cm height and for Rotojet with 30 degrees tilt angle at 46 cm height, the centroid shift of patterns for Micromax and Rotojet nozzles were significantly greater than the flat fan nozzle at 5 percent level of significance.

In general, the vertical spinning disk nozzle produced a more uniform spray pattern than the 8001 flat fan nozzle and the two horizontal spinning disk nozzles. The effect of wind speed was not as significant on the pattern shift of the vertical spinning disk nozzle compared to the flat fan nozzle as the two horizontal spinning disk nozzles when compared to the flat fan nozzle. Therefore, the Girojet may be selected for a precise and efficient application of herbicide with the operating parameters of 2200 rpm of disk

TABLE VI

T-TEST COMPARISONS OF PATTERN CENTROID SHIFT FOR ALL NOZZLES TESTED WITH CROSS WIND

Comparison	Nozzle Height (cm)	Disk Angle (deg)	Centroid Shift Difference (cm)	T-value
8001 Flat Fan / Girojet	46	--	6	0.80
8001 Flat Fan / Girojet	61	--	16	0.53
8001 Flat Fan / Micromax	46	15	114	15.74*
8001 Flat Fan / Micromax	46	30	27	53.00*
8001 Flat Fan / Micromax	61	15	117	4.2
8001 Flat Fan / Micromax	61	30	134	26.8*
8001 Flat Fan / Rotojet	46	15	173	33.09*
8001 Flat Fan / Rotojet	46	30	183	7.04
8001 Flat Fan / Rotojet	61	15	92	7.08*
8001 Flat Fan / Rotojet	61	30	40	26.80*

* Significant at 5 percent level.

speed, 9 degrees counterclockwise rotation in a plane perpendicular to the direction of travel, 0.50 L/min of flow rate per nozzle, 104 cm nozzle spacing, and 46 or 61 cm nozzle heights.

Verification of Model

The simulation model was verified in two parts. In the first part, the simulated spray patterns of a single Girojet nozzle were compared with the measured spray patterns from laboratory tests by measuring the pattern width and the beginning and the ending of deposition locations along the swath width. In the second part, the simulated spray patterns of 4 Girojet nozzles mounted on the spray boom were compared to the measured spray patterns obtained from field tests.

The centroid of both the simulated and measured spray patterns were calculated in addition to the pattern width and the beginning and ending locations of pattern. These variables were not changed by averaging the replications of the simulated spray patterns and replicated spray patterns for laboratory and field conditions. Therefore, a simulated spray pattern was compared with the average of the measured spray patterns obtained from the laboratory and the field tests.

The simulated spray pattern of Figure 22 was obtained using the model at 0 degrees, 46 cm nozzle height, 0.50 L/min, and 2200 rpm disk speed. Figure 23 from laboratory tests was used at the same operating parameters for

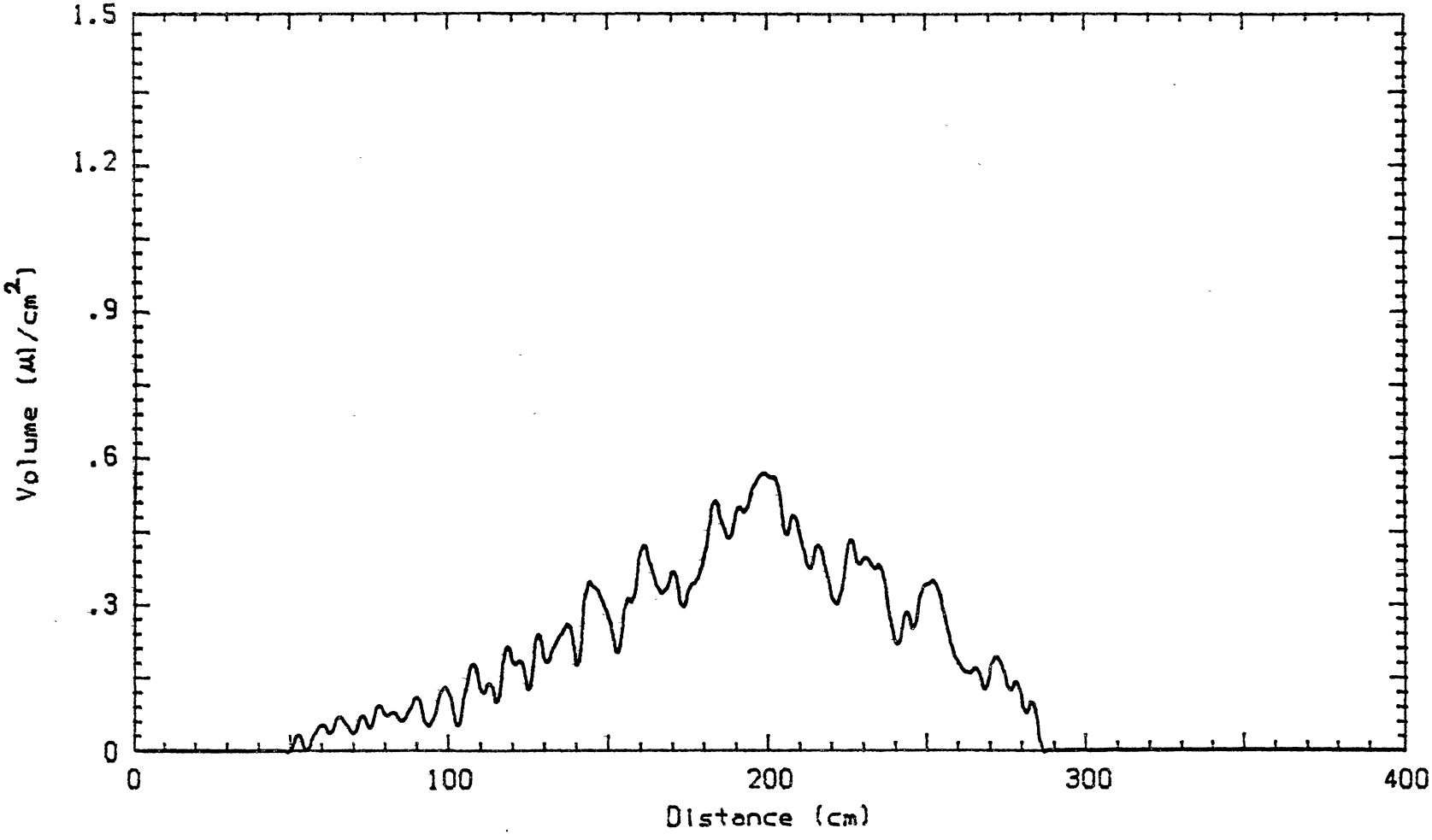

Figure 22. Simulated Pattern Distribution of Girojet Nozzle Operated at 46 cm Height, 0.50 L/min, 1.34 m/s, and 2200 rpm at 0 Degrees Angle Rotation with center located at 207 cm

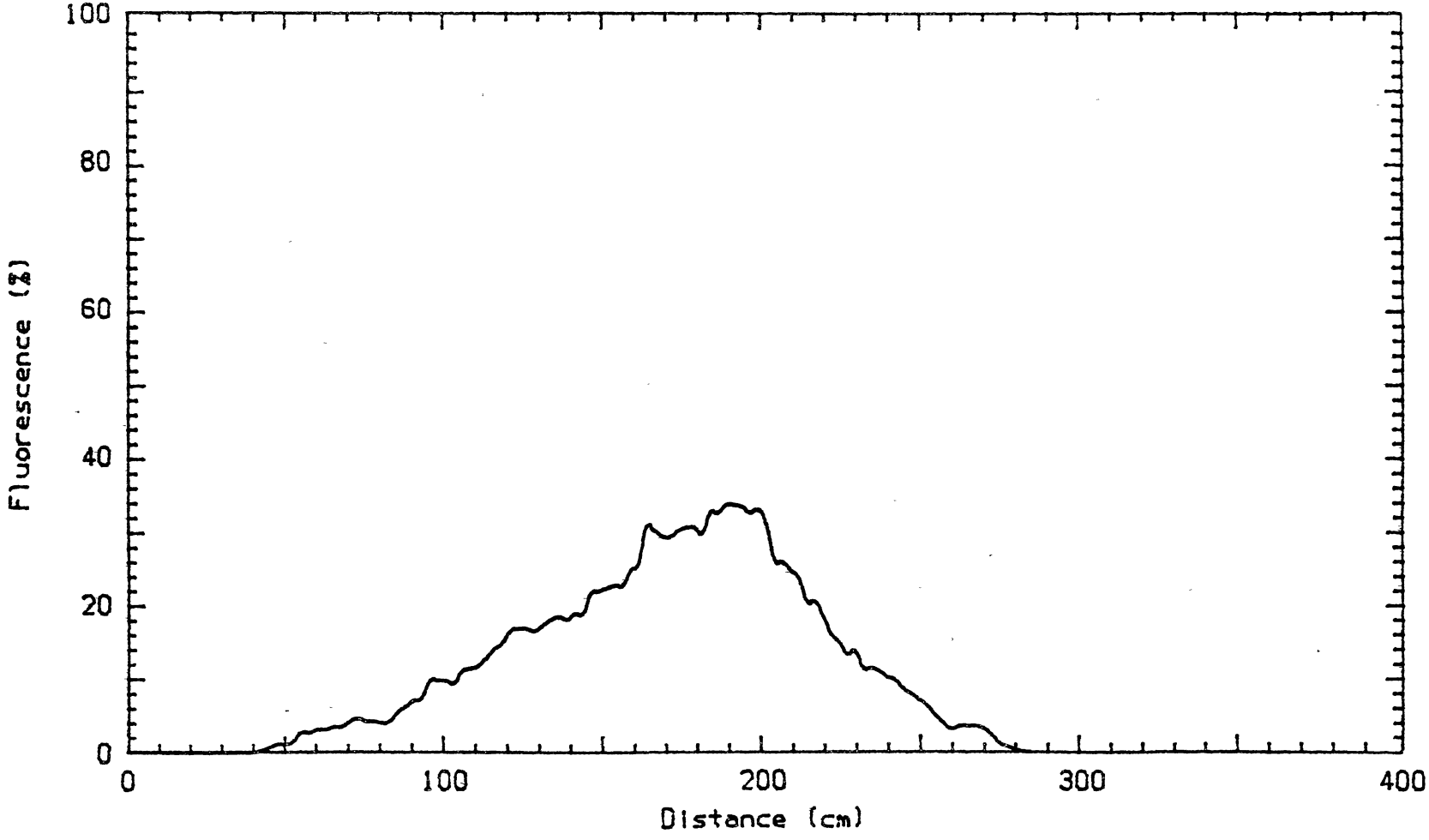

Figure 23. Average Pattern Distribution of Girojet Nozzle Operated at 46 cm Height, 0.50 L/min, 1.34 m/s, and 2200 rpm at 0 Degrees Angle Rotation with center located at 195.5 cm

comparison. The pattern width of simulated spray pattern was found to be within 10 cm of the average of measured spray pattern.

The center of the nozzle for the simulated spray pattern was at 207 cm and for the average of the measured pattern, the center of the nozzle was at 190.5 cm. The beginning and ending locations of deposition for the simulated spray pattern were at 50 cm and 286 cm, and for the average of measured spray pattern were at 44 cm and 290 cm, respectively.

The effect of nozzle height on the pattern width of the average of measured spray pattern and the simulated spray pattern were studied at the same operating parameters of 0.50 L/min, 2200 rpm, 1.47 m/s of ground speed, and 46, 61, and 71 cm of nozzle heights. Figures 24 through 29 show the simulated and the average of measured spray patterns for the 46, 61, and 71 cm nozzle heights. The center of the nozzle for the simulated spray pattern was located at 207 cm and for the average of measured spray pattern, the center was at 160 cm.

The simulated pattern widths were found to be 2 cm, 21 cm, and 7 cm greater than the average of measured spray pattern width for the 46, 61, and 71 cm nozzle height, respectively (Table VII). Study of the measured and simulated pattern width from Table VII show that an increase in nozzle height, resulted in a wider pattern.

Figure 30 shows the simulated spray pattern of four

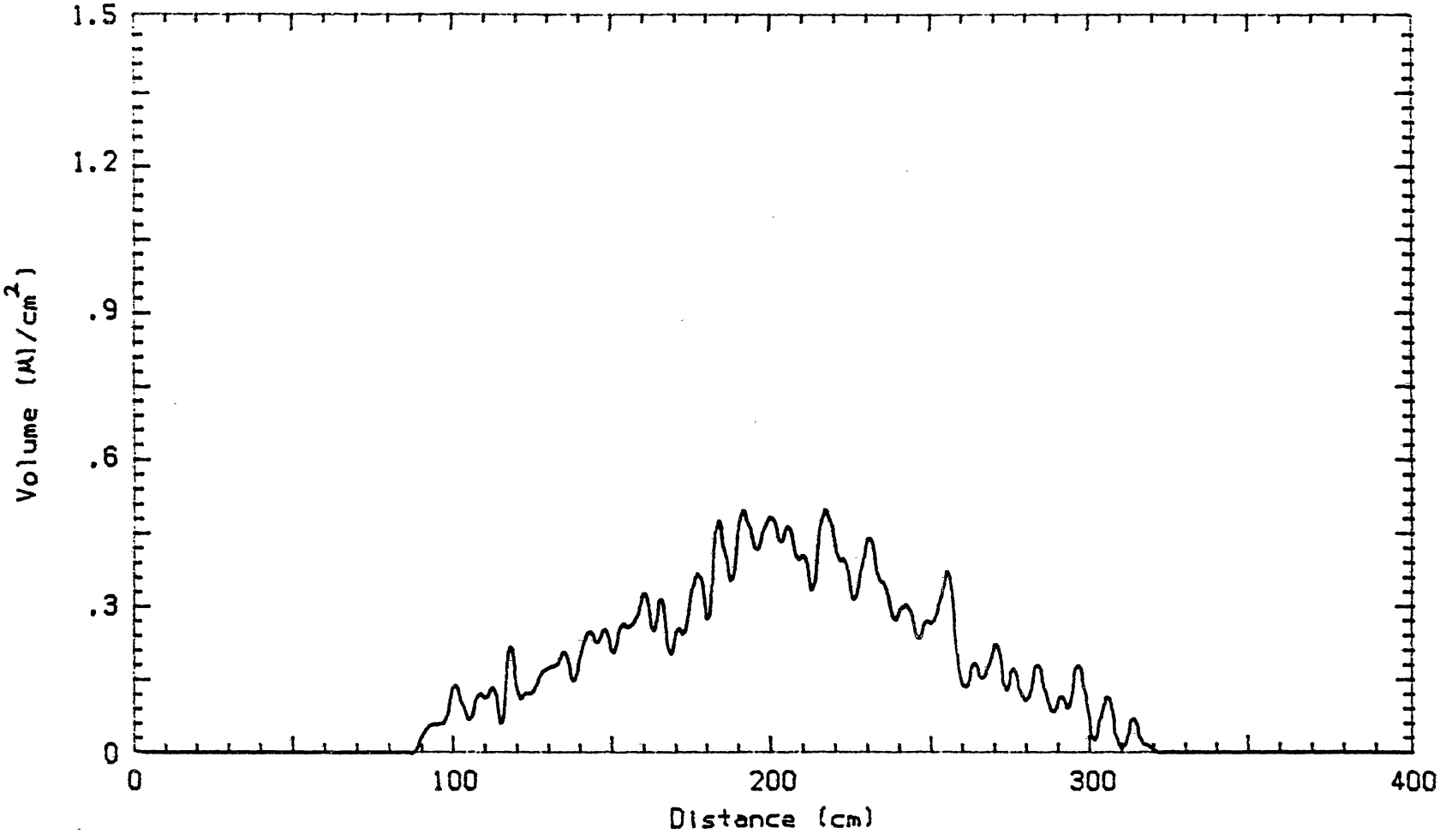

Figure 24. Simulated Pattern Distribution of Girojet Nozzle Operated at 46 cm Height, 0.50 L/min, 1.34 m/s, and 2200 rpm at 9 Degrees Angle Rotation with center located at 207 cm

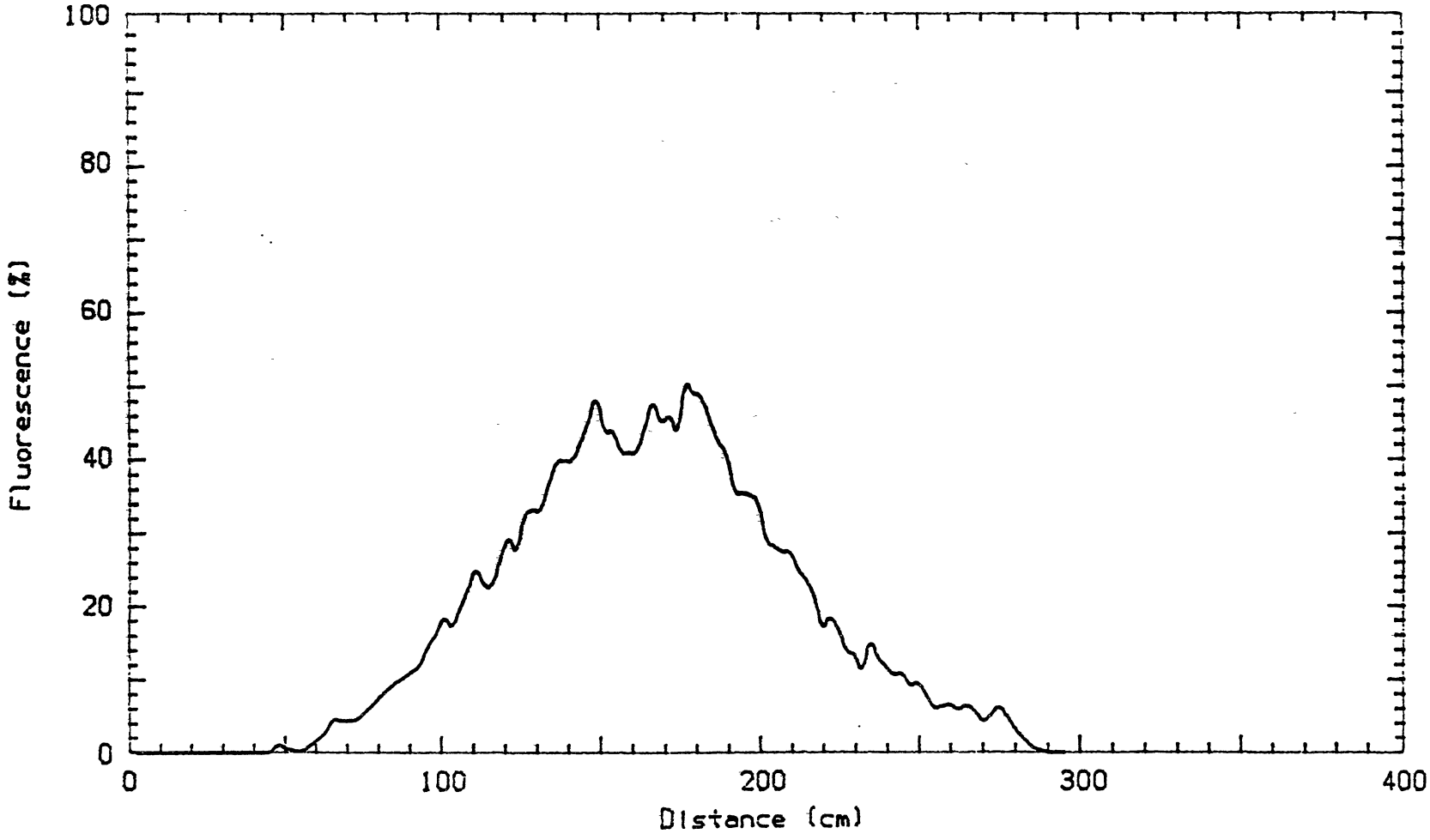

Figure 25. Average Pattern Distribution of Girojet Nozzle Operated at 46 cm Height, 0.50 L/min, 1.34 m/s, and 2200 rpm at 9 Degrees Angle Rotation with center located at 160 cm

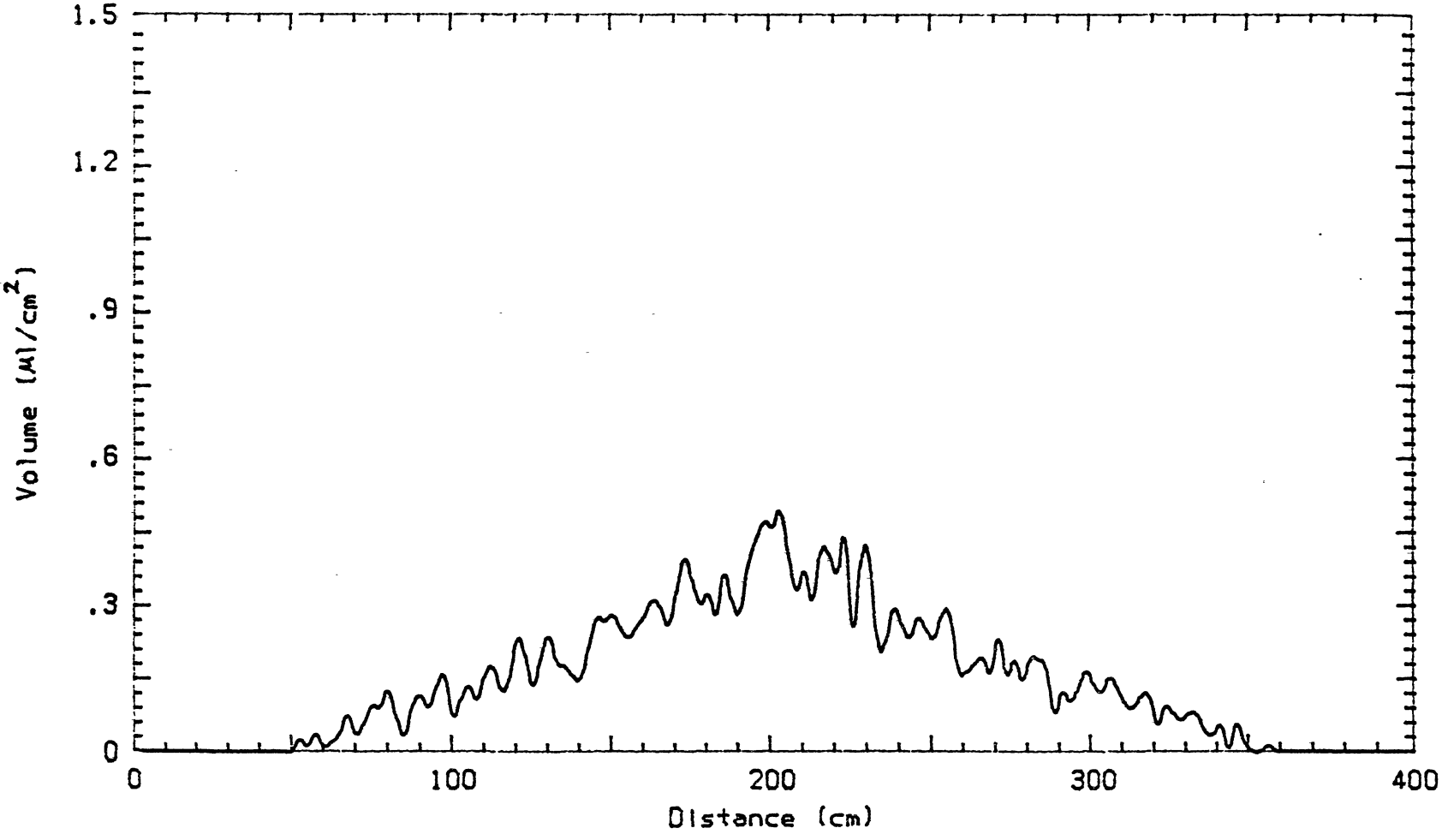

Figure 26. Simulated Pattern Distribution of Girojet Nozzle Operated at 61 cm Height, 0.50 L/min, 1.34 m/s, and 2200 rpm at 9 Degrees Angle Rotation with center located at 207 cm

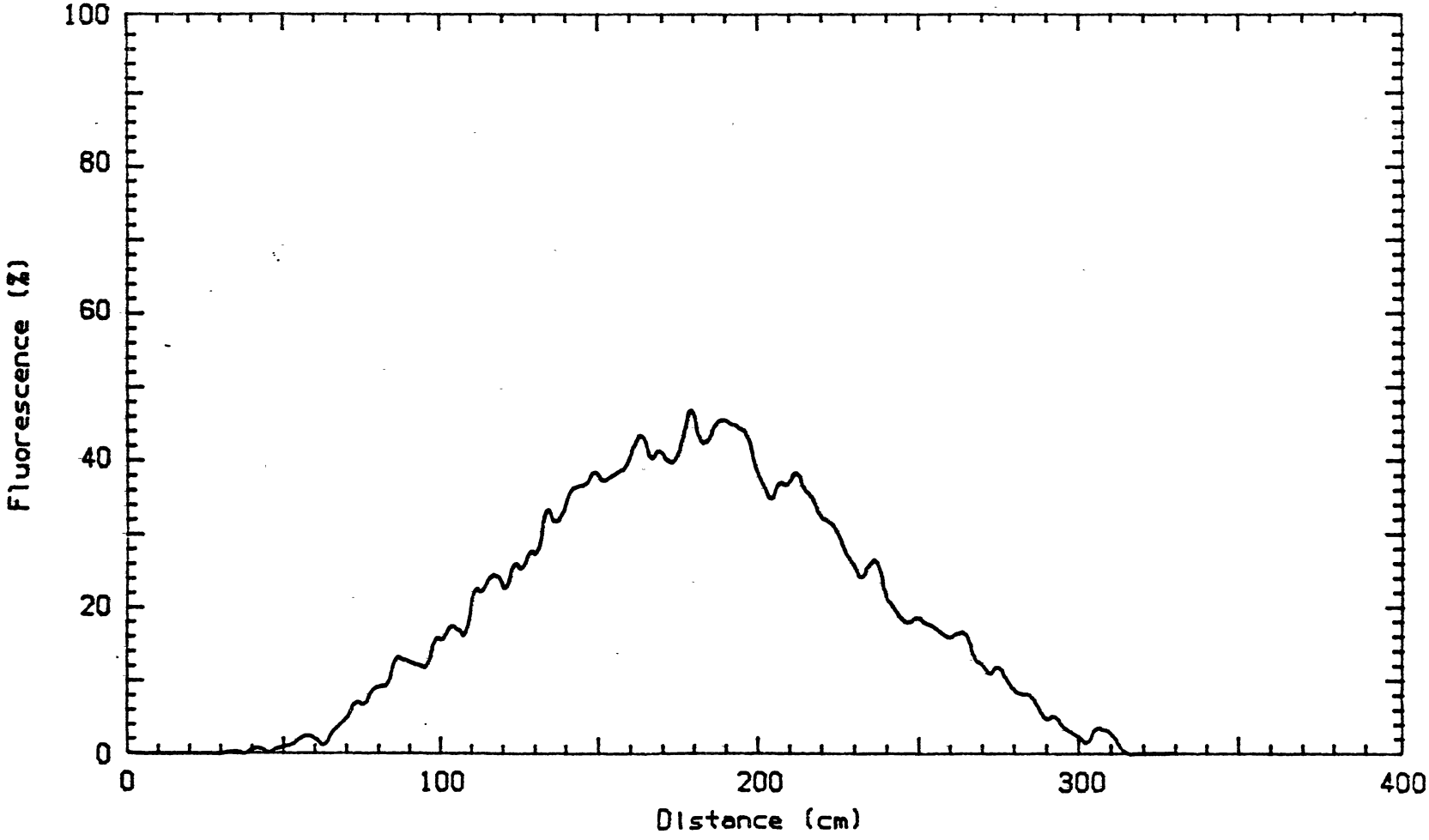

Figure 27. Average Pattern Distribution of Girojet Nozzle Operated at 61 cm Height, 0.50 L/min, 1.34 m/s, and 2200 rpm at 9 Degrees Angle Rotation with center located at 160 cm

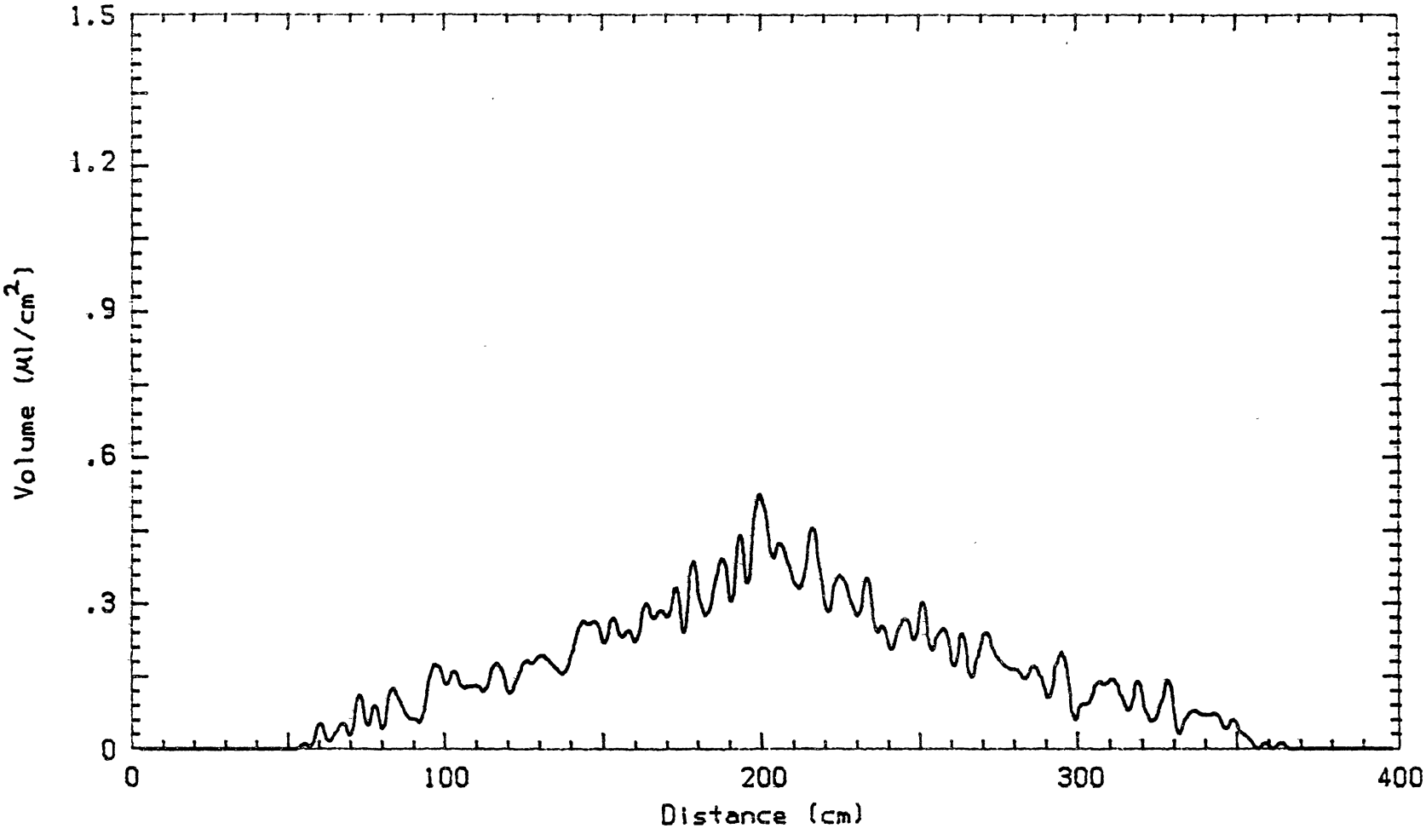

Figure 28. Simulated Pattern Distribution of Girojet Nozzle Operated at 71 cm Height, 0.50 L/min, 1.34 m/s, and 2200 rpm at 9 Degrees Angle Rotation with center located at 207 cm

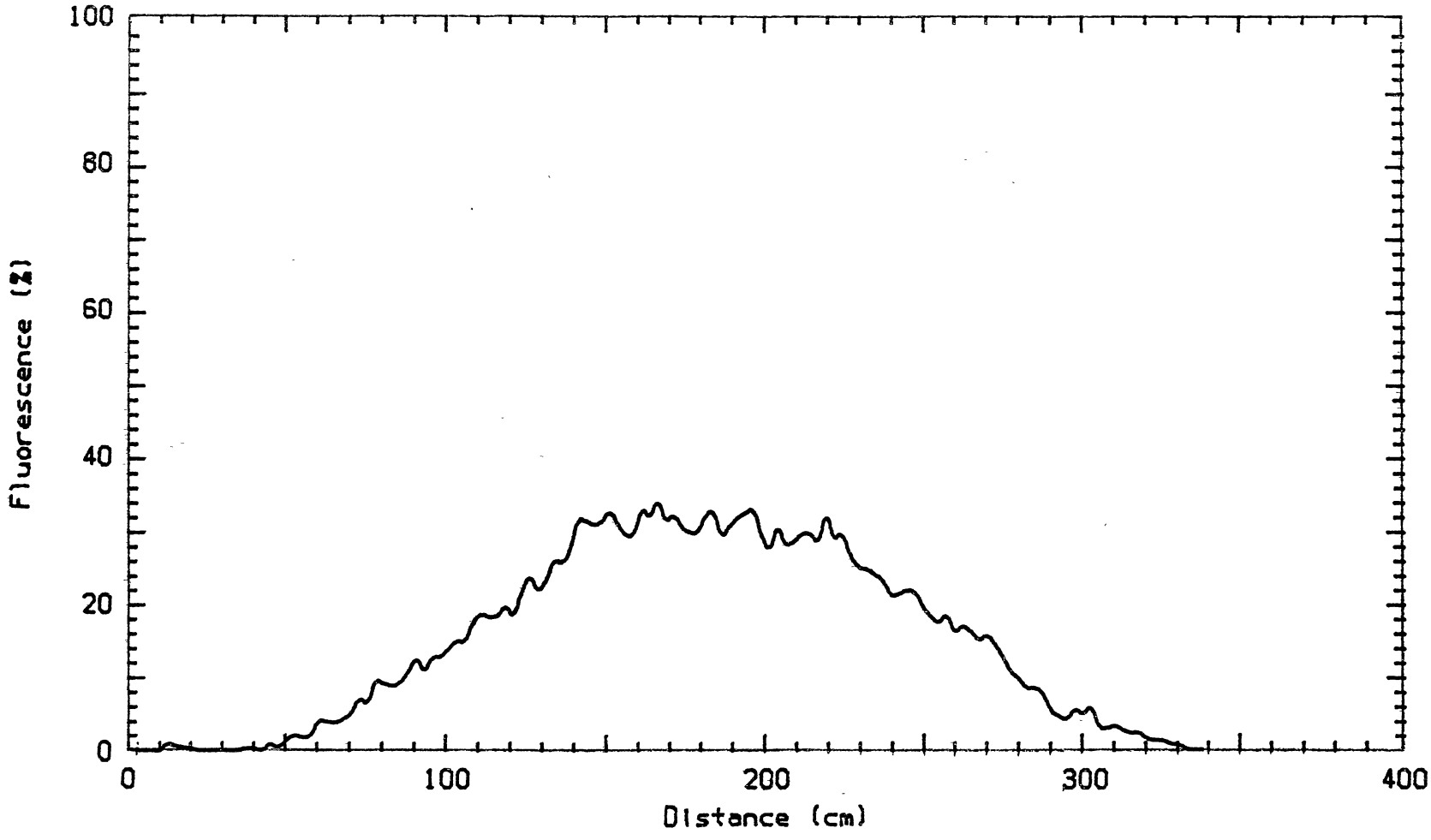

Figure 29. Average Pattern Distribution of Girojet Nozzle Operated at 71 cm Height, 0.50 L/min, 1.34 m/s, and 2200 rpm at 9 Degrees Angle Rotation with center located at 160 cm

TABLE VII

EFFECT OF NOZZLE HEIGHT ON MEASURED AND SIMULATED SPRAY PATTERN WIDTH FOR A SINGLE GIROJET NOZZLE

Nozzle Height	Pattern Width		Beginning of Deposition		Ending of Deposition		Maximum Deposition	
(cm)	Meas. (cm)	Simul. (CM)	Meas. (cm)	Simul. (cm)	Meas. (cm)	Simul. (cm)	Meas.[1] (%F)	Simul.[2] (uL/cm^2)
46	230	232	55	88	285	320	51	0.56
61	269	290	46	60	315	350	46	0.50
71	295	302	45	55	340	357	36	0.56

1) Measures percent fluorescence dye deposited on the paper type.
2) Simulated spray application rate in uL/cm^2.

Girojet nozzles mounted on a spray boom. This pattern was obtained from four simulated single nozzle patterns with different seed numbers, overlapped 104 cm apart, center to center and with the operating parameters of 46 cm nozzle height, 42 L/ha of application rate, 2200 rpm of disk speed, and forward speed of 2.235 m/s. This pattern was compared with the selected pattern obtained from the field tests with the same operating parameters as shown in Figure 31.

The center locations of nozzles for the simulated spray pattern were at 251, 355, 459, and 563 cm, respectively and for the average of measured spray pattern, the nozzle centers were located at 104 cm apart (nozzle spacing) on the spray boom, with the first nozzle at 244 cm location. The pattern width for the simulated spray pattern was measured to be 567 cm and for the average of measured spray pattern, it was 580 cm as listed in Table VIII.

At 61 cm of nozzle height, another simulated spray pattern was obtained using the model (Figure 32) with the same operating parameters as the average of measured spray pattern shown in Figure 33. The nozzle's locations remained the same for both the simulated and the measured patterns. The pattern width of the simulated spray pattern was measured to be within 6 cm of the pattern width for the averge of measured spray pattern.

The simulation model was also verified by a number of comparisons between the simulated spray patterns and the average of two sample measured spray patterns obtained from the field tests. Figures 34 and 35 show the simulated and

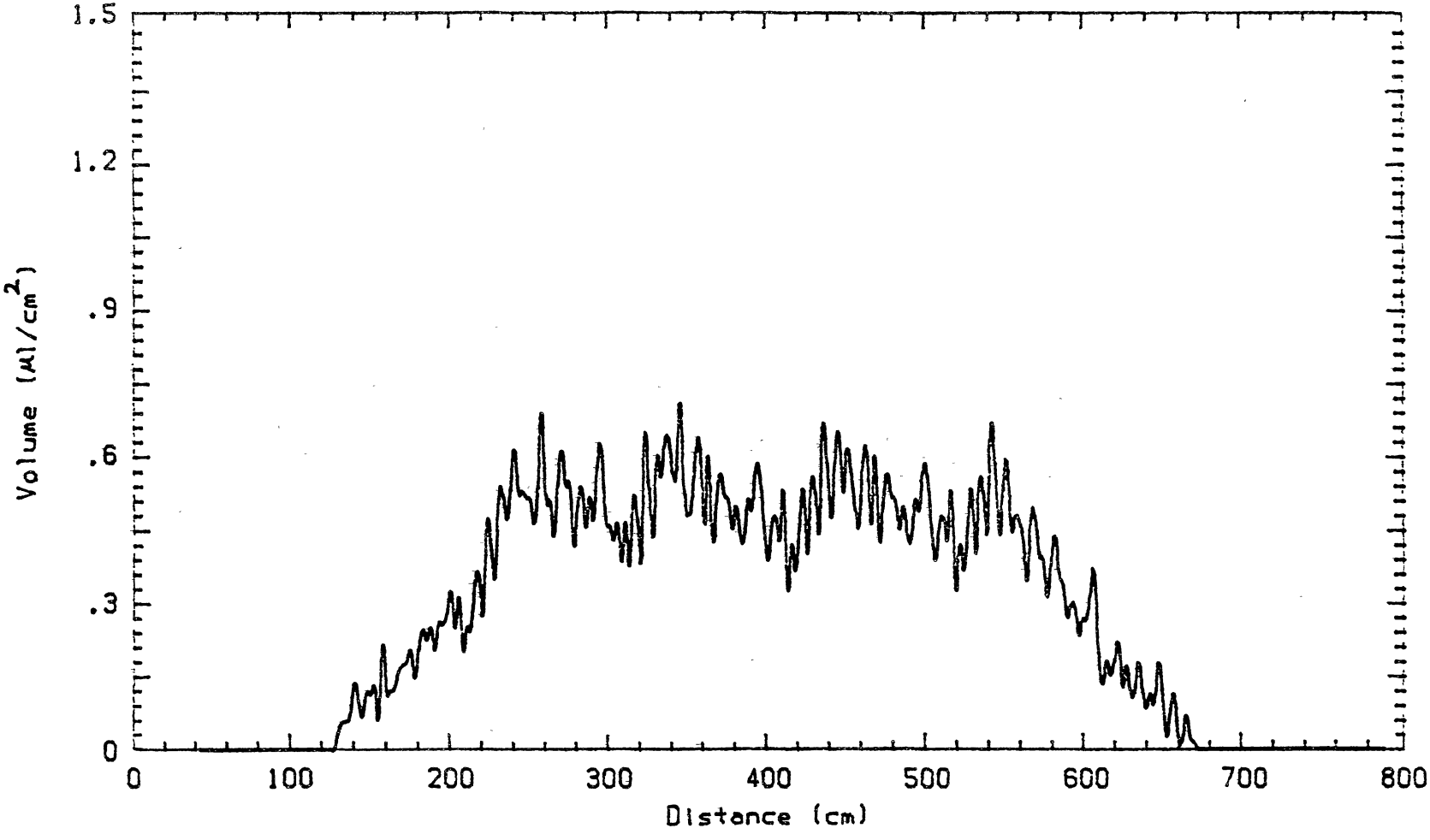

Figure 30. Simulated Pattern Distribution of 4 Girojet Nozzles Operated at 46 cm Height, 42 L/ha, 2.24 m/s, and 2200 rpm at 9 Degrees Angle Rotation with center of nozzles located at 251, 355, 459, and 563 cm

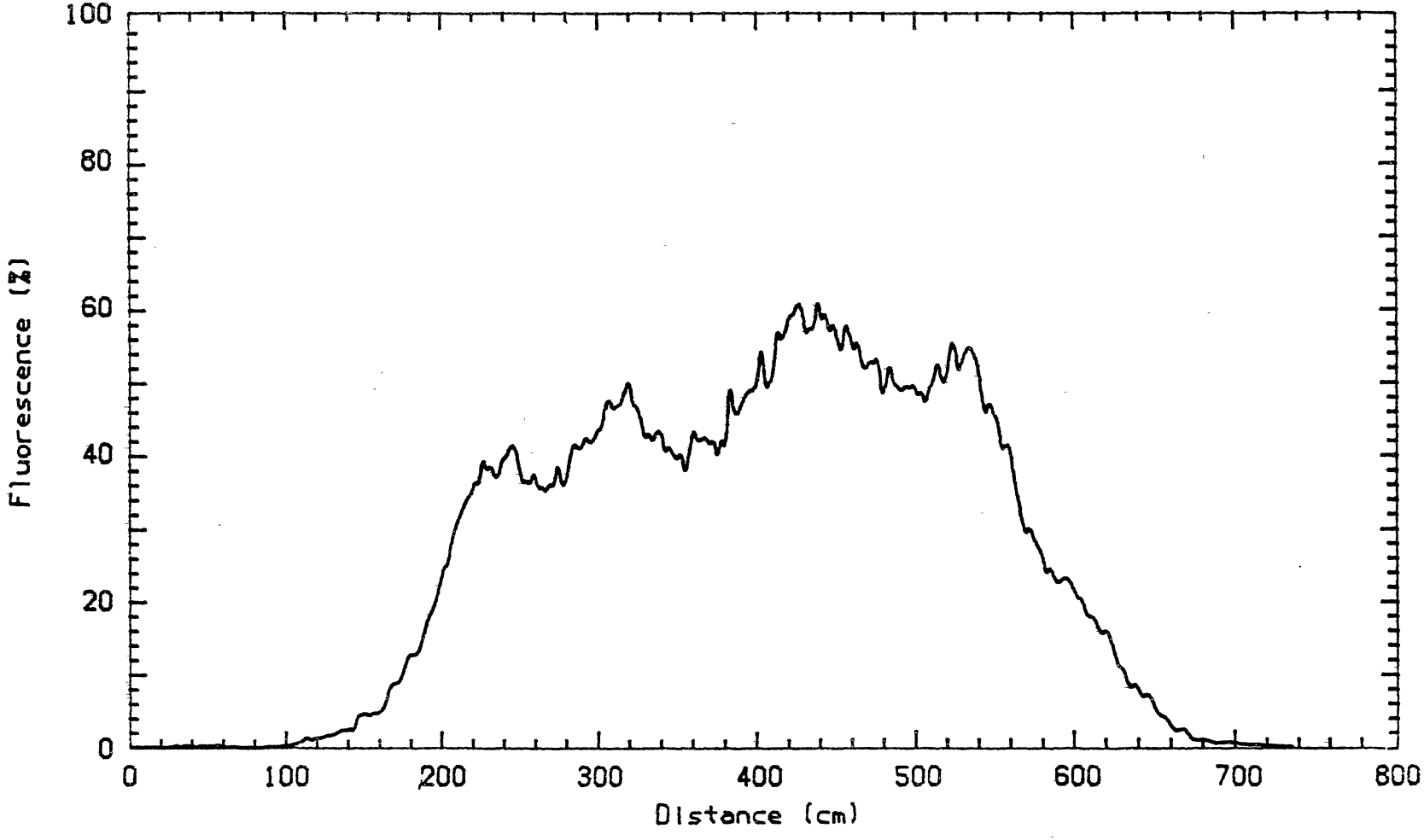

Figure 31. Measured Pattern Distribution of 4 Girojet Nozzles Operated at 46 cm Height, 42 L/ha, 2.24 m/s, and 2200 rpm at 9 Degrees Angle Rotation with center of nozzles located at 244, 348, 452, and 556 cm

TABLE VIII

EFFECT OF WIND SPEED ON MEASURED AND SIMULATED SPRAY PATTERN SHIFT OF 4 GIROJET NOZZLES MOUNTED ON A BOOM

Nozzle Height	Wind Speed	Pattern Width		Pattern Centroid		Pattern[1] Shift	
		Meas.	Simul.	Meas.	Simul.	Meas.	Simul.
(cm)	(m/s)	(cm)	(cm)	(cm)	(cm)	(cm)	(cm)
46	0	580	567	403	395	--	--
46	1.48	630	610	436	465	33	70
61	0	600	605	405	396	--	--
61	0.62	680	660	459	464	54	68
61	1.32	750	630	442	475	37	79

1) The pattern shift was obtained by subtracting the centroid of spray pattern under no cross wind from the centroid of spray pattern with cross wind.

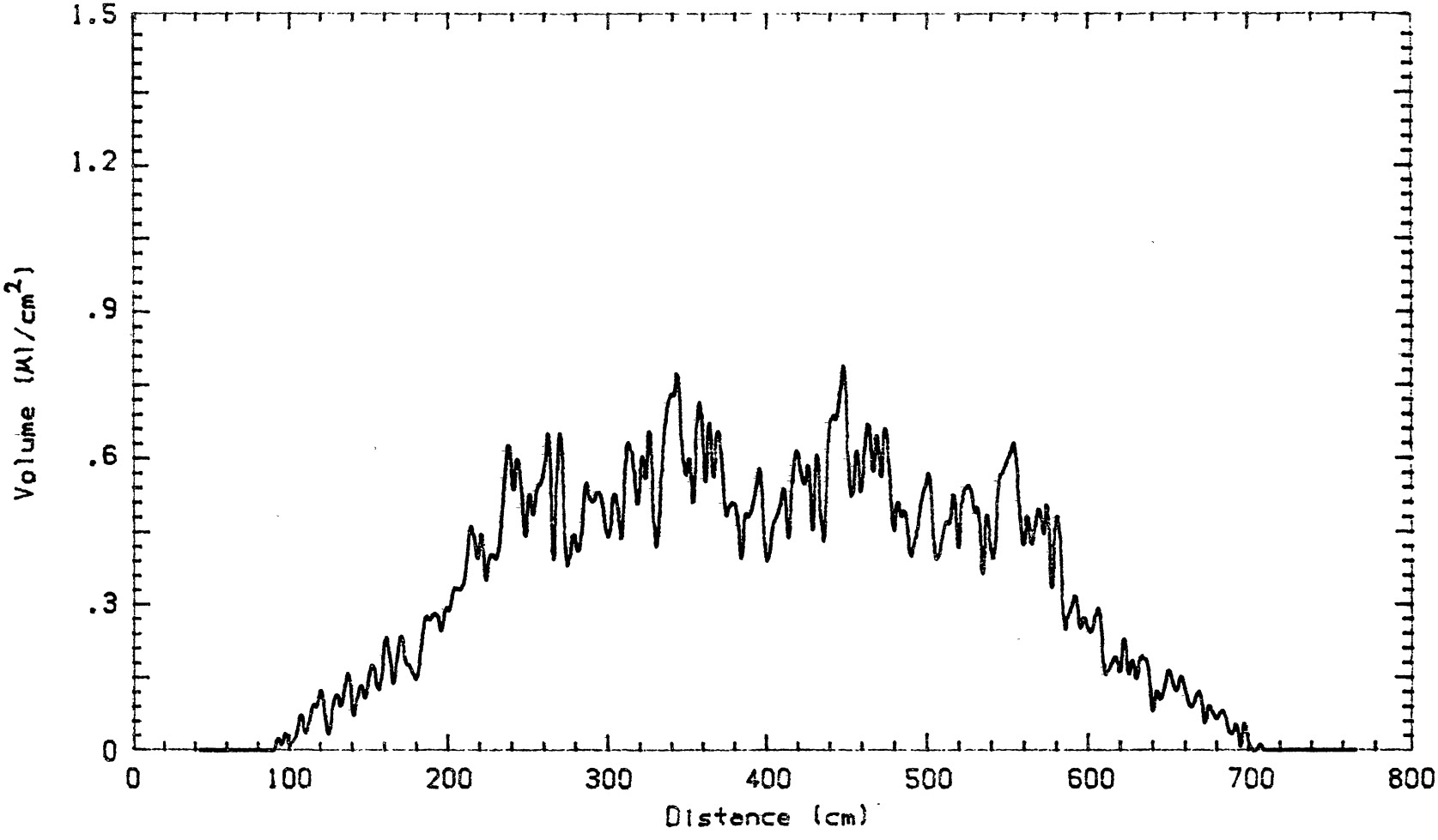

Figure 32. Simulated Pattern Distribution of 4 Girojet Nozzles Operated at 61 cm Height, 42 L/ha, 2.24 m/s, and 2200 rpm at 9 Degrees Angle Rotation with center of nozzles located at 251, 355, 459, and 563 cm

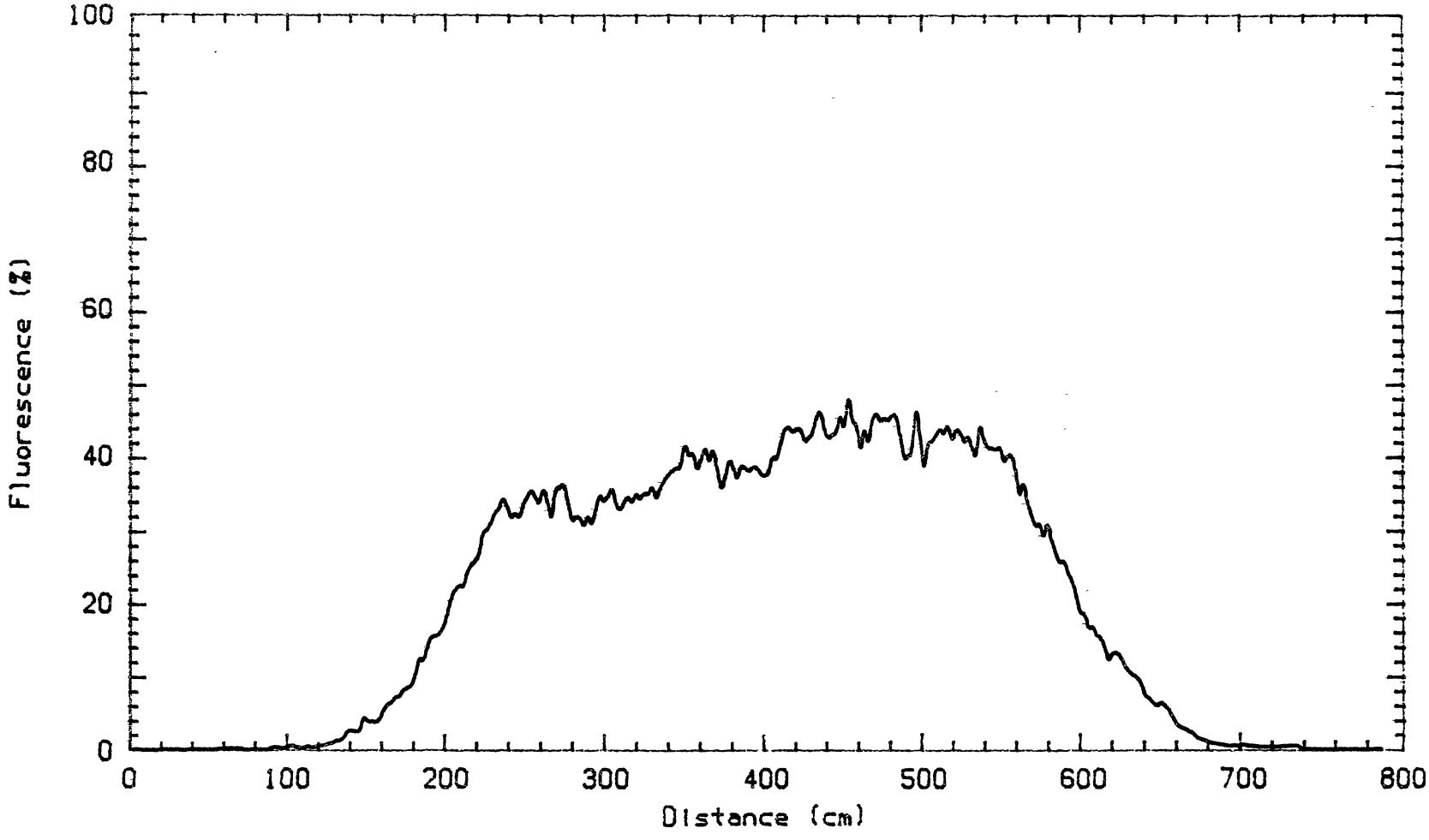

Figure 33. Measured Pattern Distribution of 4 Girojet Nozzles Operated at 61 cm Height, 42 L/ha, 2.24 m/s, and 2200 rpm at 9 Degrees Angle Rotation with center of nozzles located at 244, 348, 452, and 556 cm

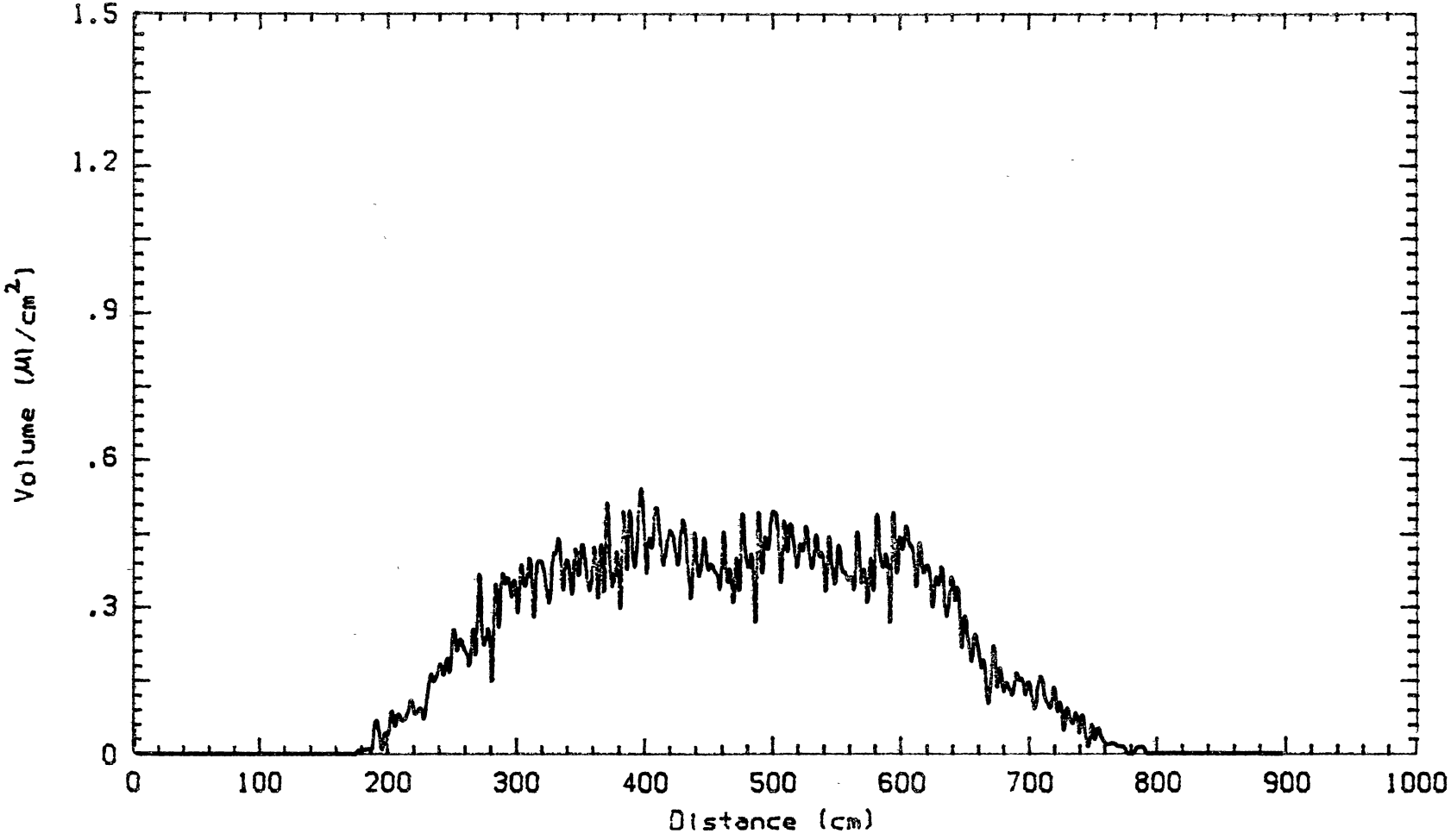

Figure 34. Simulated Pattern Distribution of 4 Girojet Nozzles Operated at 46 cm Height, 42 L/ha, 2.24 m/s, 1.48 m/s wind speed, and 2200 rpm at 9 Degrees Angle Rotation with centers located at 251, 355, 459, and 563 cm

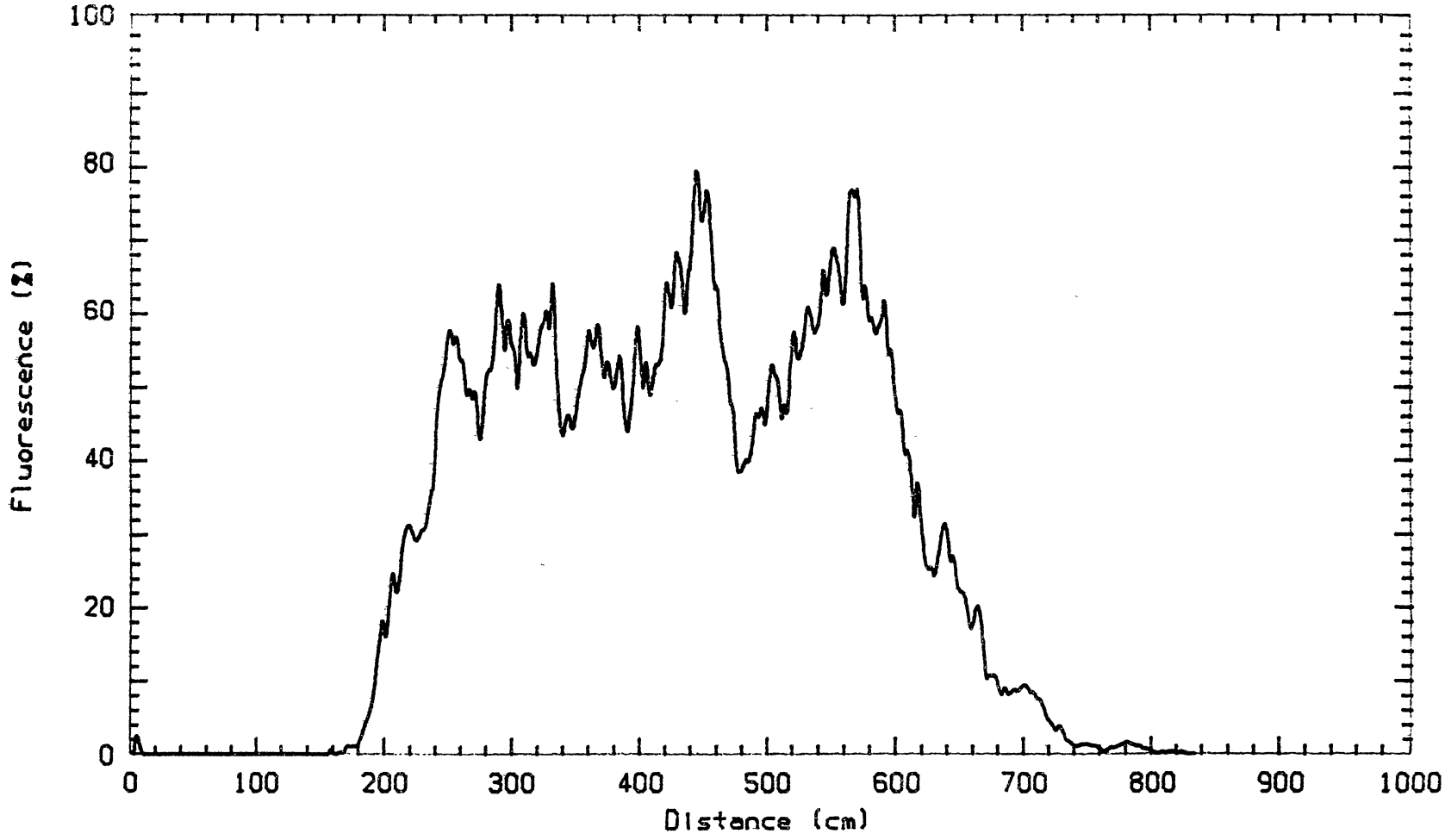

Figure 35. Measured Pattern Distribution of 4 Girojet Nozzles Operated at 46 cm Height, 42 L/ha, 2.24 m/s, 1.48 m/s wind speed, and 2200 rpm at 9 Degrees Angle Rotation with centers located at 244, 348, 452, and 556 cm

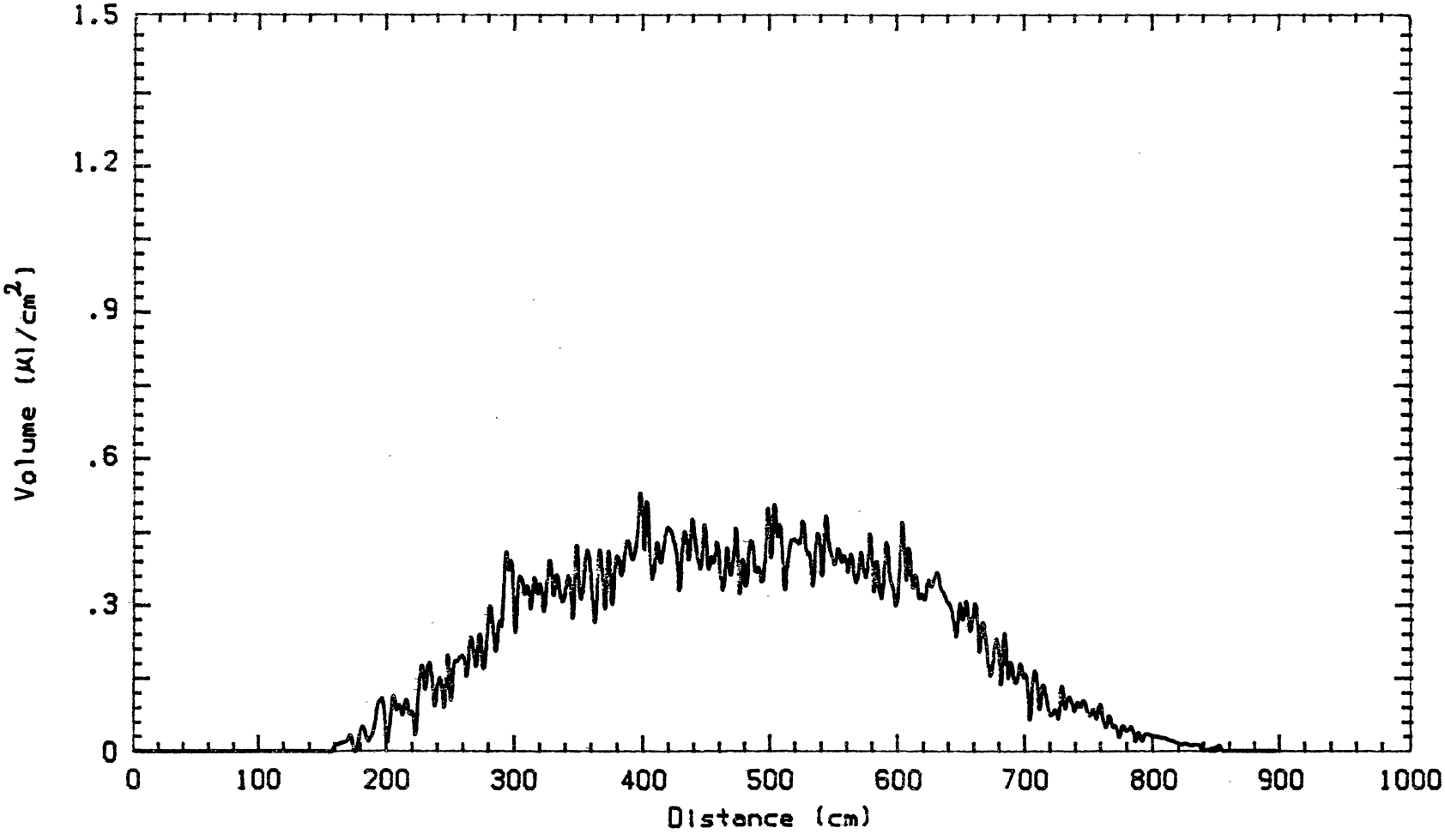

Figure 36. Simulated Pattern Distribution of 4 Girojet Nozzles Operated at 61 cm Height, 42 L/ha, 2.24 m/s, 0.62 m/s wind speed, and 2200 rpm at 9 Degrees Angle Rotation with centers located at 251, 355, 459, and 563 cm

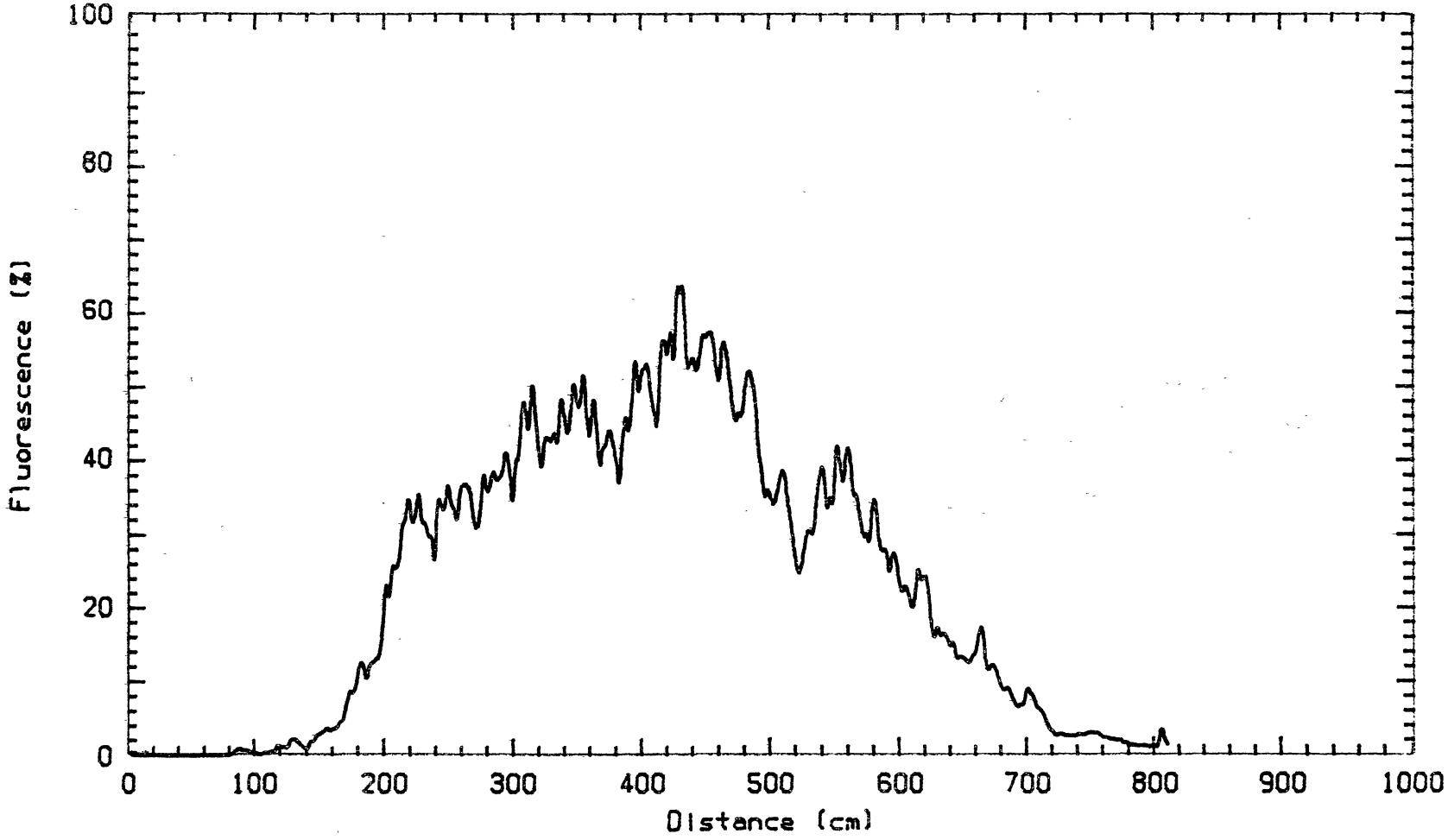

Figure 37. Measured Pattern Distribution of 4 Girojet Nozzles Operated at 61 cm Height, 42 L/ha, 2.24 m/s, 0.62 m/s wind speed, and 2200 rpm at 9 Degrees Angle Rotation with centers located at 244, 348, 452, and 556 cm

the average of two sample measured spray patterns at 46 cm nozzle height, 2200 rpm, 42 L/ha, 2200 rpm, 2.235 m/s of ground speed, and with 1.48 m of cross wind.

The pattern width and the centroid shift of spray pattern for both the simulated and the average of two sample measured patterns are listed in Table VIII. The shift of centroid for the spray patterns was determined by measuring the displacement of the centroid of the spray pattern caused by wind speed. This displacement was calculated by subtracting the spray pattern centroid under no cross wind from the shifted spray pattern centroid by cross wind.

Table VIII also shows the nozzle heights, wind speed, and pattern centroid values for the simulated and the average of two sample measured spray patterns at two level of nozzle heights. At 46 cm nozzle height, the wind caused an increase in pattern width of 20 cm for the average of two samples measured spray pattern and an increase of about 50 cm for the simulated spray pattern. This resulted in a greater shift of simulated pattern (70 cm shift for the simulated pattern compared to 33 cm shift for the average of two sample measured spray pattern).

With a cross wind of 0.62 m/s and at the 61 cm height, the measured pattern width increased about 80 cm whereas the increase of pattern width for the simulated pattern was 55 cm as listed in Table VIII and shown in the Figures 36 and 37. Even though the average of two sample measured spray pattern widths was increased more than the simulated pattern

width by wind speed, the centroid of simulated spray pattern shifted about 14 cm more than the centroid of the average of two sample measured spray pattern.

At 61 cm nozzle height, with the wind speed of 1.32 m/s (Figures 38 and 39), the pattern width for the average of two sample measured spray patterns was increased 150 cm compared to the 25 cm increase in pattern width of the simulated spray pattern. The centroid of the simulated spray pattern was shifted about 40 cm more than the measured average of two sample spray patterns.

To study how well the simulation model predicts the amount of material deposited at any location along the swath width compared to the measured amount of material deposited at that location, a number of measured spray patterns were selected from experimental data. The simulation model was used to predict the spray patterns under the same conditions as these measured spray patterns and with the same number of replications for verification of the model.

Solie and Gerling (1984), showed that the fluorescence level is linearly proportional to the amount of spray material applied. If the simulation model accurately predicts the amount of material applied at any location, then the fluorescence at any location will be linearly correlated with the predicted values.

The comparisons were made by obtaining the coefficient of determination, R-Square, between the simulated and measured data. This statistical value was calculated to show how much of the variation in the measured spray pattern

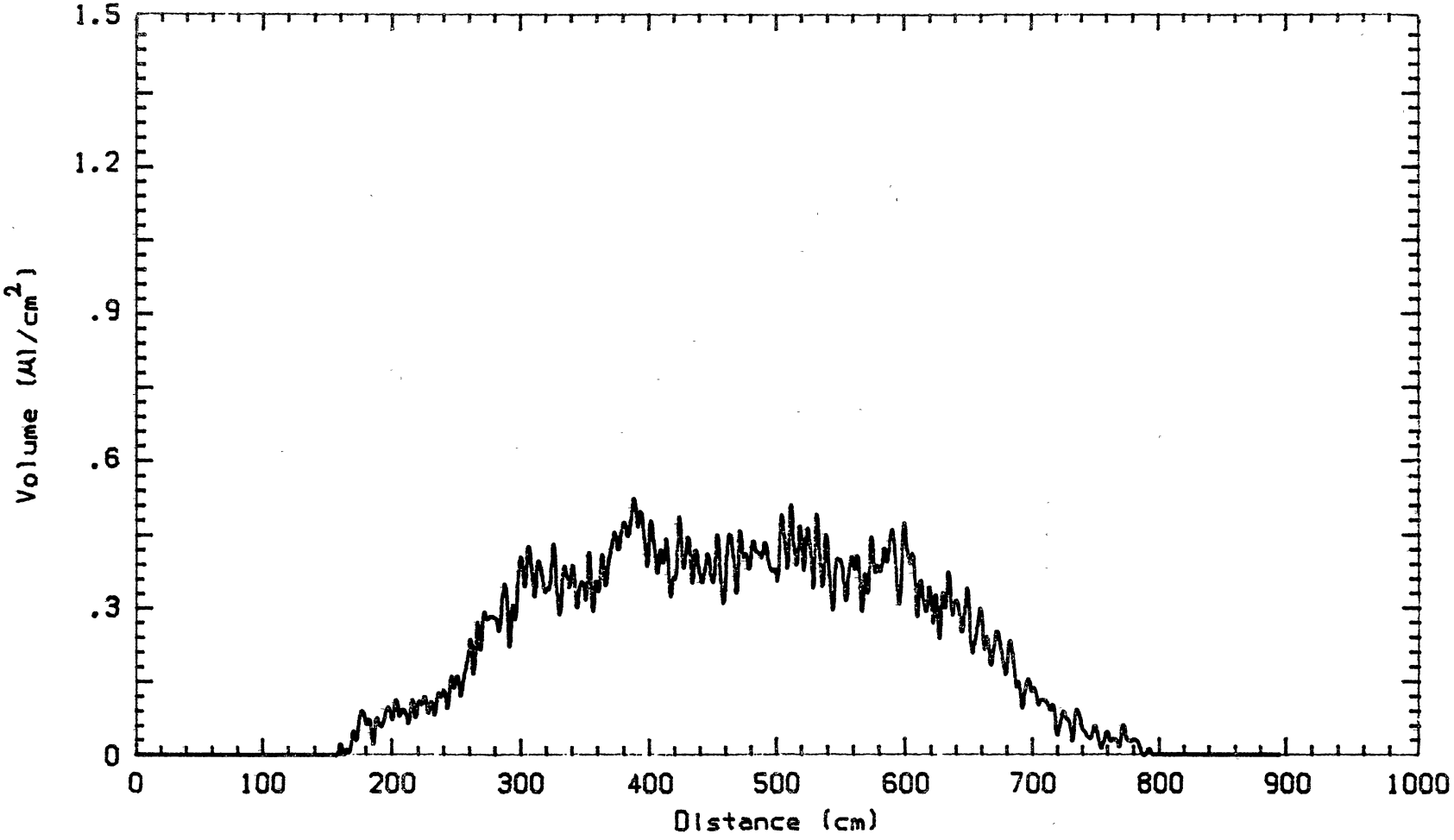

Figure 38. Simulated Pattern Distribution of 4 Girojet Nozzles Operated at 61 cm Height, 42 L/ha, 2.24 m/s, 1.32 m/s wind speed, and 2200 rpm at 9 Degrees Angle Rotation with centers located at 251, 355, 459, and 563 cm

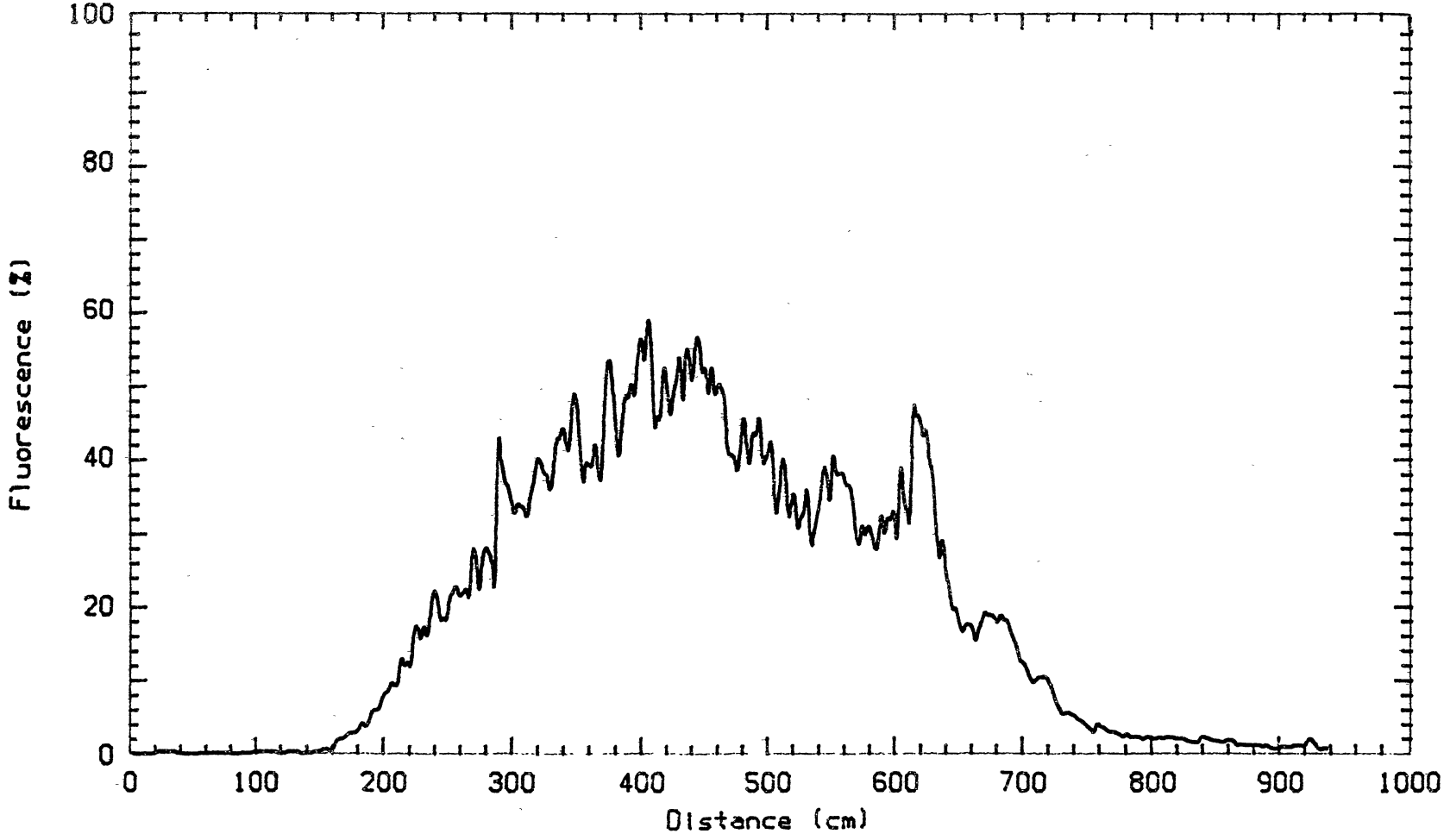

Figure 39. Measured Pattern Distribution of 4 Girojet Nozzles Operated at 61 cm Height, 42 L/ha, 2.24 m/s, 1.32 m/s wind speed, and 2200 rpm at 9 Degrees Angle Rotation with centers located at 244, 348, 452, and 556 cm

is explained by the model.

The coefficients of determination for a number of selected operating parameters are listed in Table IX. An examination of the R-Square values from Table IX show that for 46 cm nozzle height at a rotation angle of 0 degree, 89 percent of the variation of the measures fluorescence level deposited on the paper tape for the measured spray pattern was explained by the model.

When the unit was oriented 9 degrees counterclockwise, 93 percent of the variation in the measured pattern was explained by the model. When the measured spray pattern of 4 nozzles mounted on the boom with no wind was predicted by the model, 87 percent of the variation was explained by the simulated pattern.

With the cross wind of 1.48 m/s at 46 cm nozzle height, the R-Square was found to be 0.73 and at 61 cm nozzle height, an R-Square value of 0.70 was found (Table IX). The decrease of R-Square value under cross wind condition shows that the model does not explain all the variation in deposition of material across the swath width.

The discrepancy between the simulated and measured data can be explained partly by the assumptions made in simulating the boom nozzle spray patterns, that is, the effect of wind speed on the spray pattern was assumed to be the same on the upwind and downwind nozzles. The sprayer boom and body, variation in boom height during spraying, variation of flow rate and disk speed, accuracy of wind speed measurment,

TABLE IX

COEFFICIENT OF DETERMINATION FOR THE AVERAGE SIMULATED AND MEASURED SPRAY PATTERNS OF GIROJET NOZZLE

Location[1]	Nozzle Height (cm)	Wind Speed (m/s)	Angle of Rotation (Deg.)	Coefficient of Determination (R-Square)
Laboratory	46	0	0	0.89
Laboratory	46	0	9	0.93
Field	46	0	9	0.87
Field	46	1.48	9	0.73
Field	61	1.32	9	0.70

1) A single nozzle was used in the laboratory and 4 nozzle were used on the spray boom for the field tests. The tests were conducted at both locations with 2200 rpm, 0.50 L/min flow rate per nozzle.

and the assumption that the one-seventh power-law accurately predicts the boundary layer were the other factors that may cause a comparatively lower R-Square value for cross wind tests.

In general the simulated spray patterns correspond well with the measured spray pattern. In presence of wind, the simulated spray patterns were more affected by wind than the measured spray patterns. Results of the above study shows that the model has the potential of determining the effects of operating parameters and meteorological conditions on the spray pattern. Also, the model can be used to predict the results of some design changes on the spraying system.

CHAPTER V

SUMMARY AND CONCLUSIONS

The effects of operational parameters: nozzle height, disk speed, mounting angle, and flow rate on the spray distribution patterns of a vertical spinning disk nozzle (Girojet) were studied in the laboratory and the operational parameters were established.

A simulation model was developed based on the information obtained from the laboratory study. A series of spray patterns were generated by the model to study the effects of operational parameters and meteorological conditions. The experimental data obtained from the laboratory and field tests were used to verify the model under no wind and cross wind conditions.

Field tests were conducted to study the effects of operational parameters and meteorological conditions on the spray distribution patterns of a vertical spinning disk nozzle (Girojet), two horizontal spinning disk nozzles (Micromax and Rotojet), and a regular 8001 flat fan nozzle. The spray patterns of spinning disk nozzles were compared with the flat fan nozzle under cross wind conditions. The following were the conclusions of this study:

1. Girojet produced the most symmetrical spray pattern with an angle oriented 9 degrees counterclockwise in a plane

perpendicular to the direction of travel. An increase in nozzle height resulted in an increase of the pattern width but caused a decrease in pattern peak when the nozzle height was increased. The pattern width decreased as the disk speed was increased and the distribution of material near the center of nozzle tended to remain nearly constant above 3000 rpm. this level, had no effect on the pattern width, but the pattern peak was decreased. Pattern width increased as the flow rate was increased to 0.50 L/min. Beyond this level, the pattern peak tended to decrese.

2. The simulated spray patterns corresponed well with the measured spray pattern. In laboratory tests, the R-Square ranged as high as 0.93. In presence of wind, the centroid of the simulated spray patterns were shifted greater than the centroid of the measured spray patterns. The R-Square ranged 0.73 to 0.70 in the wind condition.

3. The effect of 46 cm nozzle height on the spray pattern uniformity of the spinning disk nozzles and the regular flat fan nozzle was not significant, but at 61 cm nozzle height, the Girojet produced the most uniform spray pattern and the Micromax produced the least uniform spray pattern at 15 degrees tilt angle. The centroid of spray patterns of the Girojet vertical spinning disk nozzle were not shifted significantly by wind compared to the flat fan nozzle, but a significant shift of the centroid of spray pattern was found in general for the two horizontal spinning disk nozzles compared with the flat fan nozzle.

CHAPER VI

SUGGESTION FOR FURTHER WORK

When a simulation model is developed to predict the spray pattern of a vertical spinning disk nozzle, all the parameters which may affect the spray pattern characteristics of the nozzle, must be considered in the model.

These parameters are sprayer body interfering the spray pattern under cross wind condition, vibration of spray boom, variation in the flow rate or disk speed. A valid and proven profile model must be used to accurately predict the boundary layer of wind. A good experimental technique must be selected to measure the meteorological data.

The Girojet nozzle with its vertical spinning disk reduced the effect of wind on the spray pattern compared with the horizontal spinning disk nozzles. But to be practical, a wear resistant accurate metering orifice must be designed, the sump must be redesigned to prevent material from splashing out, and a control system must be design to accurately control the disk speed.

REFERENCES CITED

Barker, G. L. 1977. Deposition of evaporating spray droplets on a three dimensional body with rectangular boundaries. Ph.D. Dissertation. Mississippi State University. 213 p.

Barker, G. L., J. F. Thompson, Jr., and E. D. Threadgill. 1978. Spray droplet deposition on a three dimensional object. Transactions of the ASAE 21(5):806-812.

Bode, L. E., B. J. Butler, S. L. Pearson, and L. F. Bouse. 1982. Characteristics and Operating Parameters of CDA Applicators. ASAE Paper No. 82-1002. American Society of Agricultural Engineers. St. Joseph, MI 49085.

Carlton, J. B. and L. F. Bouse. 1981. Characterizing spray deposit on film by light transmission. Transactions of the ASAE 24(2):277-280.

Giles, R. 1962. Fluid mechanics and hydraulics. Schaum Publishing Co. New York, NY 274 p.

Goering, C. E., L. E. Bode, and M. R. Gebhardt. 1972. Mathematical modeling of spray droplet deceleration and evaporation. Transactions of the ASAE 15(1):220-225.

Goering, C. E. and B. J. Butler. 1975. Paired field studies of herbicide drift. Transactions of the ASAE 18(1):27-34.

Goering, C. E., L. N. Shukla and D. B. Weathers. 1969. Is the analog computer obsolete? Agricultural Engineering 50(3):142-143.

Goering, C. E. and D. B. Smith. 1978. Equation for droplet size distribution in sprays. Transactions of the ASAE 21(2):209-216.

Hughes, R. R. and E. R. Gilliland. 1952. The mechanics of drops. Chemical Engineering Progress 48(10):497-504.

Marchant, J. A. 1977. Calculation of spray droplet trajectory in a moving airstream. J. of Agric. Engnr. Res. Vol. 22:93-96.

Marshall, W. R., Jr. 1954. Atomization and spray drying. Chemical Engineering Progress Monograph Series No. 2,

Vol. 50. American Institute of Chemical Engineers, New York.

Micromax Installation and Operating Manual. Micron Corporation. Houston, TX 77023.

Miles, G. E. 1972. Deposition of ULV size spray droplets of two-dimensional rectangular bodies. MS Thesis, Mississippi State University.

Roth, L. O. and J. G. Porterfield. 1965. A photographic spray-sampling apparatus and technique. Transactions of the ASAE 8(4):493-496.

Rotojet Owners Information Manual. 900 Rotojet direct drive rotary atomizer. Spraying System Co. Wheaton, Ill 60188.

Sabersky, R. H. and A. J. Acosta. 1964. Fluid flow, The Macmillan Co. New York, NY 254 p.

Sjenitzer, F. 1962. The evaporation of a liquid spray into a stream of gas. Chemical Engineering Science. 17: 309- 322.

Smith, R. M. 1970. Analog simulation of in-flight evaporation of spray droplets. Transactions of the ASAE 13(5):587-590, 593.

Smith, D. B., F. D. Harris, and C. E. Goering. 1982. Variables affecting drift from boom sprayers. Transactions of the ASAE 25(6):1499-1503.

Solie, J. B. and J. F. Gerling. 1984. A spray pattern analysis system for ground application. ASAE Paper No. 84-1002. American Society of Agricultural Engineers. St. Joseph, MI 49085.

Tecnoma Girojet Mounting Instructions-Operating Manual. Wilbur-Ellis Co. Fresno, CA 93706.

Teejet Agricultural Spray Nozzle and Accessories. Catalog No. 37. Spraying System Co. Wheaton, Ill 60187.

USDA, 1984. Inputs outlook and Situation Report. United States Department of Agriculture Publication. IOS-6.

Williamson, R. E. 1972. A simulation for the dynamics of evaporating spray droplets in agricultural spraying. Ph.D. Dissertation. Mississippi State University. 88p.

Williamson, R. E. and E. D. Threadgill. 1974. A simulation for the dynamics of evaporating spray droplets in agricultural spraying. Transactions of the ASAE

17(1):254-261.

Yates, W. E. and N. B. Akesson. 1963. Fluorescent tracers for quantitative microresidue analysis. Transactions of the ASAE 6(2):104-107,114.

APPENDIX A

LIST OF COMPUTER PROGRAM

List of Variables

RPM	=	Disk speed
BXZ, BYZ	=	Components angle in xz and yz planes
VTX	=	Sprayer speed
G	=	Gravitational acceleration
R	=	Disk radius
VAY0	=	Wind speed measured at the center of nozzle in y direction
MV	=	Molecular weight of diffusing vapor
MM	=	Mean Molecular weight of gas mixture in transfer path
DV	=	The diffusivity of water vapor in air
DA	=	Density of air
DL	=	Density of droplet
KVA	=	Kinematic viscosity of air
DP	=	Vapor pressure difference
PF	=	Partial pressure of air
APP	=	Application rate
HW	=	Height in which the wind speed was measured
D	=	Droplet diameter
VTT	=	Cumulative volume before evaporation
F	=	Ejection angle
VP	=	Initial velocity of droplet
VR	=	Relative velocity of droplet
VRX, VRY, VRZ	=	Components of relative velocity of droplet
VAY	=	Calculated wind speed at the droplet height
RE	=	Reynolds Number
SC	=	Schmidt Number
CD	=	Drag coefficient
AX, AY, AZ	=	Components of Droplet acceleration
VX, VY, VZ	=	Components of droplet velocity
X, Y, Z	=	Components of droplet trajectory
DD	=	Rate of change of droplet diameter
HC	=	New calculated droplet height
VPX, VPY, VPZ	=	Components of initial droplet velocity
DIST	=	Calculated droplet trajectory in y direction at the origin
CY	=	Calculated droplet trajectory from the reference point
Q	=	Calculated droplet volume after evaporation
VOLT	=	Acumulated droplet volume after evaporation
T	=	Total time
H	=	Step size time
N	=	Random generator number

COMPUTER PROGRAM

```
1000 REM ************************************************
1010 REM * The 3-Dimentional Simulation Program in BASIC *
1020 REM * for an IBM-PC Computer. The Program Generates *
1030 REM * the Spray Distribution Pattern of a Vertical  *
1040 REM *      Spinning Disk Nnzzle (Girojet)           *
1050 REM ********** INITIAL VALUES **********
1060 REM Disk Radius: R
1070 REM Constant PI Value: PIE
1080 REM Sprayer Speed: VTX
1090 REM Kinematic Viscocity of Air: KVA
1100 REM Disk Speed : RPM = 2200
1110 REM Wind Speed at the Center of Nozzle: VAY0
1120 REM Molecular Weight of Diffusing Vapor: MV
1130 REM Mean Molecular Weight of Gas Mixture
1140 REM in the Transfer Path: MM
1150 REM Diffusivity of Water Vapor in air: DV
1160 REM Density of Air: DA
1170 REM Density of Droplet: DL
1180 REM Vapor Pressure Difference: DP
1190 REM Partial Pressure of Air: PF
1200 REM Application Rate: APP
1210 REM Wind Speed Measurement Height: HW
1220 REM Droplet Diameter: D
1230 REM Acumulated Droplet Volume After Evaporation: VOLT
1240 REM Random Generator Number: N
1250 REM Cumulative Volume Before Evaporation: VTT
1260 REM Ejection Angle: F
1270 ERM New Calculated Droplet Height: HC
1280 REM Components of Droplet Acceleration: AX, AY, AZ
1290 REM Components of Droplet Velocity: VX, VY, VZ
1300 REM Components of Droplet Trajectory: X, Y, Z
1310 REM Components of Relative Velocity: VRX, VRY, VRZ
1320 REM Initial Velocity of Droplet:VP
1330 REM Relative Velocity of Droplet
1340 REM Reynolds Number: RE
1350 REM Schmidt Number: SC
1360 REM Evaporated Droplet Diameter: DD
1370 REM Calculated Droplet Volume After Evaporation: Q
1380 REM Total Time:T , Step Size Time: H
1390      R=0.0706:PIE=3.1416:VTX=2.235:KVA=1.5E-04
1400      RPM=2200:VAY0=1.48:MV=18:MM=29:DV=0.2377E-04
1410      DA=1.145:DL=1000:DP/PA=0.0038:APP=0.1094:HW=1.0
1420      DIM VX(500),X(500),VY(500),Y(500),VZ(500),Z(500)
          D(500),VOLT(500)
1430      OPEN "B:D100" FOR OUTPUT AS #1
1440      FOR J=1 TO 5000
1450 REM ********** DROPLET SIZE **********
1460      N=RND*(100-8.5)+8.5
1470      D=FIX(173-3.59*N-.072*(N^2))/10^4
1480      VTT=VTT+0.5236*(D^3)
1480      IF VTT>APP THEN 1970:D=D/100
1500 REM ********** EJECTION ANGLE **********
1510      F=RND*(2.79-.35)+.35:BYZ=F
1520 REM ********** VELOCITY COMPONENTS **********
1530      VP=(2*PIE*R/60)*RPM
1540      VZ=VP*SIN(BYZ):VY=VP*COS(BYZ)+VAY:VX=VTX
1550      VRY=VP*COS(BYZ)-VAY:VRZ=VZ:VRX=VX
1560      VR=(VRX^2+VRY^2+VRZ^2)^.5
1570      FOR I=30 TO 1000
1580      D(0)=D:VAY:VAY0
1590      RE=D*VR/KVA:SC=DV/KVA
1600 REM ********** EVAPORATION OF DROPLET **********
1610      DEF FNDE(D)=-2*(MV/MM)*(DV/D)*(DA/DL)*(DP/PF)*(2+
                  0.6*SC^(1/3)+RE^(0.5))
1620      KD1=FNDE(D(I))
1630      KD2=FNDE(D(I)+.5*KD1)
1640      KD3=FNDE(D(I)+.5*KD2)
1650      KD4=FNDE(D(I)+KD3)
1660      D(I+1)=D(I)+(H/6)*(KD1+2*KD2+2*KD3+KD4)
1670      DD=D(I+1)
1680      D=D(I)
```

```
1690      RE=DD*VR/KVA
1700 REM ************* DRAG COEFFICIENT ******************
1710      IF RE<=.5 THEN CD=24/RE
1720      IF RE>.5 AND RE<=150 THEN CD=0.49+26.38*RE^(-.845)
1730      IF RE>150 AND RE<=1000 THEN CD=7.86*RE^(-.44)
1740 REM ***************** X-TRAJECTORY ********************
1750      VX(I)=VX
1760      X(0)=0
1770      AX=-(0.75*CD*D*DA*VR*VRX)/(DL*D)-3*VRX*DD/D
1780      DEF FNAE(VX)=AX
1790      KX1=H*FNAE(VX(I))
1800      KX2=H*FNAE(VX(I)+KX1/2)
1810      KX3=H*FNAE(VX(I)+KX2/2)
1820      KX4=H*FNAE(VX(I)+KX3)
1830      VX(I+1)=VX(I)+H*(VX(I)+(KX1+2*KX2+2*KX3+KX4)/6
1840      X(I+1)=X(I)+H*(VX(I)+(KX1+KX2+KX3)/6)
1850 REM *************** Y-TRAJECTORY *********************
1860      VY(I)=VY
1870      Y(0)=0
1880      AY=-(0.75*CD*D*DA*VR*VRY)/(DL*D)-3*VRY*DD/D
1890      DEF FNBE(VY)=AY
1900      KY1=H*FNBE(VY(I))
1910      KY2=H*FNBE(VY(I)+KY1/2)
1920      KY3=H*FNBE(VY(I)+KX2/2)
1930      KY4=H*FNBE(VY(I)+KX3)
1940      VY(I+1)=VY(I)+(KY1+2*KY2+2*KY3+KY4)/6
1950      Y(I+1)=Y(I)+H*(VY(I)+(KY1+KY2=KY3)/6)
1960 REM ************** Z-TRAJECTORY **********************
1970      VZ(I)=VZ
1980      Z(0)=0
1990      AZ=G-(0.75*CD*D*DA*VR*VRZ)/(DL*D)-3*VRZ*DD/D
2000      DEF FNCE(VZ)=AZ
2010      KZ1=H*FNCE(VZ(I))
2020      KZ2=H*FNCE(VZ(I)+KZ1/2)
2030      KZ3=H*FNCE(VZ(I)+KZ2/2)
2040      KZ4=H*FNCE(VZ(I)+KZ3)
2050      VZ(I+1)=VZ(I)+(KZ1+2*KZ2+2*KZ3+KZ4)/6
2060      Z(I+1)=Z(I)+H*(VZ(I)+(KZ1+KZ2=KZ3)/6)
2070 REM ************* NEW VELOCITY COMPONENTS *************
2080      T=T+H
2090      HC=.5278-.0706*COS(F)
2100      IF Y(I+1)>=HC THEN 1
2110      VAY=VAY0*((HC-Z(I+1))/HW)^(1/7)
2120      VPX=VX(I+1):VX=VPX
2130      VPY=VY(I+1)+VAY:VY=VPY
2140      VPZ=VZ(I+1):VZ=VPZ
2150      BYZ=ATN(VZ/VY)):BXZ=ATN(VZ/VX)
2160      VRX=VPX:VRY=VPY-VAY:VRZ=VPZ
2170      VR=(VRX^2+VRY^2+VRZ^2)^.5
2180      D=DD
2190      IF I<15 THEN H=.005
2200      IF I>15 THEN H=.008
2210      IF I>40 THEN H=.010
2220      NEXT I
2230 REM ******** PATTERN WIDTH AND VOLUME APPLIED ********
2240      DIST=Y(I+1)+.0706-.0706*SIN(F)
2250      LY=INT(40*DIST)+200
2260      Q=15499*((PIE/6)*D^3):VOLT(LY)=VOLT(LY)+Q
2270      D=D*10^6
2280      PRINT J,D,VTT
2290      VP=(2*PIE*R/60)*RPM:T=0:H=0
2300      NEXT J
2310      FOR LY=1 TO 400
2320      CY=LY/0.4+0.0706
2330      WRITE #1,CY,VOLT(LY)
2340      NEXT LY
2350      CLOSE #1
2360      END
```

APPENDIX B

AVERAGE OF FIVE SPRAY PATTERN PROFILES OF A SINGLE GIROJET NOZZLE TESTED ON SPRAY CARRIAGE

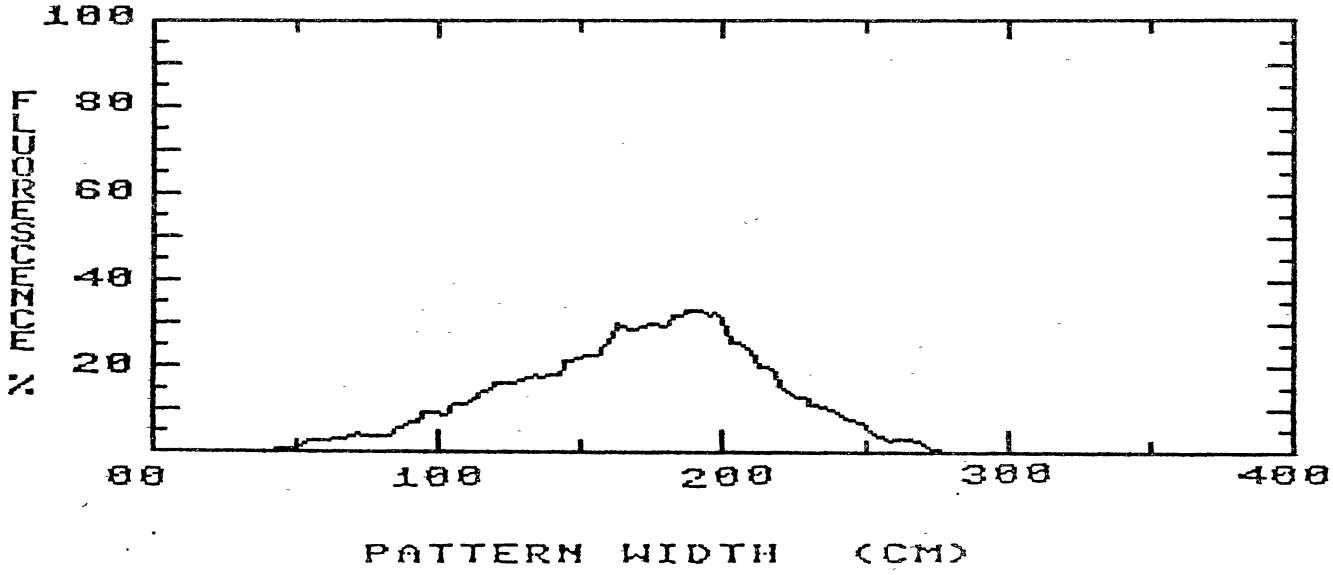

Figure 40. Average Pattern Distribution of Girojet Nozzle Operated at 46 cm Height, 0.50 L/min, 1.34 m/s, and 2200 rpm at 0 Degrees Angle Rotation with center located at 195.5 cm

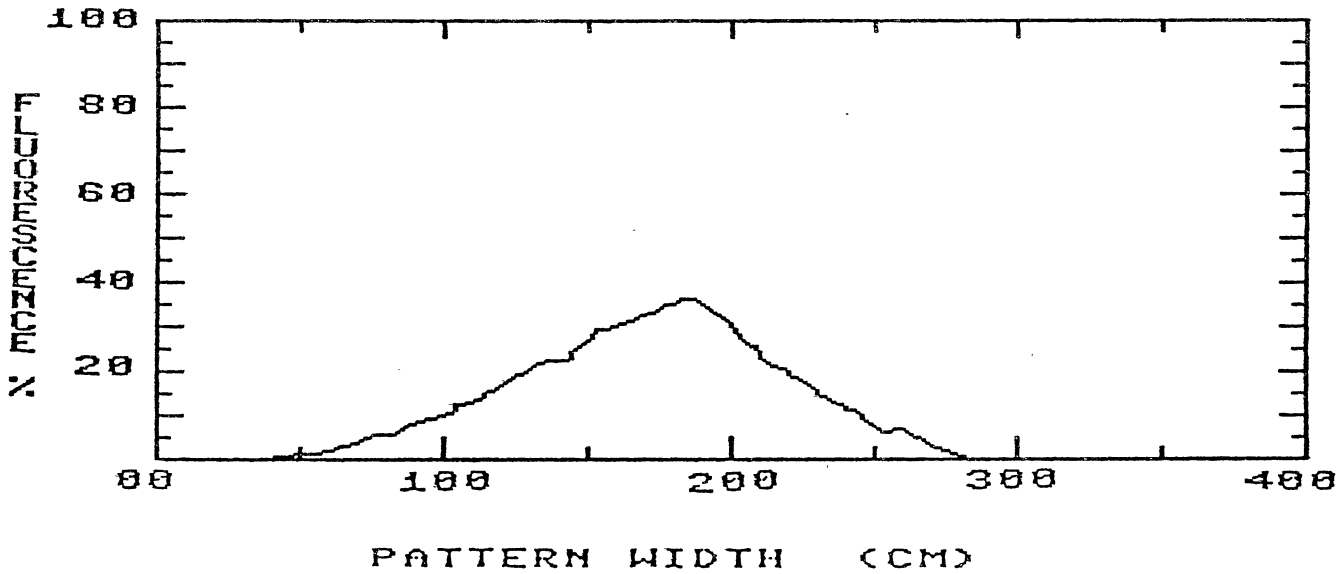

Figure 41. Average Pattern Distribution of Girojet Nozzle Operated at 46 cm Height, 0.50 L/min, 1.34 m/s, and 2200 rpm at 3 Degrees Angle Rotation with center located at 160 cm

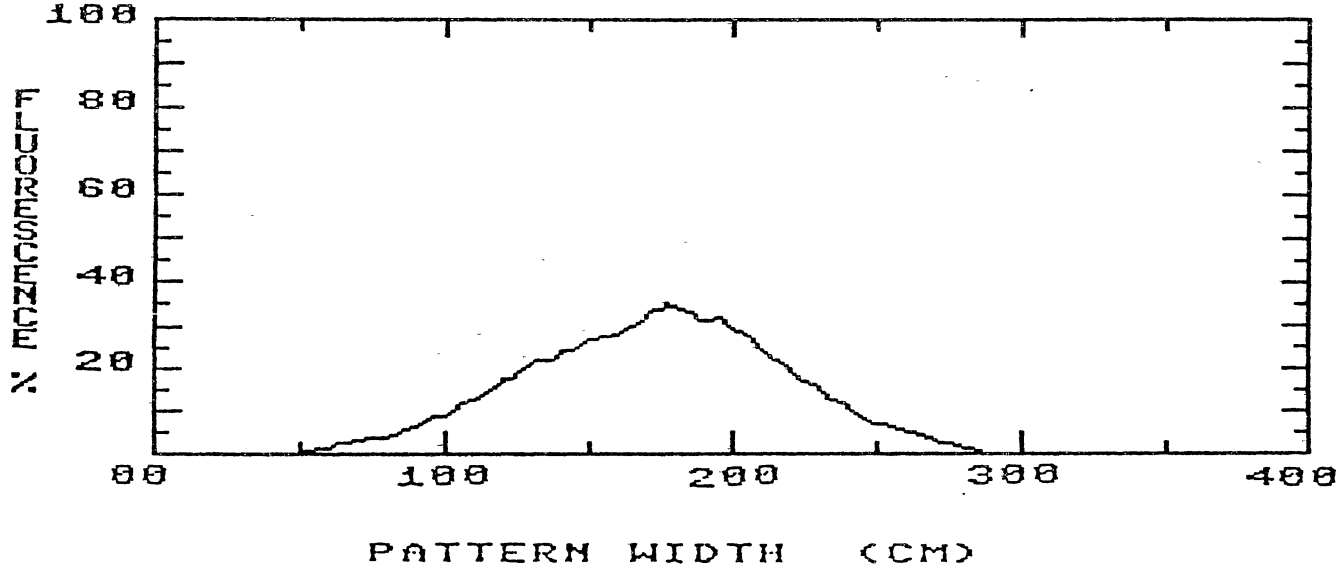

Figure 42. Average Pattern Distribution of Girojet Nozzle Operated at 46 cm Height, 0.50 L/min, 1.34 m/s, and 2200 rpm at 6 Degrees Angle Rotation with center located at 160 cm

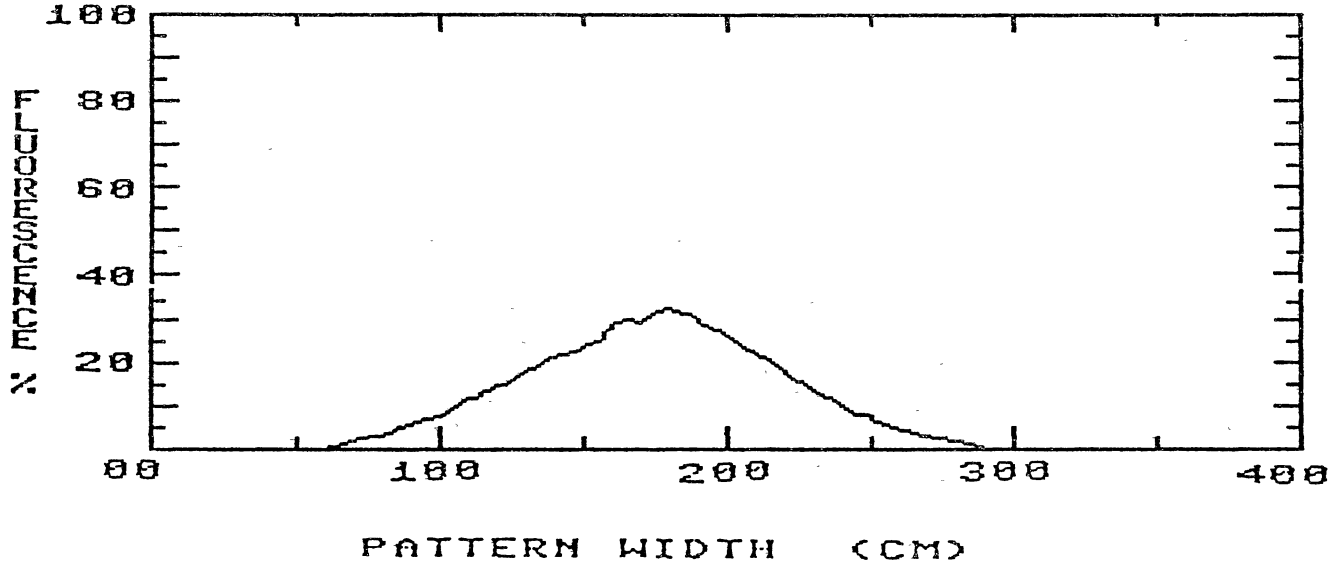

Figure 43. Average Pattern Distribution of Girojet Nozzle Operated at 46 cm Height, 0.50 L/min, 1.34 m/s, and 2200 rpm at 9 Degrees Angle Rotation with center located at 160 cm

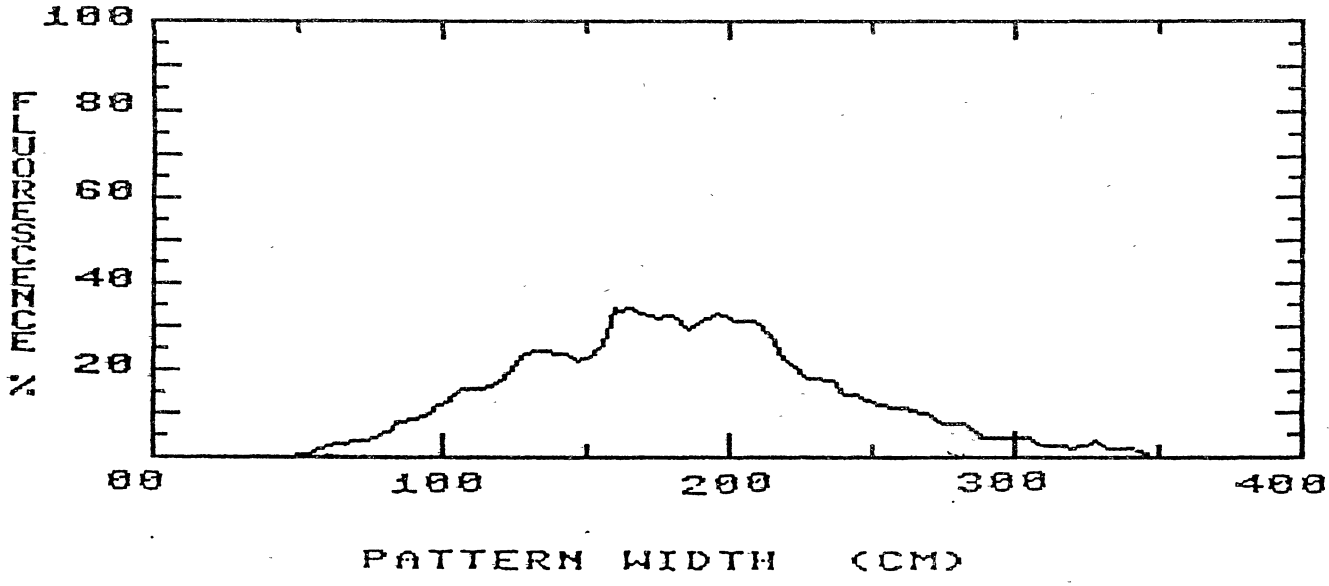

Figure 44. Average Pattern Distribution of Girojet Nozzle Operated at 46 cm Height, 0.50 L/min, 1.34 m/s, and 2200 rpm at 12 Degrees Angle Rotation with center located at 160 cm

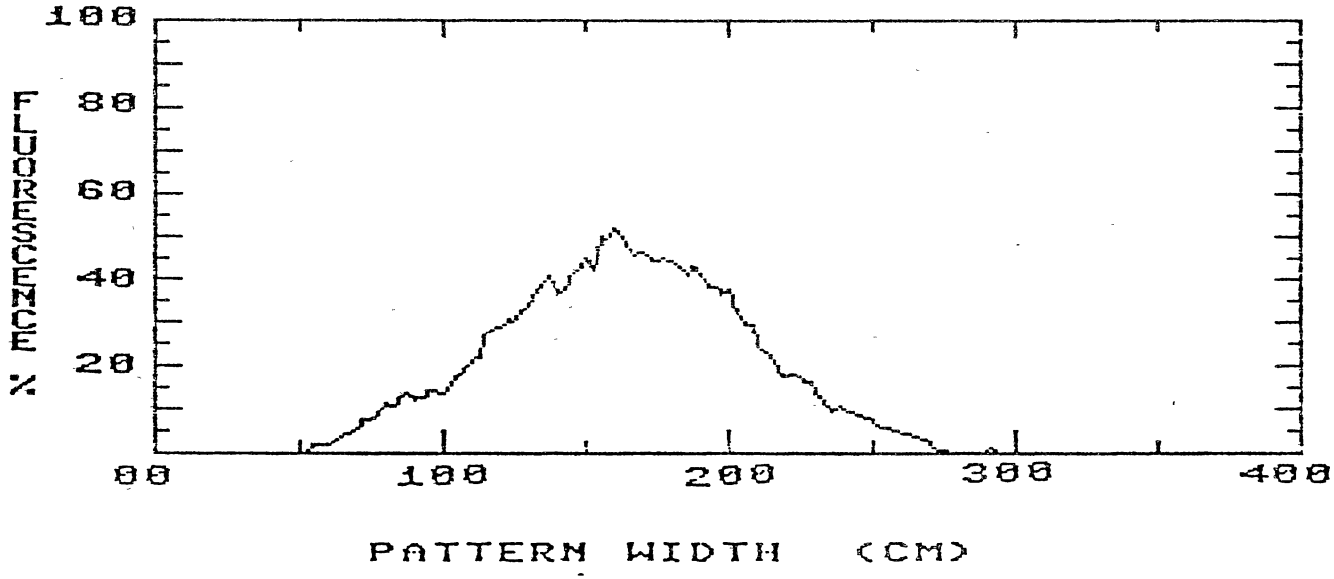

Figure 45. Average Pattern Distribution of Girojet Nozzle at 51 cm Height, 0.50 L/min, 1.34 m/s, and 2200 rpm at 9 Degrees Angle Rotation with center located at 160 cm (Pattern Peak=52 % and Pattern Width=225 cm)

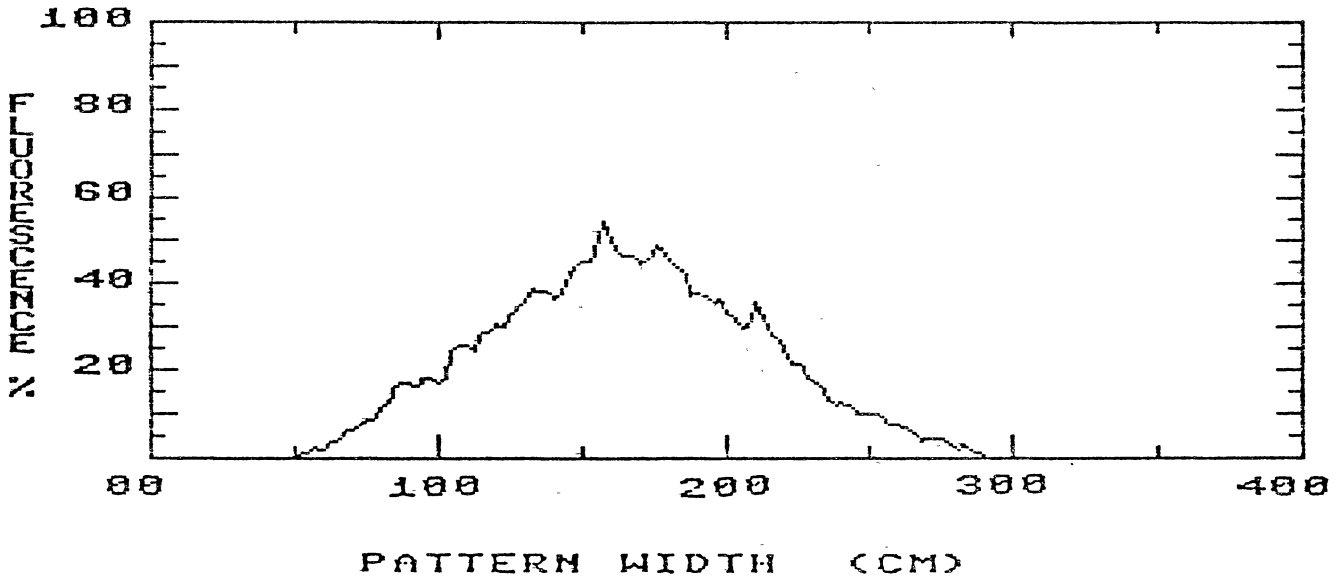

Figure 46. Average Pattern Distribution of Girojet Nozzle at 56 cm Height, 0.50 L/min, 1.34 m/s, and 2200 rpm at 9 Degrees Angle Rotation with center located at 160 cm (Pattern Peak=45.% and Pattern Width=240 cm)

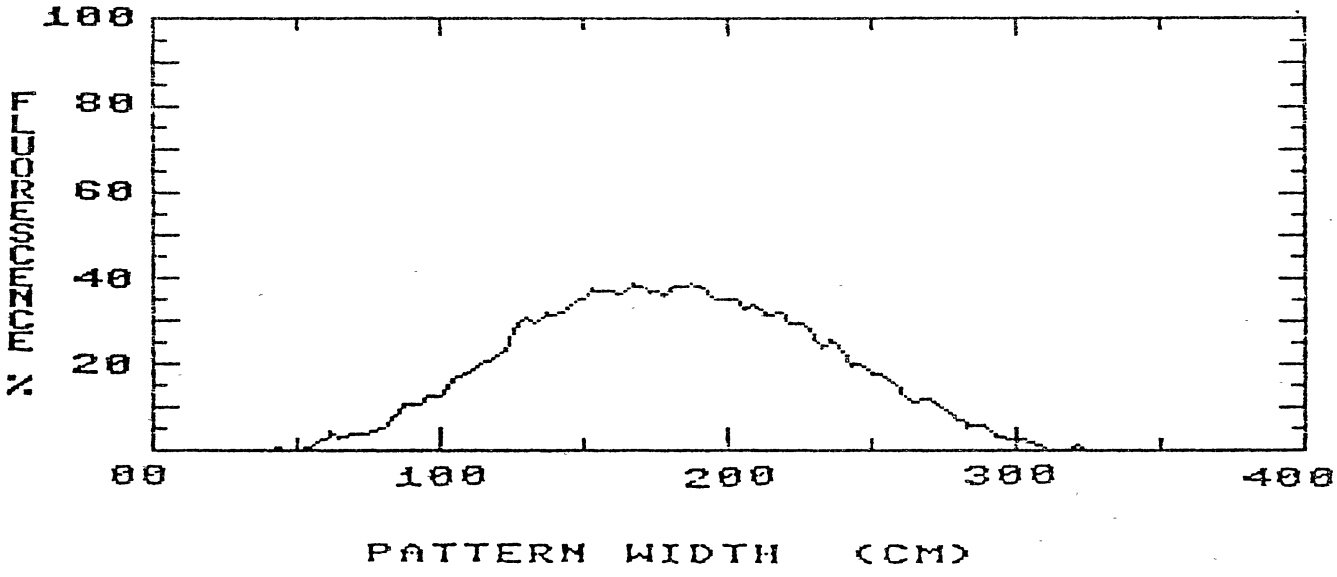

Figure 47. Average Pattern Distribution of Girojet Nozzle at 66 cm Height, 0.50 L/min, 1.34 m/s, and 2200 rpm at 9 Degrees Angle Rotation with center located at 160 cm (Pattern Peak=38 % and Pattern Width=280 cm)

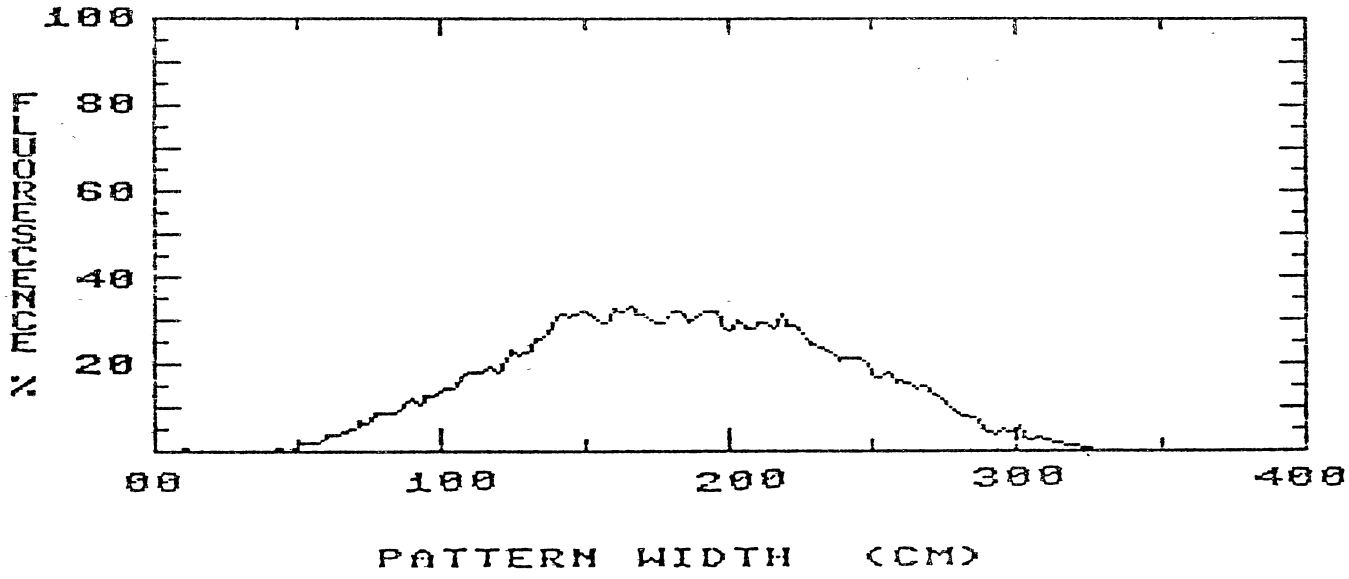

Figure 48. Average Pattern Distribution of Girojet Nozzle at 71 cm Height, 0.50 L/min, 1.34 m/s, and 2200 rpm at 9 Degrees Angle Rotation with center located at 160 cm (Pattern Peak=30 % and Pattern Width=280 cm)

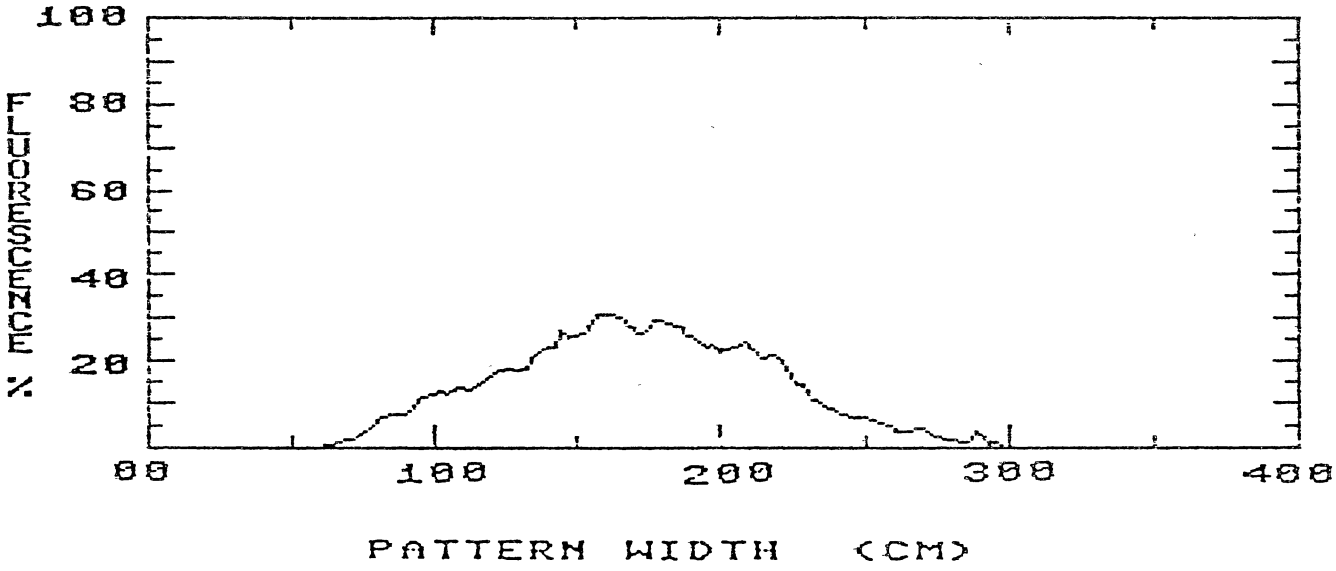

Figure 49. Average Pattern Distribution of Girojet Nozzle at 46 cm Height, 0.50 L/min, 1.34 m/s, and 1400 rpm at 9 Degrees Angle Rotation with center located at 160 cm (Pattern Peak=28 % and Pattern Width=240 cm)

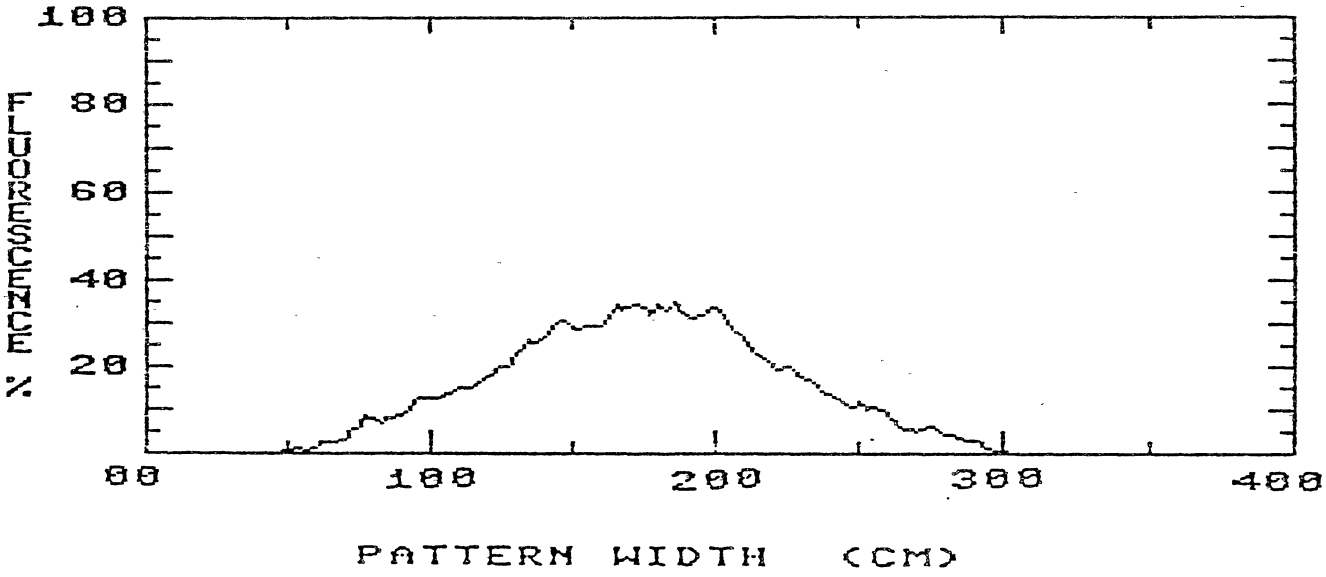

Figure 50. Average Pattern Distribution of Girojet Nozzle at 46 cm Height, 0.50 L/min, 1.34 m/s, and 1600 rpm at 9 Degrees Angle Rotation with center located at 160 cm (Pattern Peak=34 % and Pattern Width=250 cm)

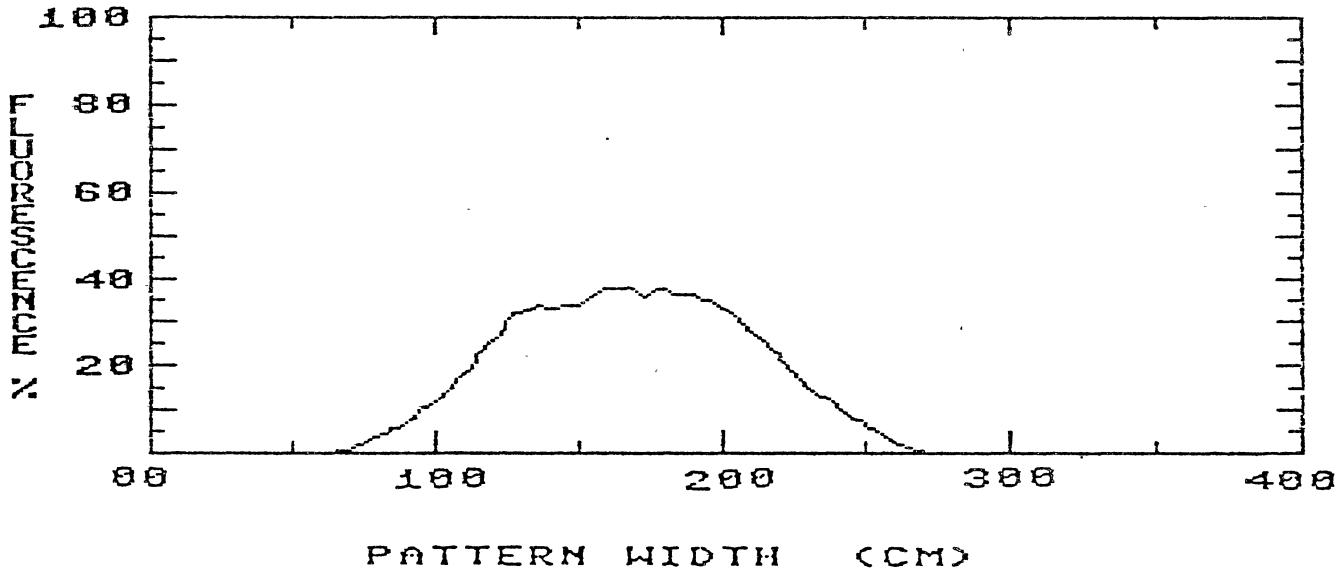

Figure 51. Average Pattern Distribution of Girojet Nozzle at 46 cm Height, 0.50 L/min, 1.34 m/s, and 3250 rpm at 12 Degrees Angle Rotation with center located at 160 cm (Pattern Peak=38 % and Pattern Width=200 cm)

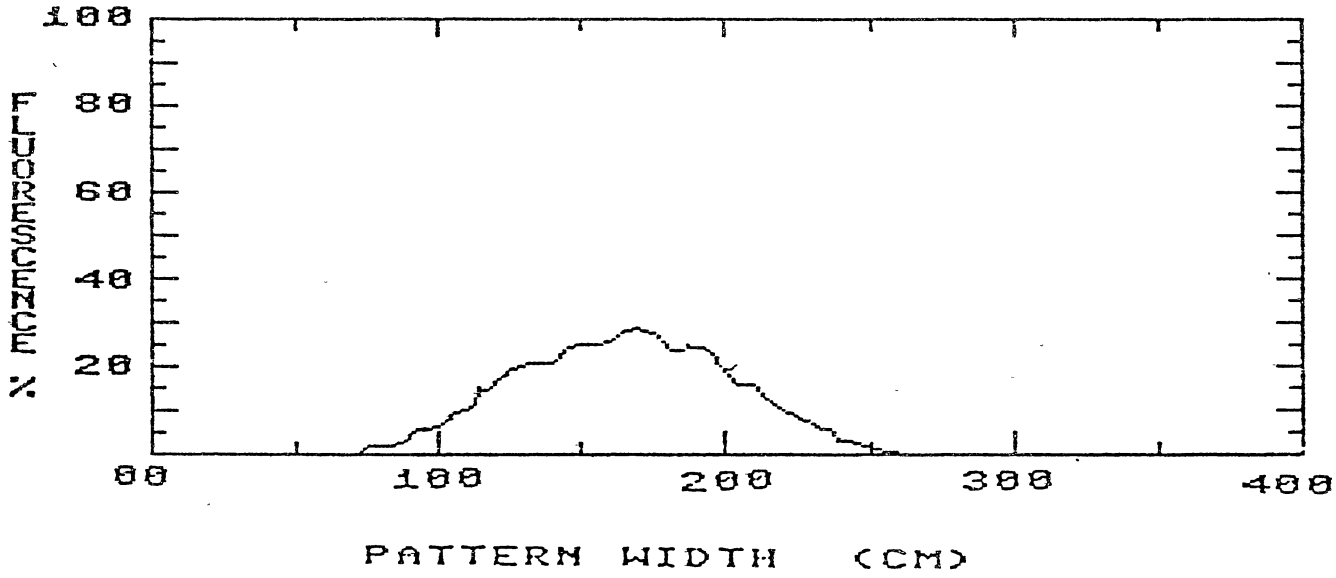

Figure 52. Average Pattern Distribution of Girojet Nozzle at 46 cm Height, 0.30 L/min, 1.34 m/s, and 2200 rpm at 9 Degrees Angle Rotation with center located at 160 cm (Pattern Peak=30 % and Pattern Width=180 cm)

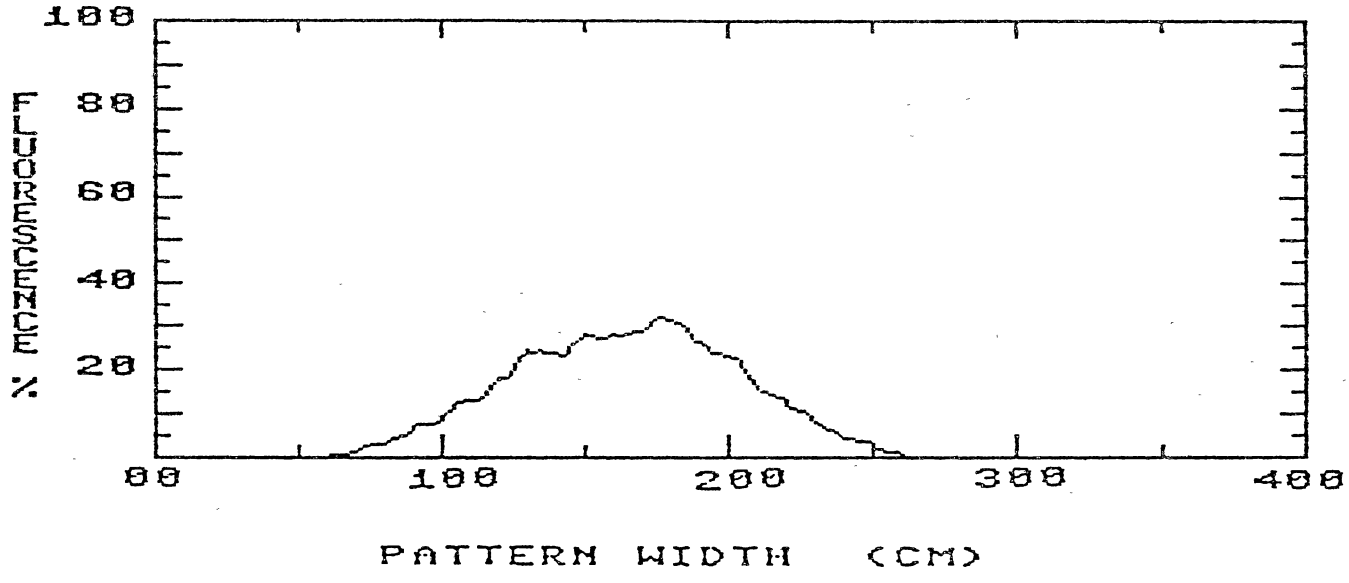

Figure 53. Average Pattern Distribution of Girojet Nozzle at 46 cm Height, 0.35 L/min, 1.34 m/s, and 2200 rpm at 9 Degrees Angle Rotation with center located at 160 cm (Pattern Peak=33 % and Pattern Width=190 cm)

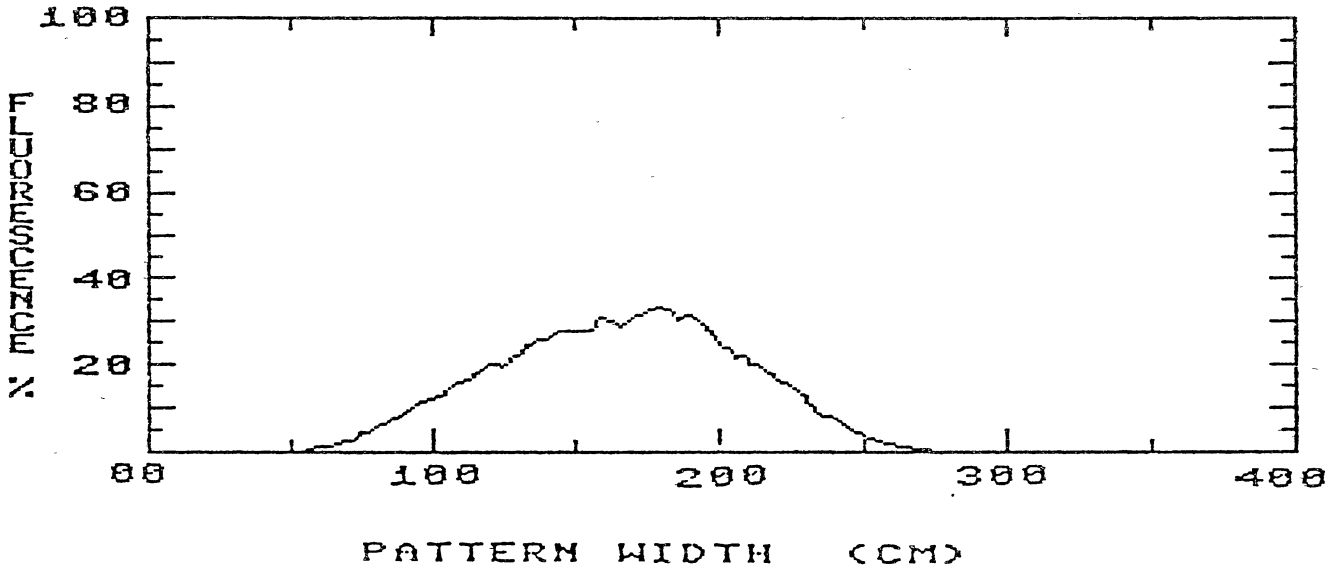

Figure 54. Average Pattern Distribution of Girojet Nozzle at 46 cm Height, 0.40 L/min, 1.34 m/s, and 2200 rpm at 9 Degrees Angle Rotation with center located at 160 cm (Pattern Peak=35 % and Pattern Width=200 cm)

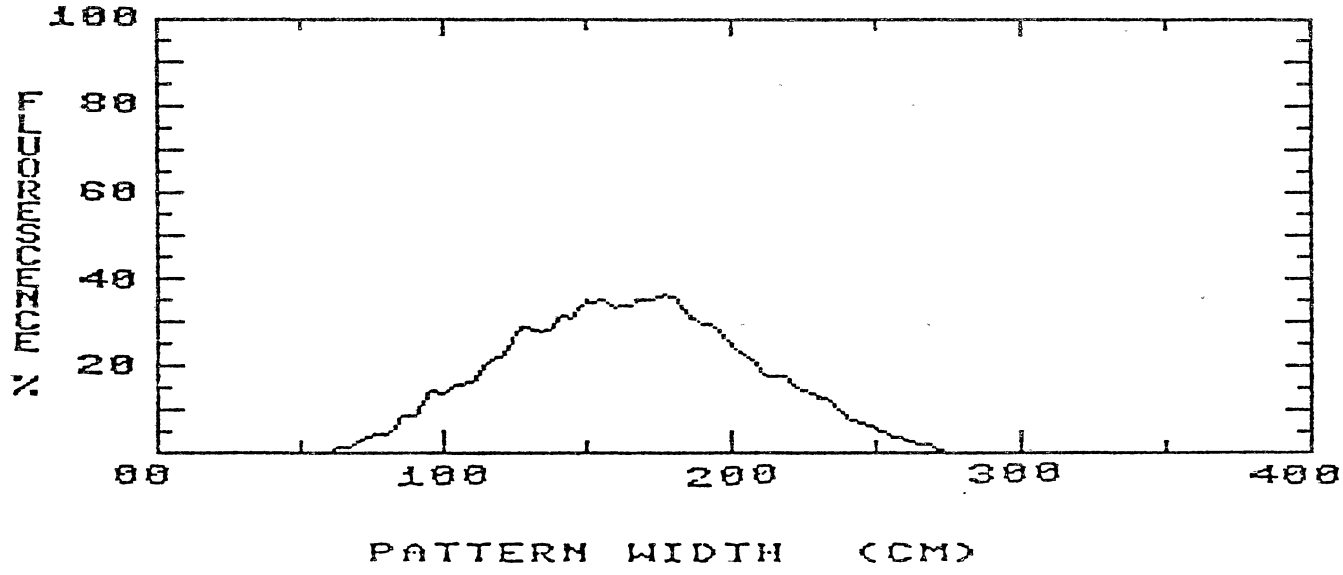

Figure 55. Average Pattern Distribution of Girojet Nozzle at 46 cm Height, 0.45 L/min, 1.34 m/s, and 2200 rpm at 9 Degrees Angle Rotation with center located at 160 cm (Pattern Peak=38 % and Pattern Width=220 cm)

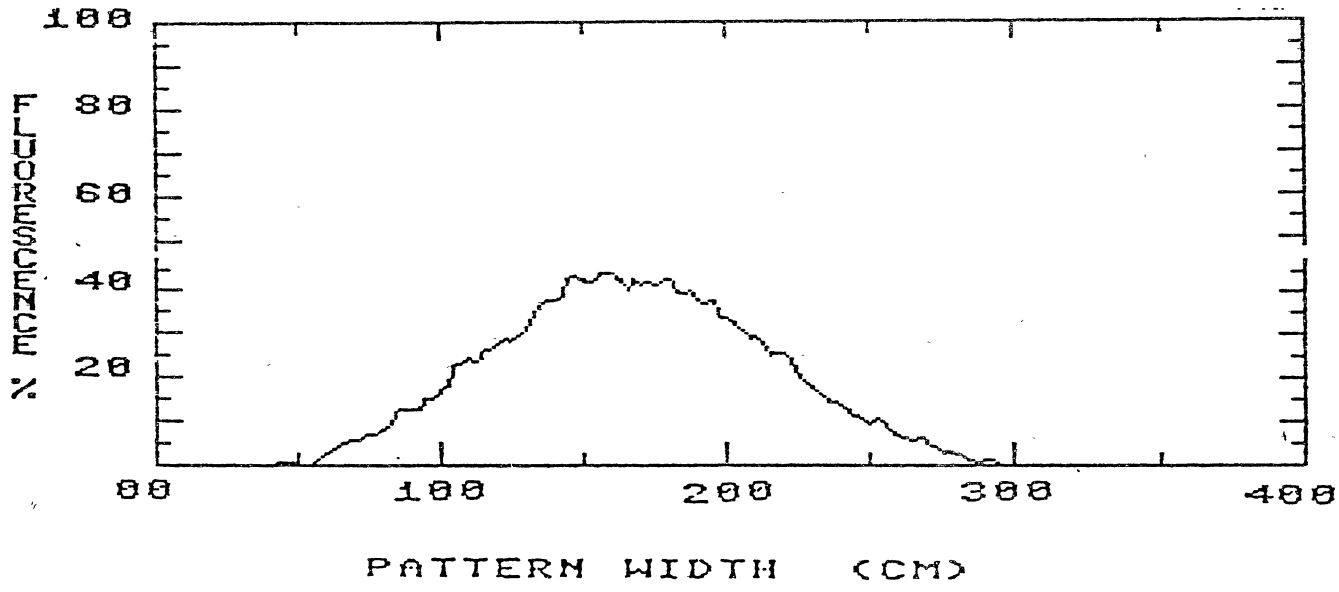

Figure 56. Average Pattern Distribution of Girojet Nozzle at 46 cm Height, 0.55 L/min, 1.34 m/s, and 2200 rpm at 9 Degrees Angle Rotation with center located at 160 cm (Pattern Peak=45 % and Pattern Width=240 cm)

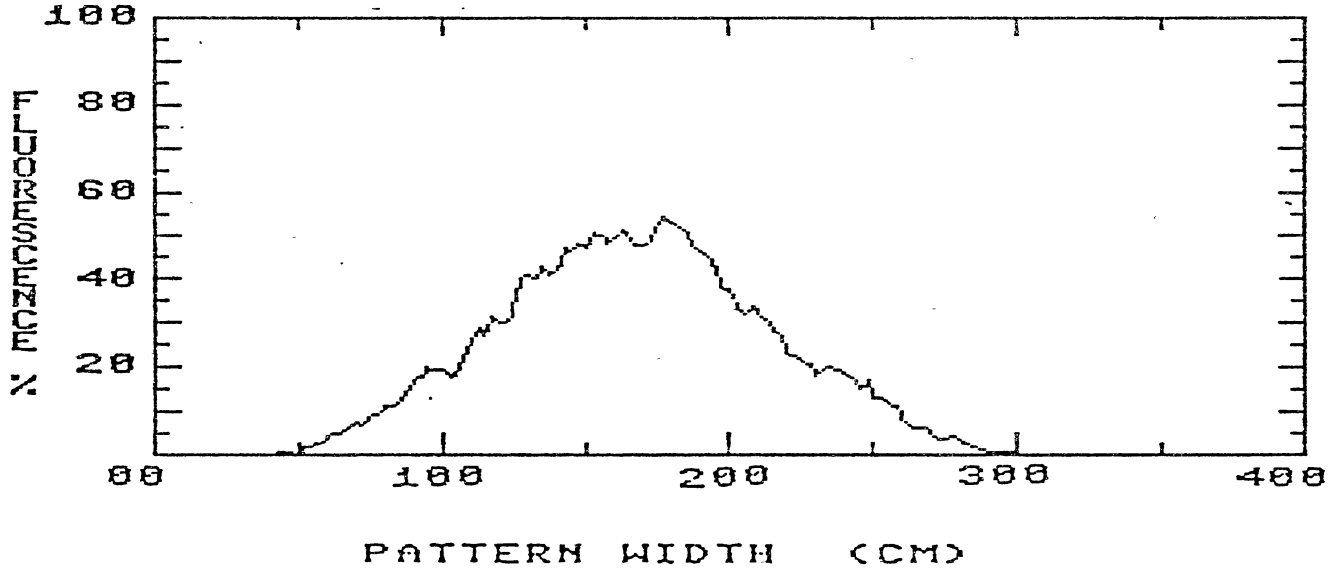

Figure 57. Average Pattern Distribution of Girojet Nozzle at 46 cm Height, 0.60 L/min, 1.34 m/s, and 2200 rpm at 9 Degrees Angle Rotation with center located at 160 cm (Pattern Peak=54 % and Pattern Width=240 cm)

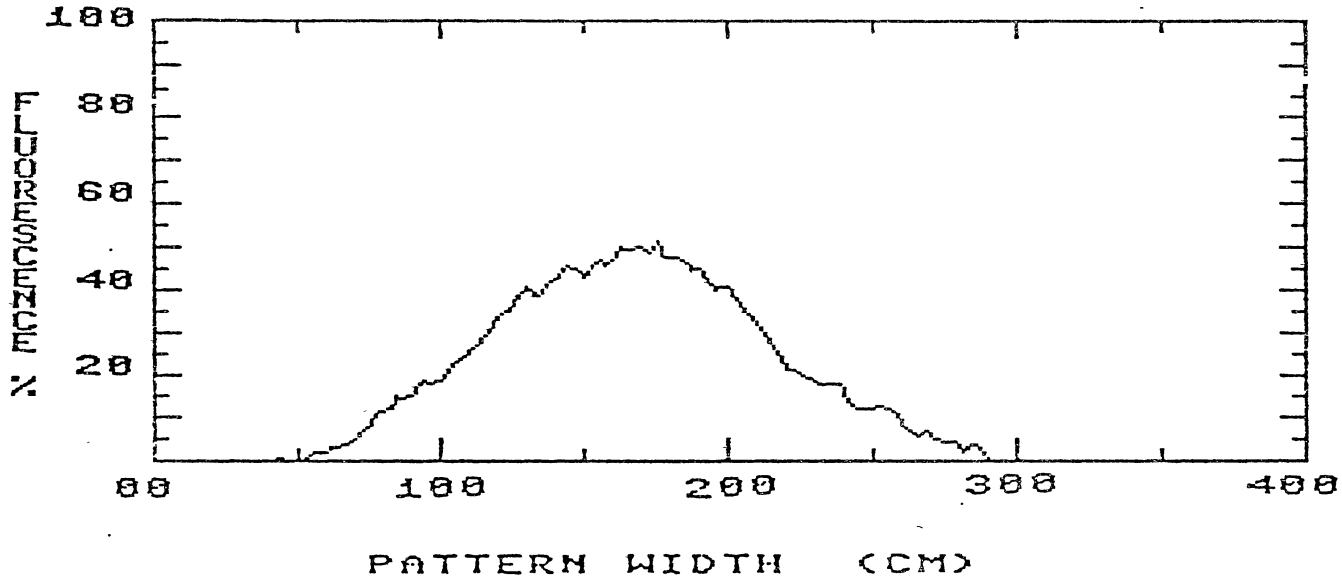

Figure 58. Average Pattern Distribution of Girojet Nozzle at 46 cm Height, 0.65 L/min, 1.34 m/s, and 2200 rpm at 9 Degrees Angle Rotation with center located at 160 cm (Pattern Peak=50 % and Pattern Width=240 cm)

APPENDIX C

AVERAGE OF TWO SAMPLES SPRAY PATTERN DATA FOR ALL NOZZLES TESTED ON SPRAYER BOOM WITH NO CROSS WIND

AVERAGE OF TWO SAMPLES COEFFICIENT OF VARIATION AND CENTROID OF SPRAY PATTERNS WITH NO CROSS WIND[1]

Pass No.	Pressure (KPa)	Nozzle Height (cm)	Nozzle Spacing (cm)	C.V. (%)	Pattern Centroid (cm)
		8001-Flat Fan			
1	150	46	--	36.45	209
2	150	46	--	33.50	200
3	150	46	--	26.70	215
4	289	61	--	28.20	227
5	289	61	--	19.35	219
6	289	61	--	19.50	213
		Girojet			
7	276	46	--	35.50	420
8	276	46	--	23.39	397
9	276	46	--	21.40	394
10	276	61	--	23.20	410
11	276	61	--	24.00	409
12	276	61	--	16.75	405
		Micromax			
13	221	46	15	34.15	391
14	221	46	15	50.15	415
15	221	46	15	33.00	396
16	221	46	30	30.25	409
17	221	46	30	41.90	425
18	221	46	30	30.65	405
19	221	61	15	48.65	409

(Continued)

Pass No.	Pressure (KPa)	Nozzle Height (cm)	Nozzle Angle (cm)	C.V. (%)	Pattern Centroid (cm)
20	221	61	15	37.05	417
21	221	61	15	43.95	386
22	221	61	30	39.95	412
23	221	61	30	35.70	413
24	221	61	30	37.80	418
		Rotojet			
25	221	46	15	22.10	376
26	221	46	15	33.50	405
27	221	46	15	33.45	386
28	221	46	30	20.15	376
29	221	46	30	26.20	387
30	221	46	30	37.20	429
31	221	61	15	32.80	383
32	221	61	15	34.00	405
33	221	61	15	33.60	344
34	221	61	30	28.90	387
35	221	61	30	34.50	390
36	221	61	30	29.75	358

1) Flat fan was operated with a nozzle spacing of 51 cm and 76 cm at 46 and 61 cm nozzle heights, respectively. Girojet was operated at 104 cm nozzle spacing and 2200 rpm, Micromax at 114 cm nozzle spacing and 2000 rpm, and Rotojet at 102 cm nozzle spacing and 2500 rpm. The temperature and relative humidity were measured to be 35°C and 64 %, respectively.

APPENDIX D

AVERAGE OF TWO SAMPLES AND THREE PASSES OF SPRAY PATTERN PROFILES FOR ALL NOZZLES TESTED ON SPRAYER BOOM WITH NO CROSS WIND

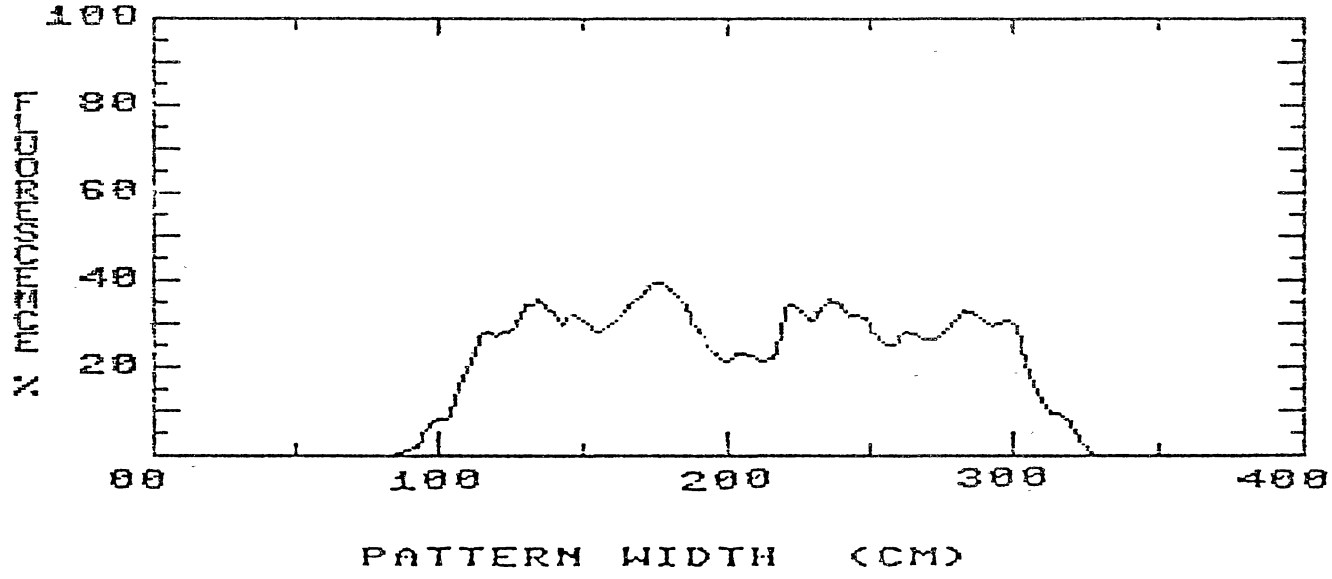

Figure 59. Average Pattern Distribution of 4-Flat Fan Nozzles Operated at 46 cm Nozzle Height, 42 L/ha, 2.235 m/s, and Center of Nozzles located at 1.31, 1.81, 2.33, and 2.83 m

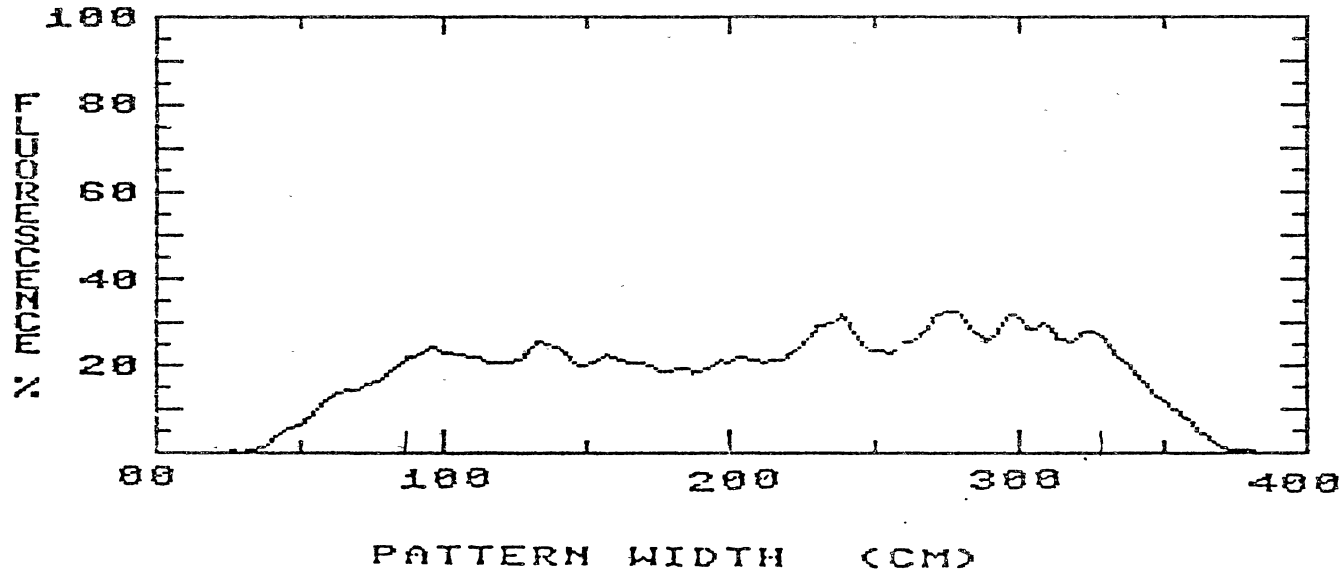

Figure 60. Average Pattern Distribution of 4-Flat Fan Nozzles Operated at 61 cm Nozzle Height, 42 L/ha, 2.235 m/s, and Center of Nozzles located at 0.93, 1.69, 2.45, and 3.21 m

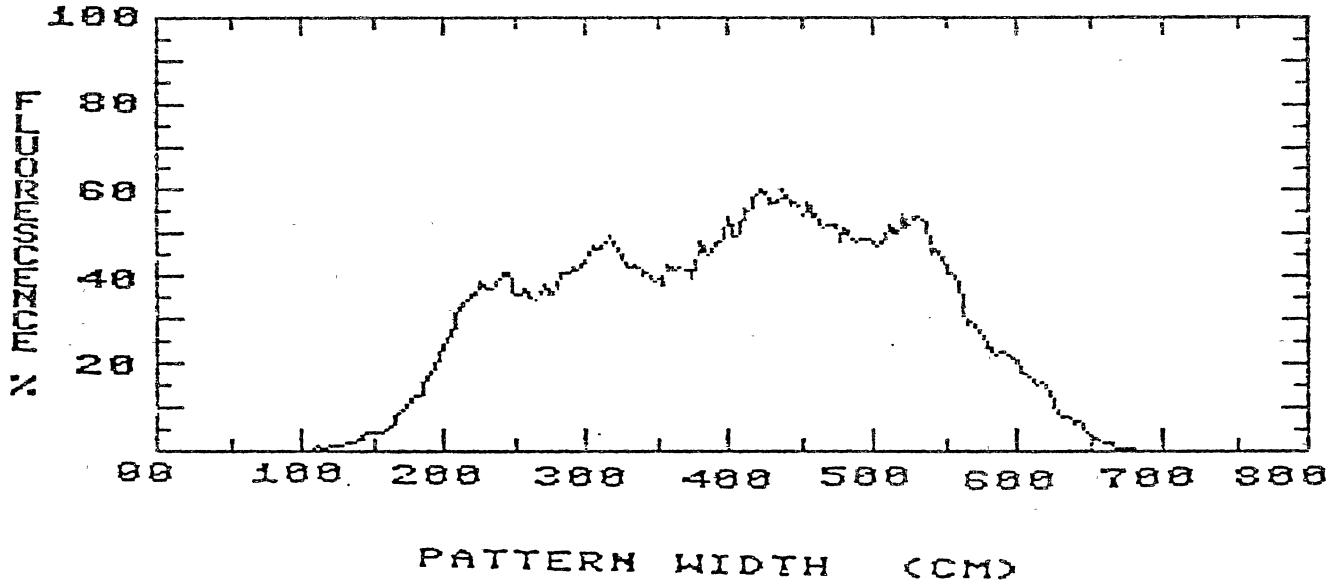

Figure 61. Average Pattern Distribution of 4-Girojet Nozzles Operated at 46 cm Nozzle Height, 42 L/Ha, 2.235 m/s, 2200 rpm, and Center of Nozzles located at 2.44, 3.48, 4.52, and 5.56 m

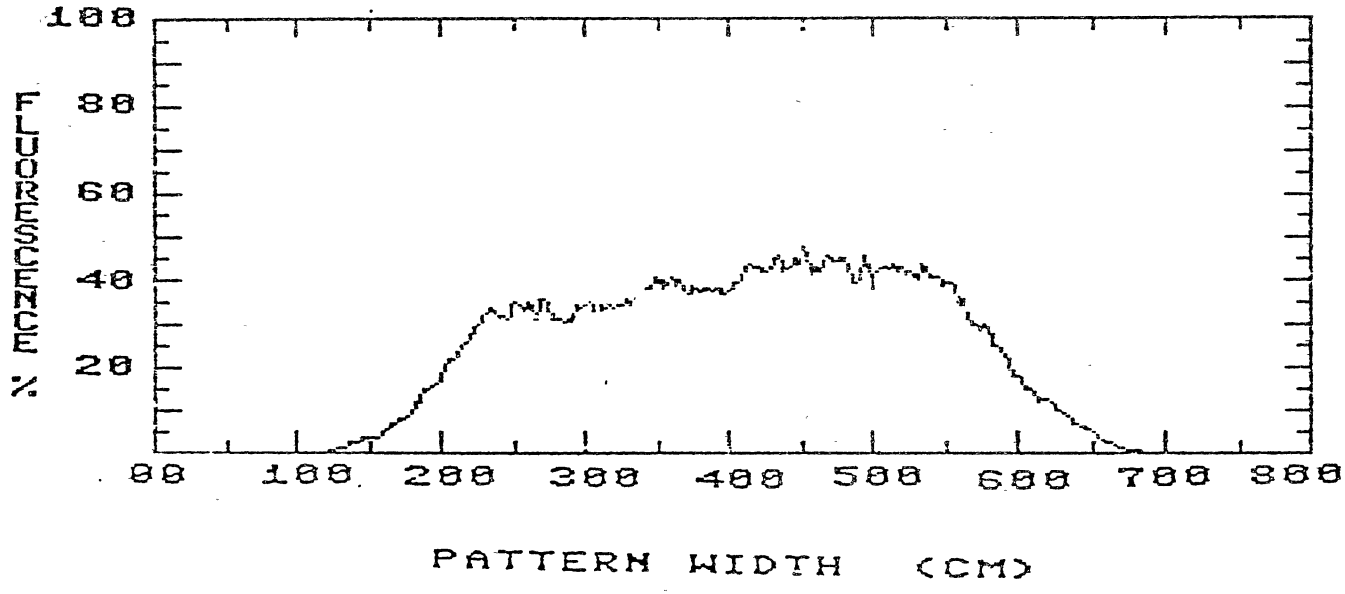

Figure 62. Average Pattern Distribution of 4-Girojet Nozzles Operated at 61 cm Nozzle Height, 42 L/Ha, 2.235 m/s, 2200 rpm, and Center of Nozzles located at 2.44, 3.48, 4.52, and 5.56 m

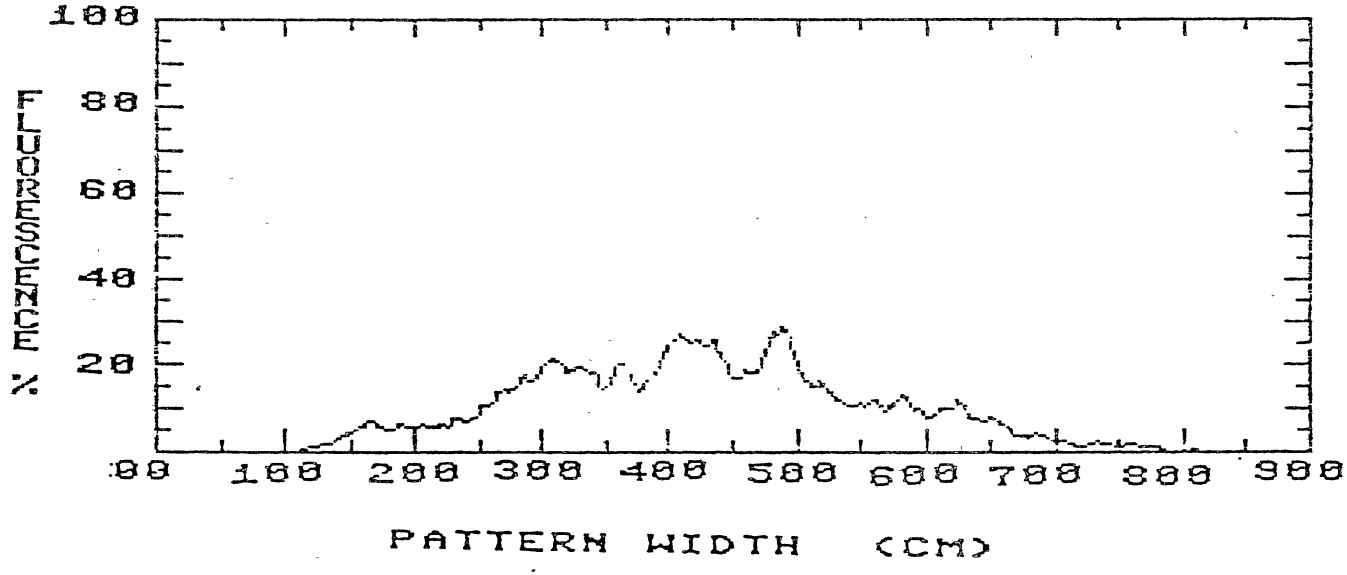

Figure 63. Average Pattern Distribution of 4-Micromax Nozzles Operated at 46 cm Nozzle Height, 42 L/Ha, 2.235 m/s, 2000 rpm, 15 Degrees Tilt Angle, and Center of Nozzles located at 2.29, 3.43, 4.57, and 5.71 m

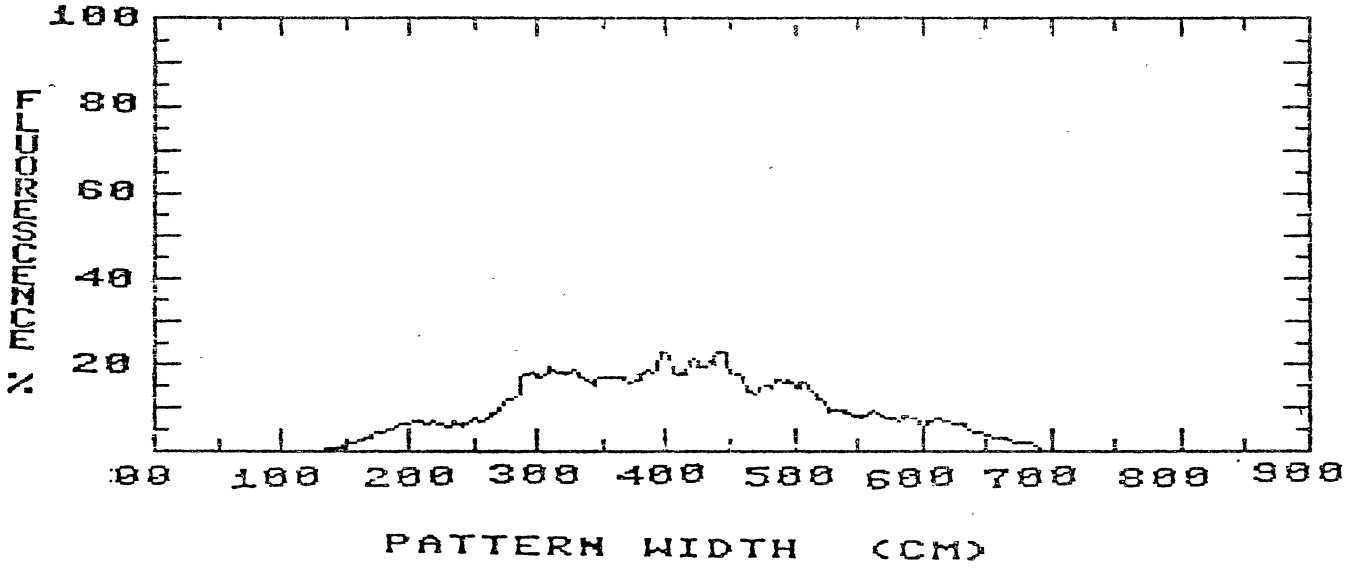

Figure 64. Average Pattern Distribution of 4-Micromax Nozzles Operated at 46 cm Nozzle Height, 42 L/Ha, 2.235 m/s, 2000 rpm, 30 Degrees Tilt Angle, and Center of Nozzles located at 2.29, 3.43, 4.57, and 5.71 m

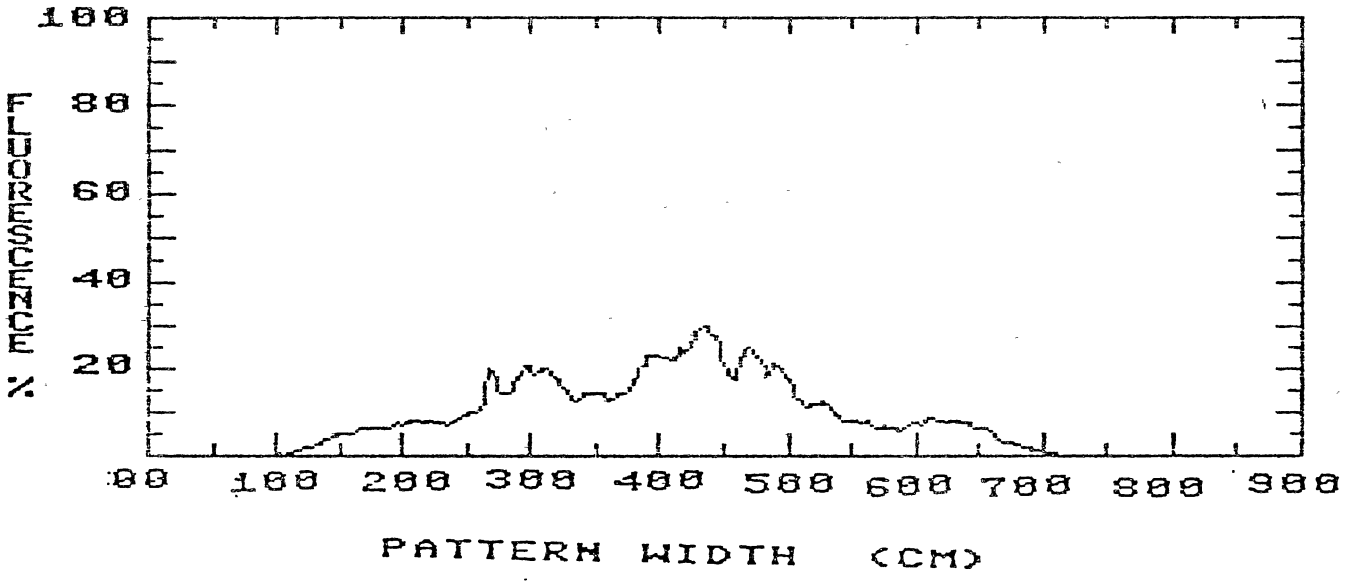

Figure 65. Average Pattern Distribution of 4-Micromax Nozzles Operated at 61 cm Nozzle Height, 42 L/Ha, 2.235 m/s, 2000 rpm, 15 Degrees Tilt Angle, and Center of Nozzles located at 2.29, 3.43, 4.57, and 5.71 m

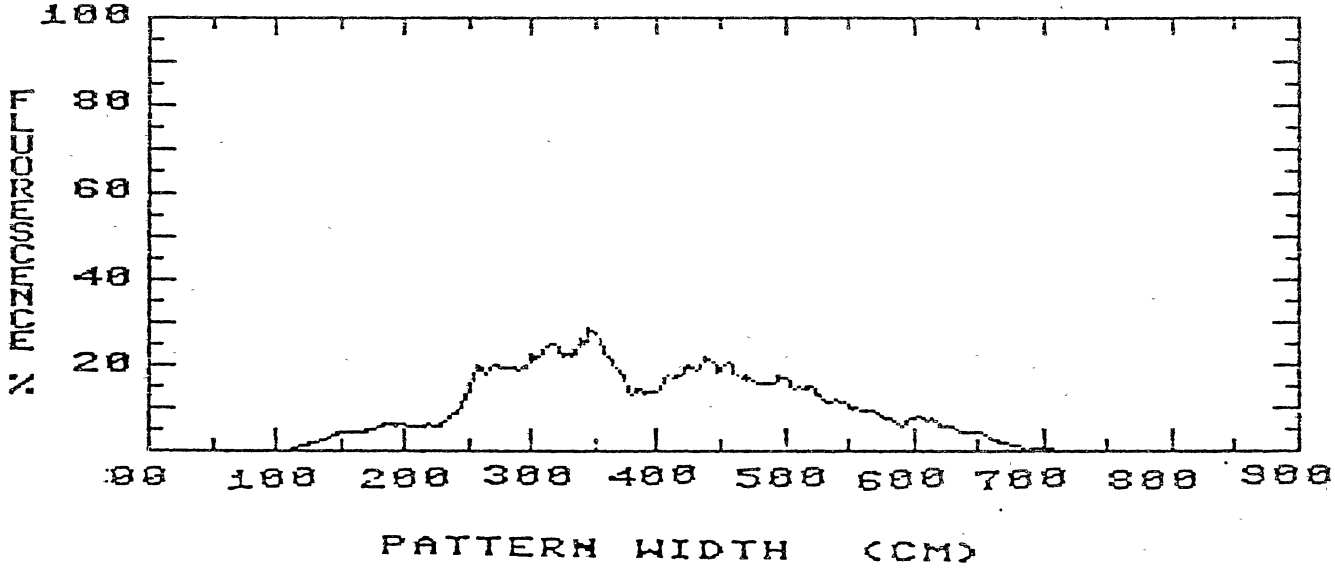

Figure 66. Average Pattern Distribution of 4-Micromax Nozzles Operated at 61 cm Nozzle Height, 42 L/Ha, 2.235 m/s, 2000 rpm, 30 Degrees Tilt Angle, and Center of Nozzles located at 2.29, 3.43, 4.57, and 5.71 m

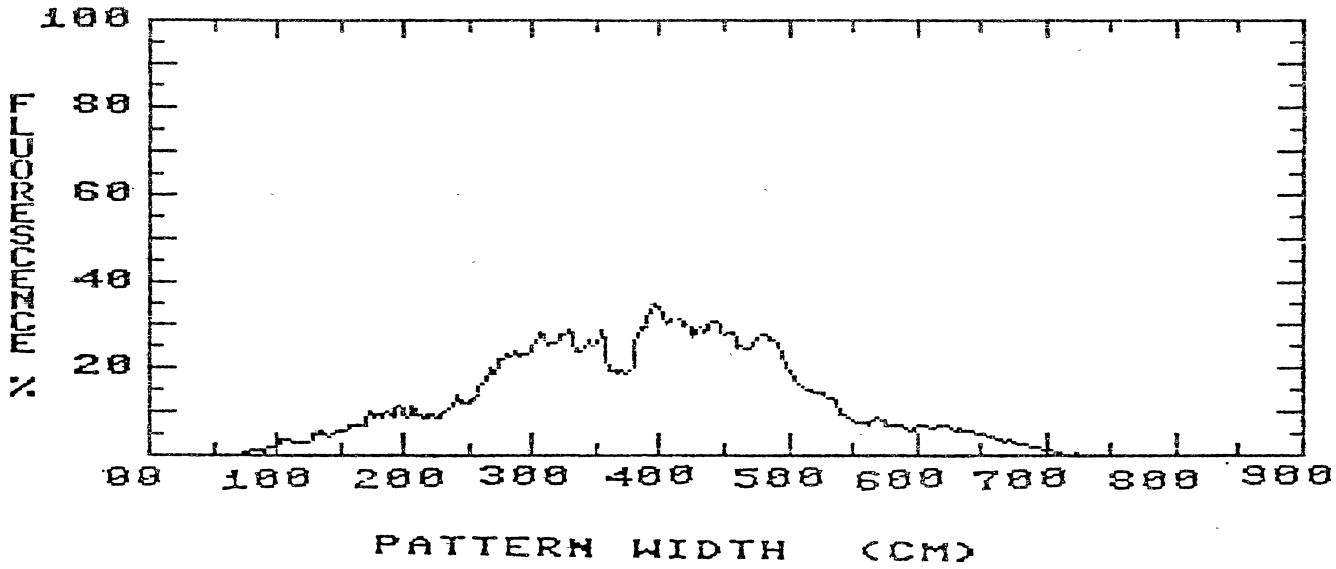

Figure 67. Average Pattern Distribution of 4-Rotojet Nozzles Operated at 46 cm Nozzle Height, 42 L/Ha, 2.235 m/s, 2500 rpm, 15 Degrees Tilt Angle, and Center of Nozzles located at 2.47, 3.49, 4.51, and 5.53 m

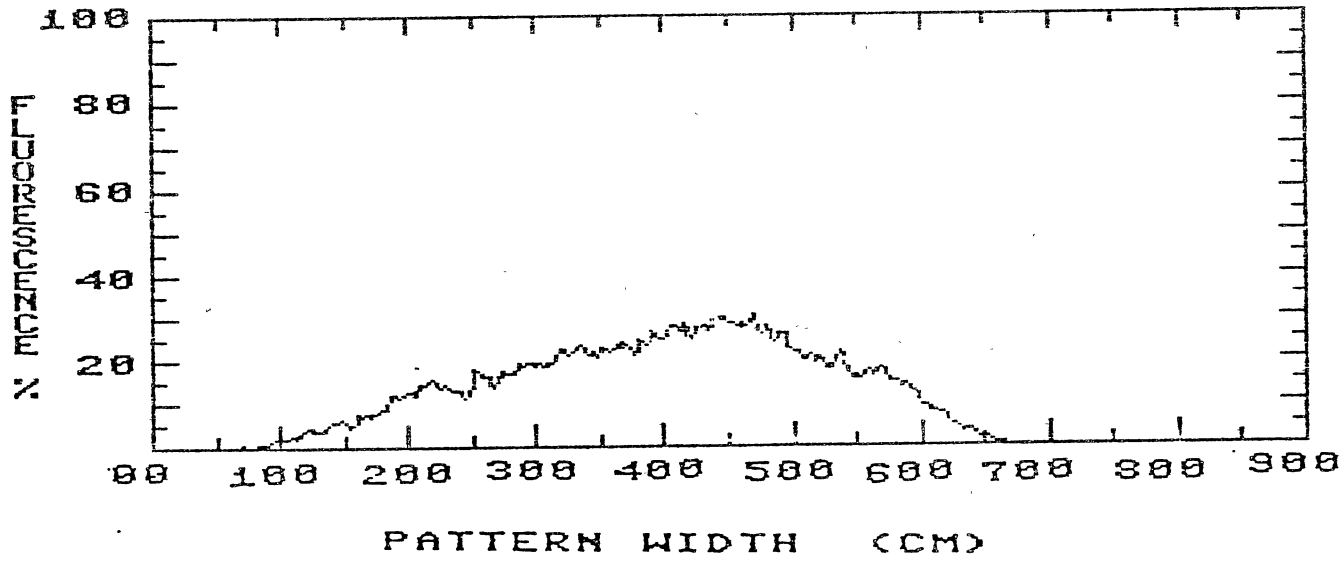

Figure 68. Average Pattern Distribution of 4-Rotojet Nozzles Operated at 46 cm Nozzle Height, 42 L/Ha, 2.235 m/s, 2500 rpm, 30 Degrees Tilt Angle, and Center of Nozzles located at 2.49, 3.49, 4.51, and 5.53 m

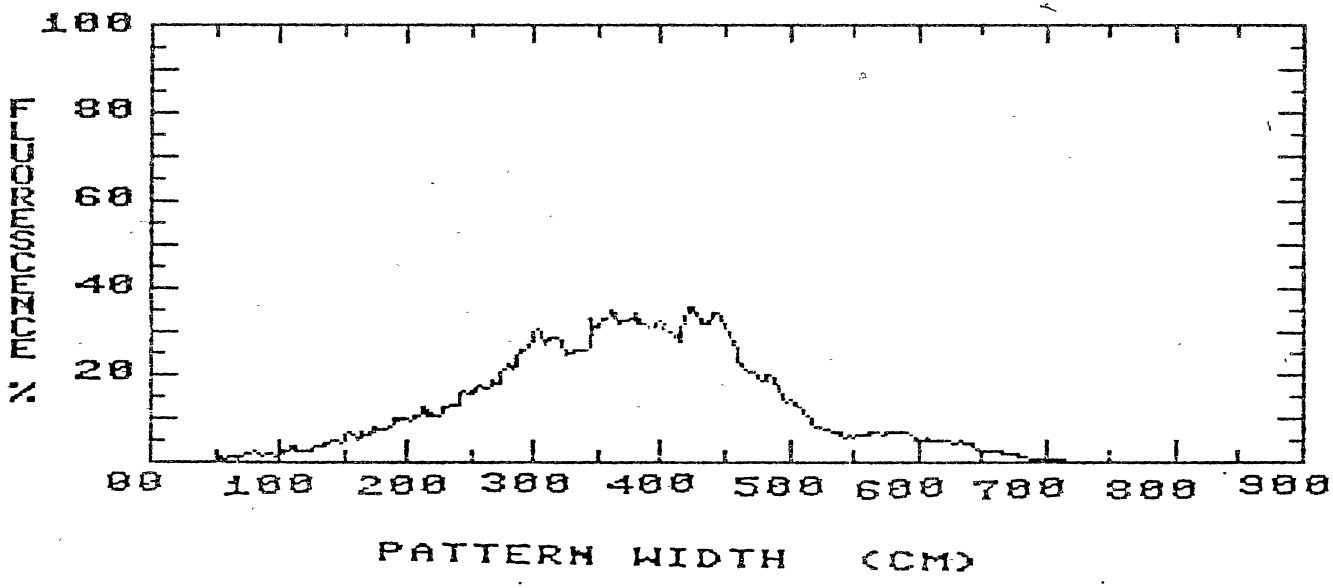

Figure 69. Average Pattern Distribution of 4-Rotojet Nozzles Operated at 61 cm Nozzle Height, 42 L/Ha, 2.235 m/s, 2500 rpm, 15 Degrees Tilt Angle, and Center of Nozzles located at 2.47, 3.49, 4.51, and 5.53 m

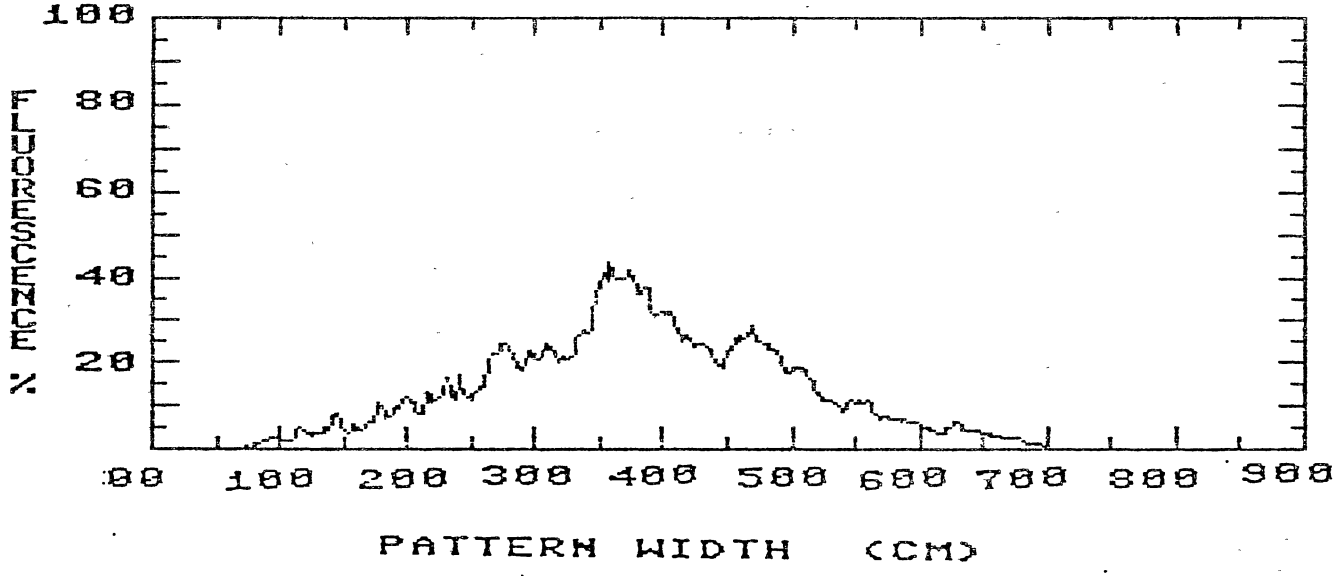

Figure 70. Average Pattern Distribution of 4-Rotojet Nozzles Operated at 61 cm Nozzle Height, 42 L/Ha, 2.235 m/s, 2500 rpm, 30 Degrees Tilt Angle, and Center of Nozzles located at 2.47, 3.49, 4.51, and 5.53 m

APPENDIX E

AVERAGE OF TWO SAMPLES SPRAY PATTERN DATA FOR ALL NOZZLES TESTED ON SPRAYER BOOM WITH CROSS WIND

AVERAGE OF TWO SAMPLES COEFFICIENT OF VARIATION AND CENTROID OF SPRAY PATTERNS WITH CROSS WIND[1]

Pass No.	Nozzle Height (cm)	Disk Angle (deg)	Wind Speed (m/s)	Wind Dir. (deg)	C.V. (%)	Pattern Centroid (cm)
			8001 Flat-Fan			
1	46	--	1.72	6	26.35	223
2	46	--	1.54	4	23.30	229
3	46	--	1.48	20	30.45	230
4	46	--	1.66	-20	30.25	236
5	46	--	0.69	-6	31.21	240
6	46	--	1.29	-4	25.95	215
7	46	--	0.81	-24	31.15	231
8	61	--	0.76	-18	22.85	264
9	61	--	1.10	-28	24.20	238
10	61	--	0.98	7	25.15	256
11	61	--	1.10	6	29.35	267
12	61	--	1.04	-10	23.05	261
13	61	--	1.72	14	24.20	238
14	61	--	1.37	-24	31.65	293
15	61	--	0.56	10	20.24	254
16	61	--	1.60	22	43.15	263
17	61	--	1.59	0	24.45	284

(Continued)

Pass No.	Nozzle Height (cm)	Disk Angle (cm)	Wind Speed (m/s)	Wind Dir. (deg)	C.V. (%)	Pattern Centroid (cm)
			Girojet			
18	46	--	1.48	10	19.20	436
19	46	--	1.44	28	28.20	414
20	46	--	1.49	7	26.10	414
21	61	--	1.71	7	18.60	454
22	61	--	1.32	-6	16.95	422
23	61	--	0.62	16	18.40	459
			Micromax			
24	46	15	1.48	24	46.65	5.22
25	46	15	1.76	18	28.20	516
26	46	15	1.70	27	37.65	517
27	46	15	1.71	25	21.65	517
28	46	30	1.52	27	34.35	440
29	61	15	0.98	-7	25.35	548
30	61	15	1.10	-24	17.50	596
31	61	15	0.75	-27	31.90	530
32	61	30	1.01	24	29.30	584
33	61	30	1.07	3	24.30	580

(Continued)

Pass No.	Nozzle Height (cm)	Disk Angle (cm)	Wind Speed (m/s)	Wind Dir. (deg)	C.V. (%)	Pattern Centroid (cm)
			Rotojet			
34	46	15	1.45	3	16.40	560
35	46	15	1.55	16	20.60	581
36	46	15	1.26	13	15.90	562
37	46	30	1.61	-7	26.90	614
38	46	30	1.62	13	17.90	561
39	61	15	1.57	21	25.50	539
40	61	30	1.01	-1	25.40	483
41	61	30	1.38	-15	22.50	503

1) Flat fan nozzle was operated at 155 KPa and 51 cm nozzle spacing at 46 cm nozzle height,and at 289 KPa and 76 cm nozzle spacing at 61 cm nozzle height. Girojet was operated at 276 kPa and 2200 rpm, Micromax at 221 KPa and 2000 rpm, and Rotojet at 221 KPa and 2500 rpm at both 46 and 61 cm nozzle heights. The temperature and relative humidity were measured to be 36°C and 64 %, respectively.

APPENDIX F

AVERAGE OF TWO SAMPLES SPRAY PATTERN PROFILES FOR ALL NOZZLES TESTED ON SPRAYER BOOM WITH CROSS WIND

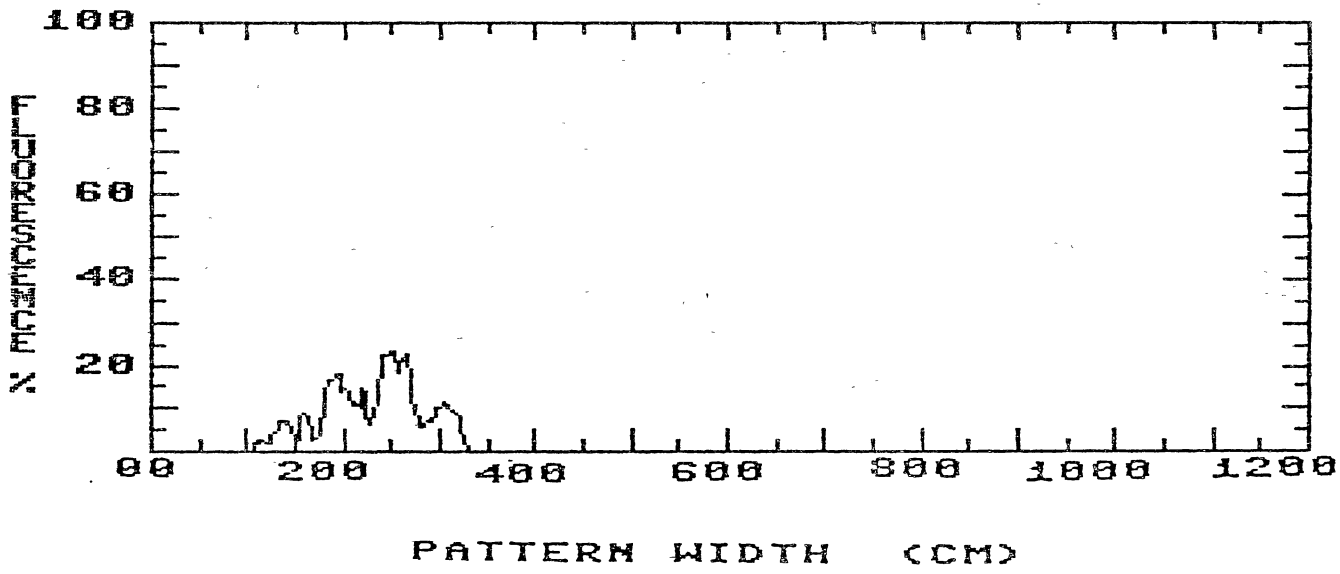

Figure 71. Average of Two Samples Pattern Distribution of 4-Flat Fan Nozzles Operated at 46 cm Nozzle Height, 42 L/ha, 2.235 m/s Sprayer Speed, 1.72 m/s Wind Speed, 6 Degrees Wind Direction, and Center of Nozzles located at 1.31, 1.81, 2.33, and 2.83 m

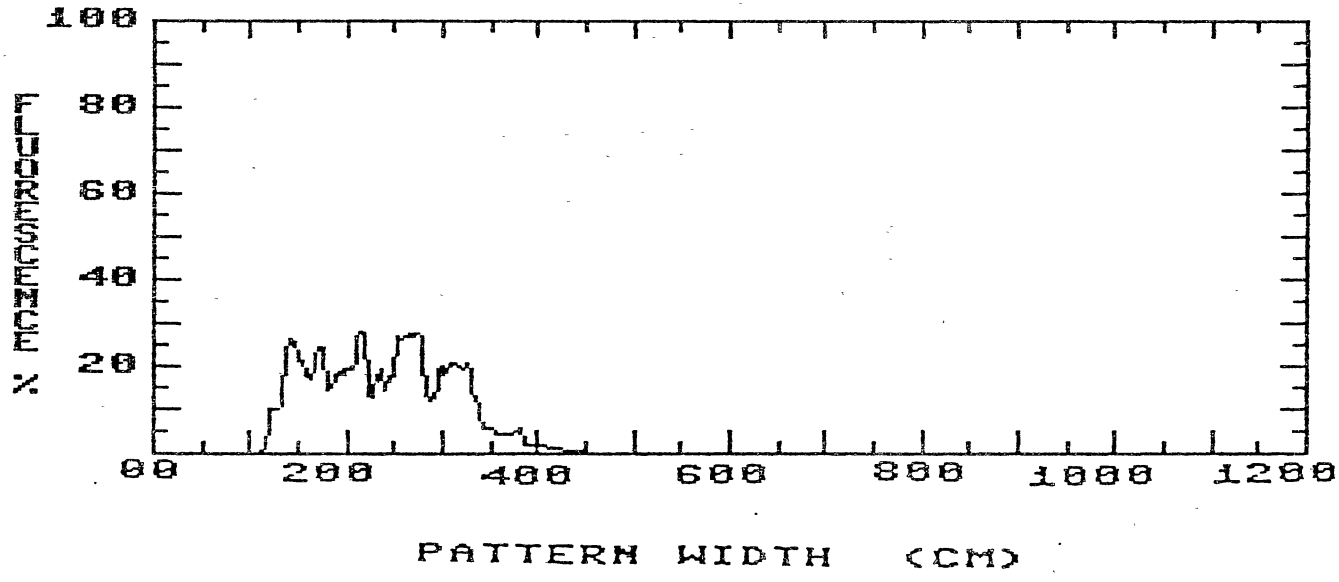

Figure 72. Average of Two Samples Pattern Distribution of 4-Flat Fan Nozzles Operated at 46 cm Nozzle Height, 42 L/ha, 2.235 m/s Sprayer Speed, 1.54 m/s Wind Speed, 4 Degrees Wind Direction, and Center of Nozzles located at 1.31, 1.81, 2.33, and 2.83 m

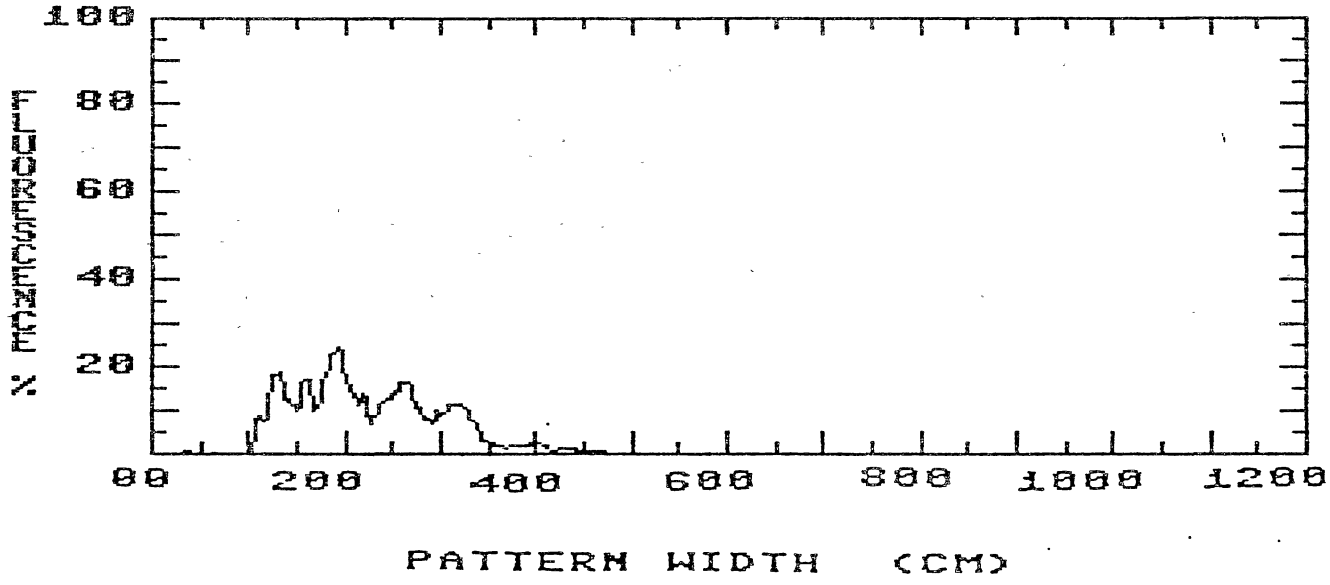

Figure 73. Average of Two Samples Pattern Distribution of 4-Flat Fan Nozzles Operated at 46 cm Nozzle Height, 42 L/ha, 2.235 m/s Sprayer Speed, 1.48 m/s Wind Speed, 20 Degrees Wind Direction, and Center of Nozzles located at 1.31, 1.81, 2.33, and 2.83 m

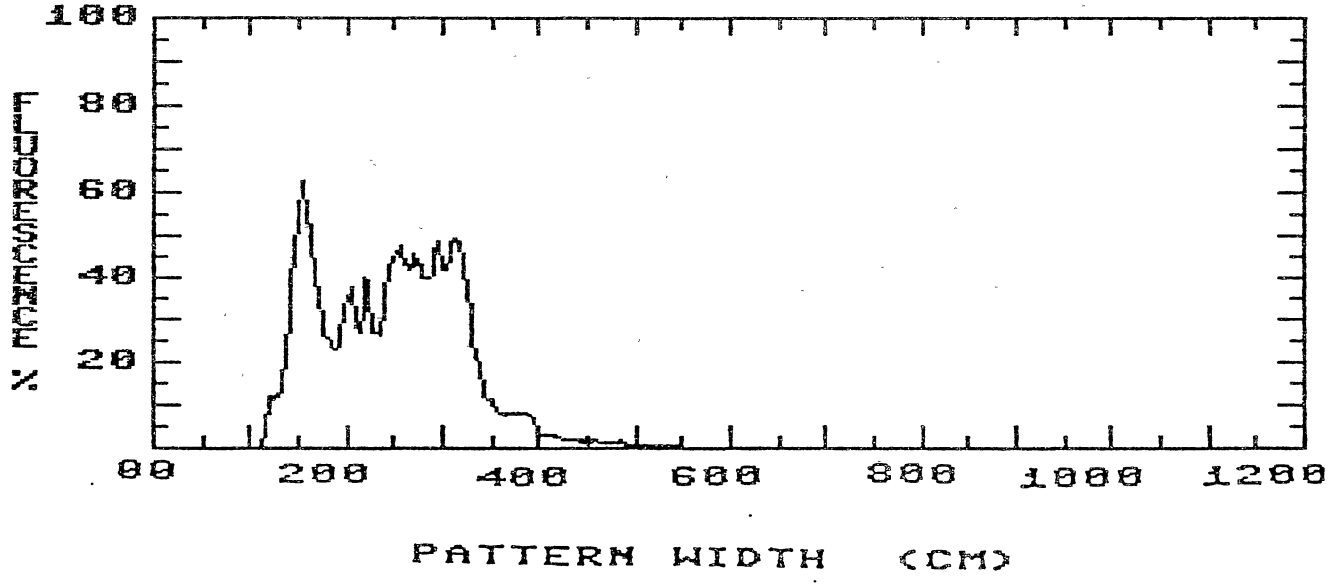

Figure 74. Average of Two Samples Pattern Distribution of 4-Flat Fan Nozzles Operated at 46 cm Nozzle Height, 42 L/ha, 2.235 m/s Sprayer Speed, 1.66 m/s Wind Speed, -20 Degrees Wind Direction, and Center of Nozzles located at 1.31, 1.81, 2.33, and 2.83 m

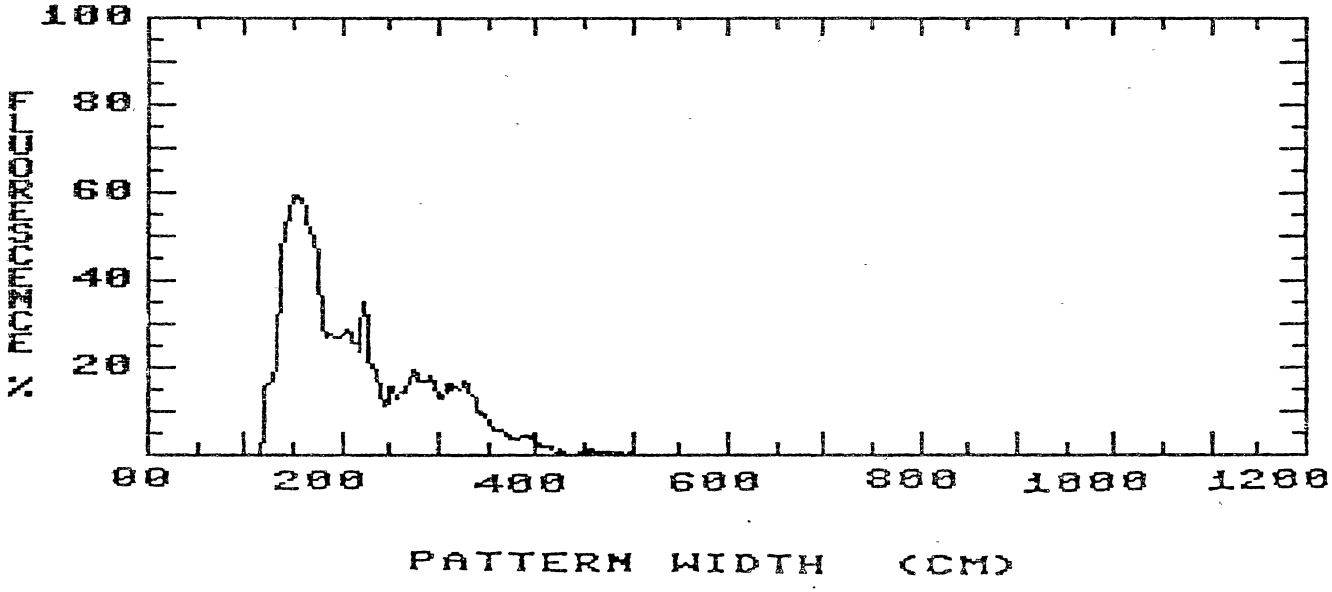

Figure 75. Average of Two Samples Pattern Distribution of 4-Flat Fan Nozzles Operated at 46 cm Nozzle Height, 42 L/ha, 2.235 m/s Sprayer Speed, 0.69 m/s Wind Speed, -6 Degrees Wind Direction, and Center of Nozzles located at 1.31, 1.81, 2.33, and 2.83 m

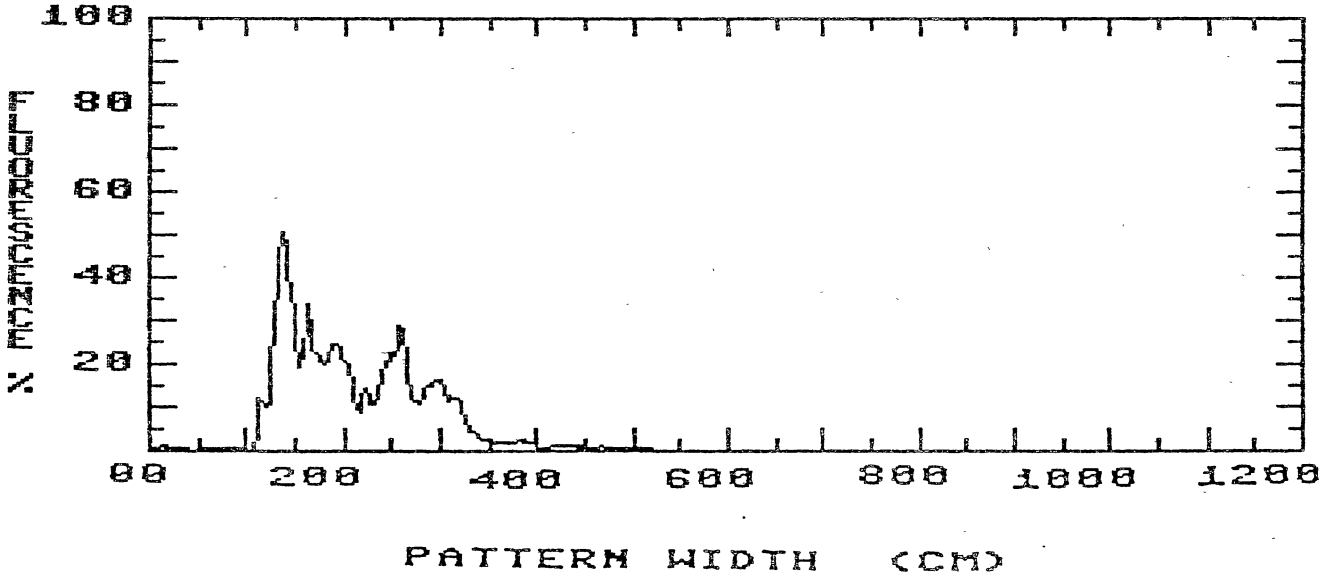

Figure 76. Average of Two Samples Pattern Distribution of 4-Flat Fan Nozzles Operated at 46 cm Nozzle Height, 42 L/ha, 2.235 m/s Sprayer Speed, 1.29 m/s Wind Speed, -4 Degrees Wind Direction, and Center of Nozzles located at 1.31, 1.81, 2.33, and 2.83 m

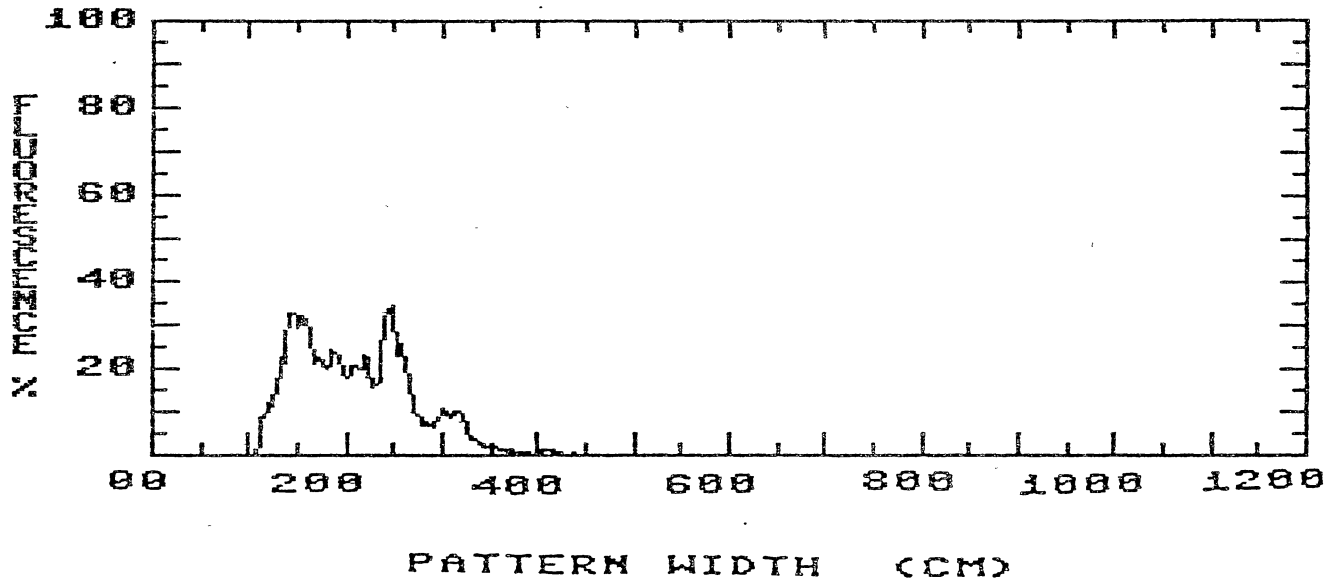

Figure 77. Average of Two Samples Pattern Distribution of 4-Flat Fan Nozzles Operated at 46 cm Nozzle Height, 42 L/ha, 2.235 m/s Sprayer Speed, 0.81 m/s Wind Speed, -24 Degrees Wind Direction, and Center of Nozzles located at 1.31, 1.81, 2.33, and 2.83 m

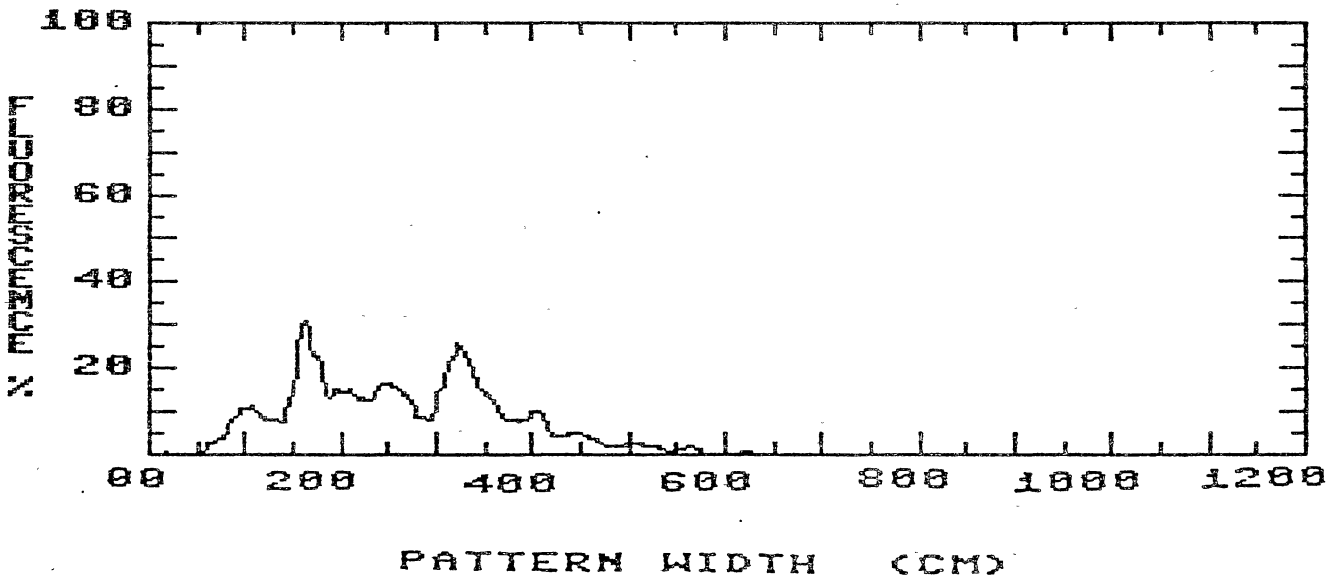

Figure 78. Average of Two Samples Pattern Distribution of 4-Flat Fan Nozzles Operated at 61 cm Nozzle Height, 42 L/ha, 2.235 m/s Sprayer Speed, 0.76 m/s Wind Speed, -18 Degrees Wind Direction, and Center of Nozzles located at 0.93, 1.69, 2.45, and 3.21 m

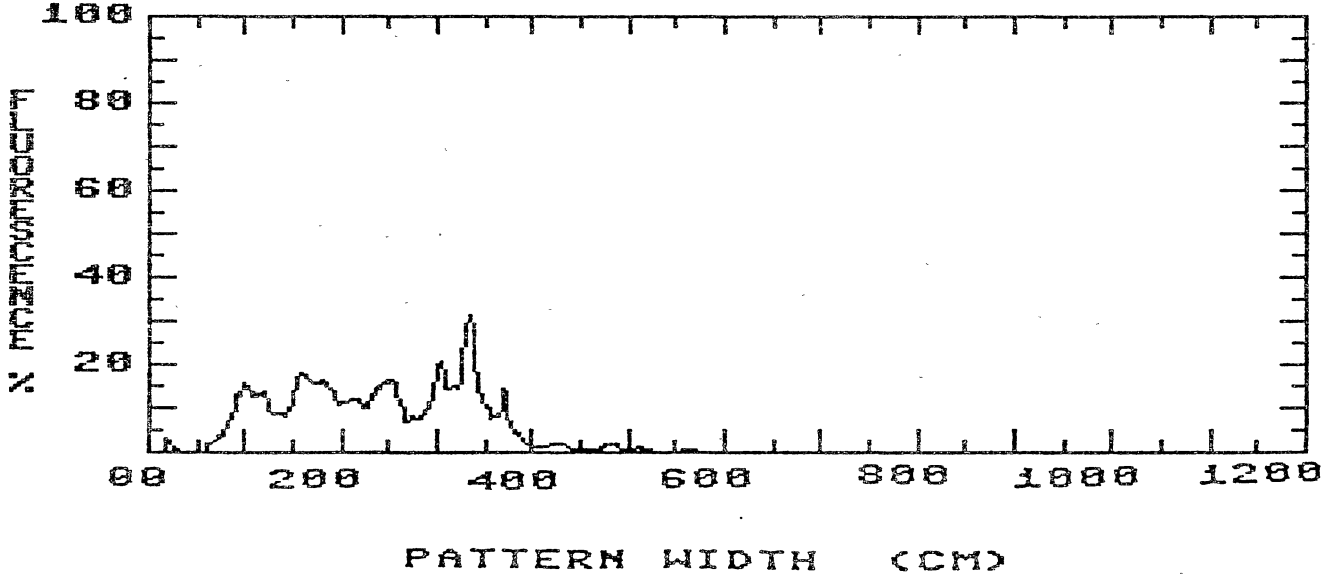

Figure 79. Average of Two Samples Pattern Distribution of 4-Flat Fan Nozzles Operated at 61 cm Nozzle Height, 42 L/ha, 2.235 m/s Sprayer Speed, 1.10 m/s Wind Speed, -28 Degrees Wind Direction, and Center of Nozzles located at 0.93, 1.69, 2.45, and 3.21 m

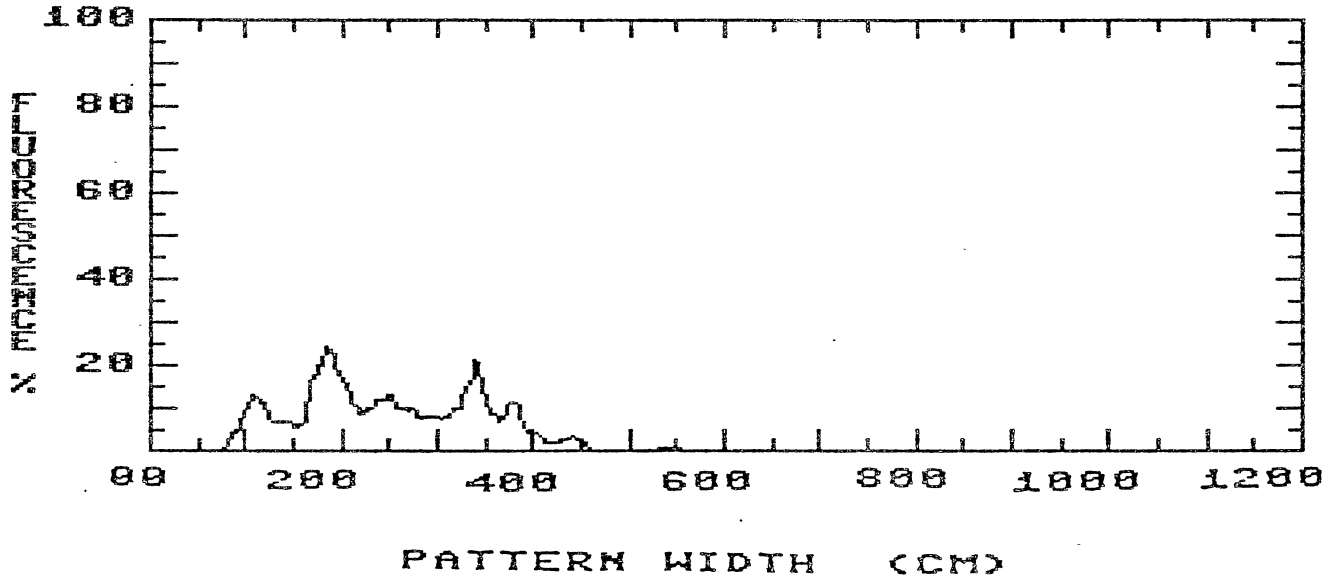

Figure 80. Average of Two Samples Pattern Distribution of 4-Flat Fan Nozzles Operated at 61 cm Nozzle Height, 42 L/ha, 2.235 m/s Sprayer Speed, 0.98 m/s Wind Speed, 7 Degrees Wind Direction, and Center of Nozzles located at 0.93, 1.69, 2.45, and 3.21 m

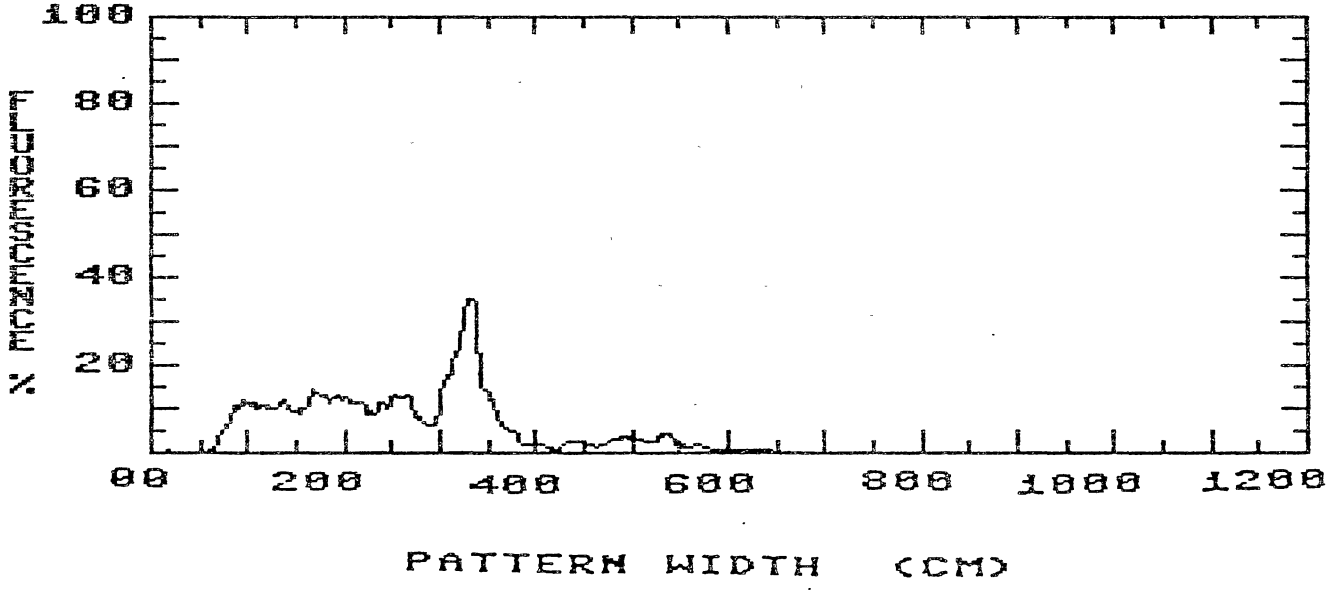

Figure 81. Average of Two Samples Pattern Distribution of 4-Flat Fan Nozzles Operated at 61 cm Nozzle Height, 42 L/ha, 2.235 m/s Sprayer Speed, 1.10 m/s Wind Speed, 6 Degrees Wind Direction, and Center of Nozzles located at 0.93, 1.69, 2.45, and 3.21 m

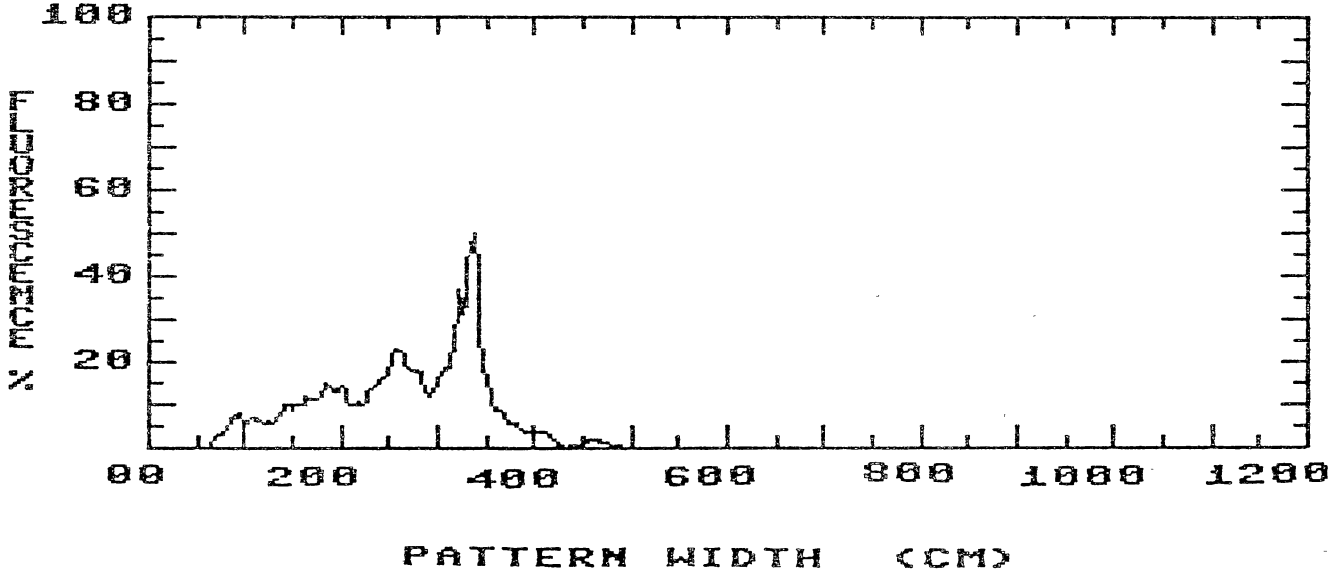

Figure 82. Average of Two Samples Pattern Distribution of 4-Flat Fan Nozzles Operated at 61 cm Nozzle Height, 42 L/ha, 2.235 m/s Sprayer Speed, 1.04 m/s Wind Speed, -10 Degrees Wind Direction, and Center of Nozzles located at 0.93, 1.69, 2.45, and 3.21 m

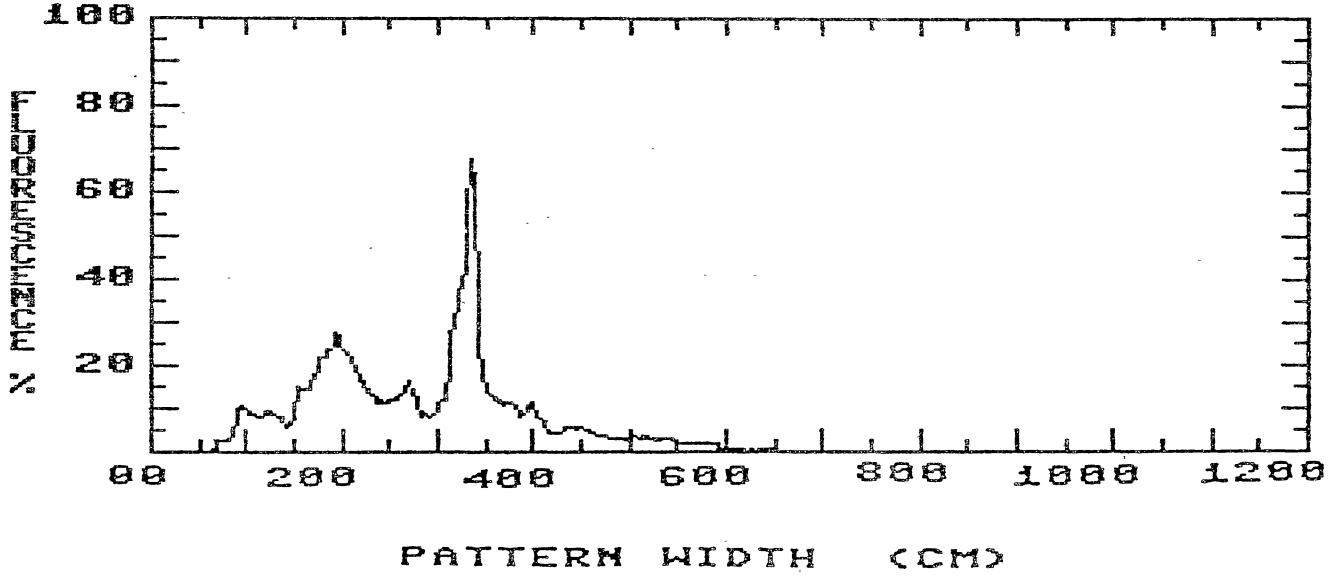

Figure 83. Average of Two Samples Pattern Distribution of 4-Flat Fan Nozzles Operated at 61 cm Nozzle Height, 42 L/ha, 2.235 m/s Sprayer Speed, 1.72 m/s Wind Speed, 14 Degrees Wind Direction, and Center of Nozzles located at 0.93, 1.69, 2.45, and 3.21 m

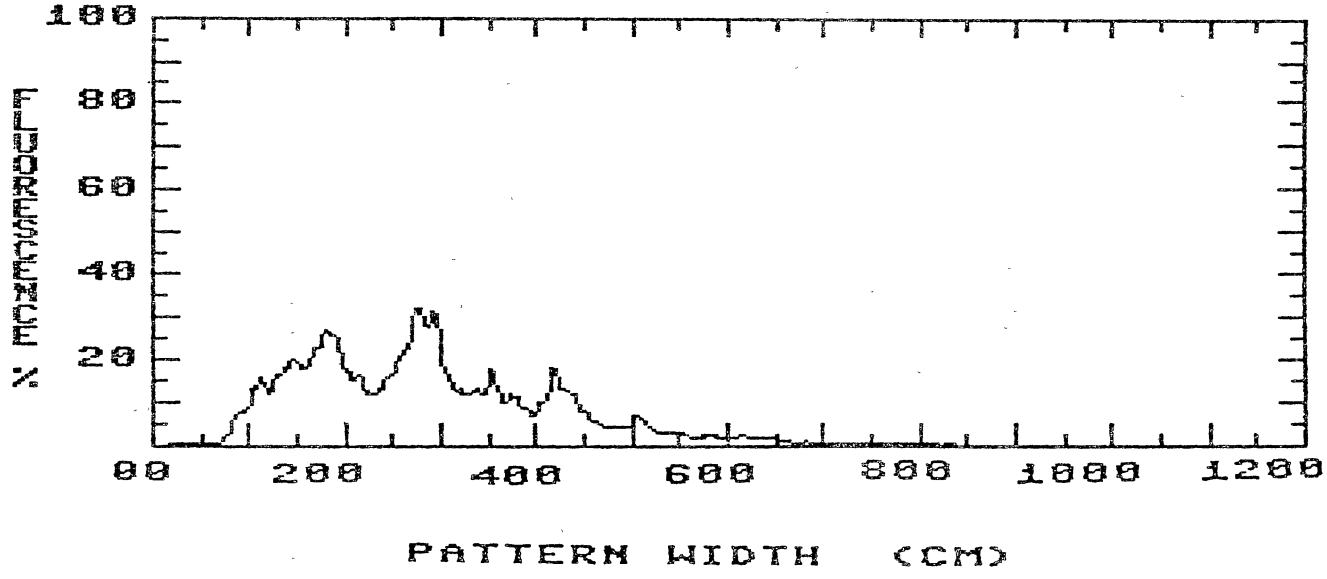

Figure 84. Average of Two Samples Pattern Distribution of 4-Flat Fan Nozzles Operated at 61 cm Nozzle Height, 42 L/ha, 2.235 m/s Sprayer Speed, 1.37 m/s Wind Speed, -24 Degrees Wind Direction, and Center of Nozzles located at 0.93, 1.69, 2.45, and 3.21 m

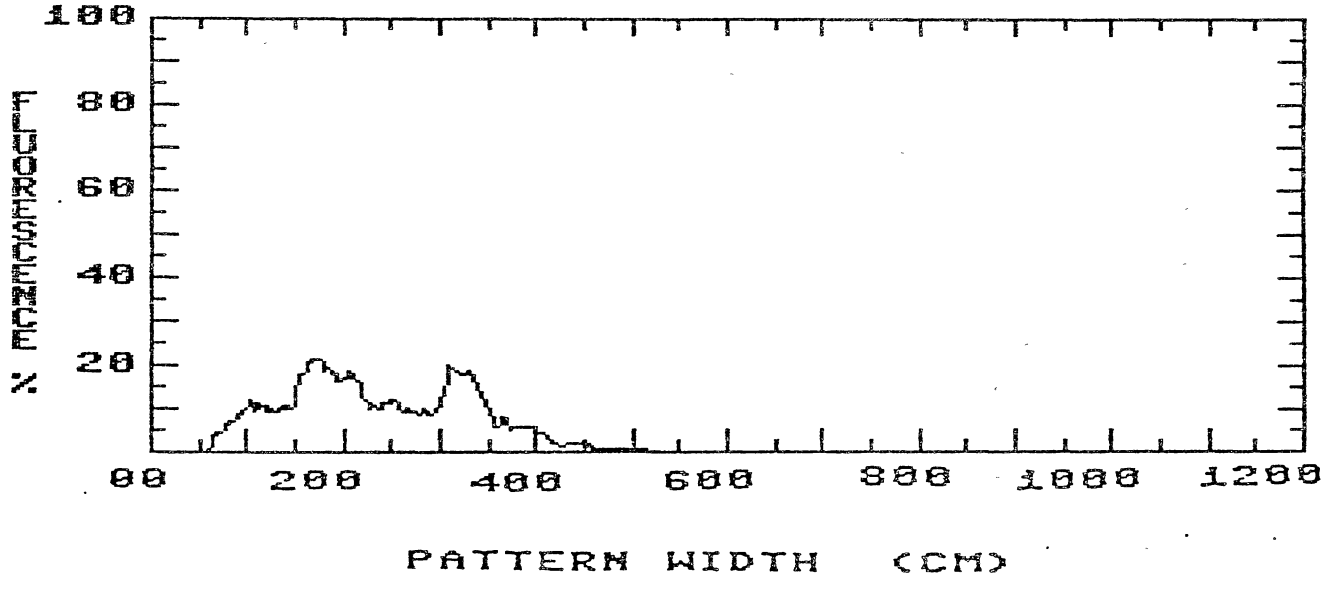

Figure 85. Average of Two Samples Pattern Distribution of 4-Flat Fan Nozzles Operated at 61 cm Nozzle Height, 42 L/ha, 2.235 m/s Sprayer Speed, 0.56 m/s Wind Speed, 10 Degrees Wind Direction, and Center of Nozzles located at 0.93, 1.69, 2.45, and 3.21 m

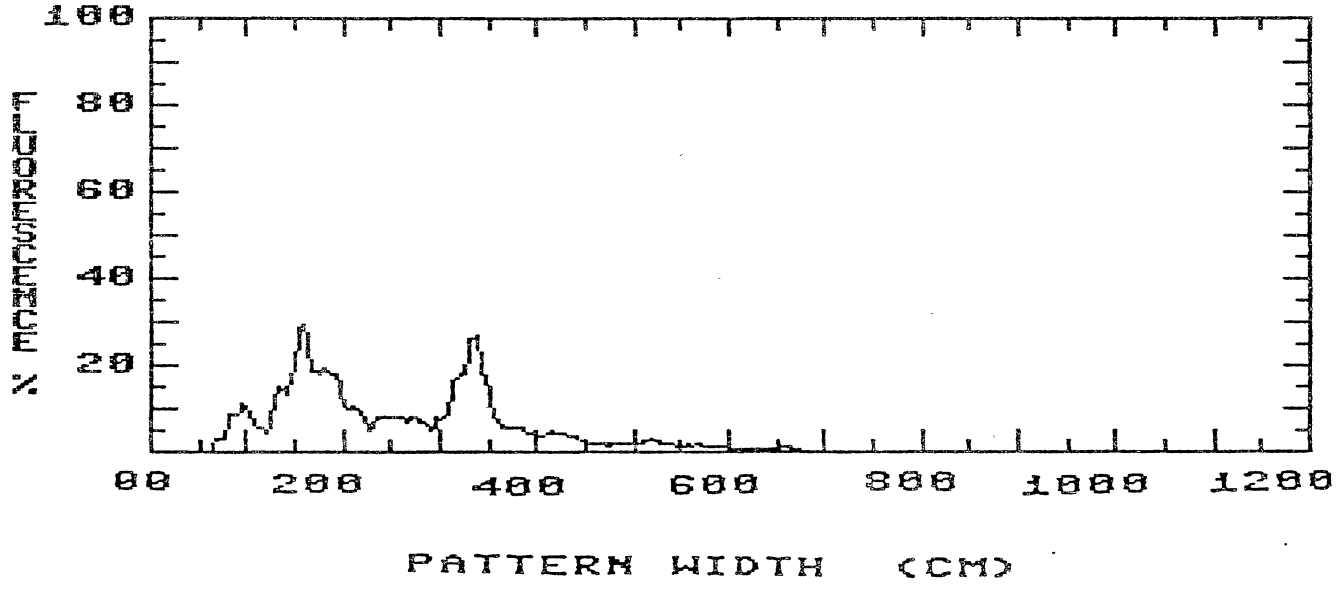

Figure 86. Average of Two Samples Pattern Distribution of 4-Flat Fan Nozzles Operated at 61 cm Nozzle Height, 42 L/ha, 2.235 m/s Sprayer Speed, 1.60 m/s Wind Speed, 22 Degrees Wind Direction, and Center of Nozzles located at 0.93, 1.69, 2.45, and 3.21 m

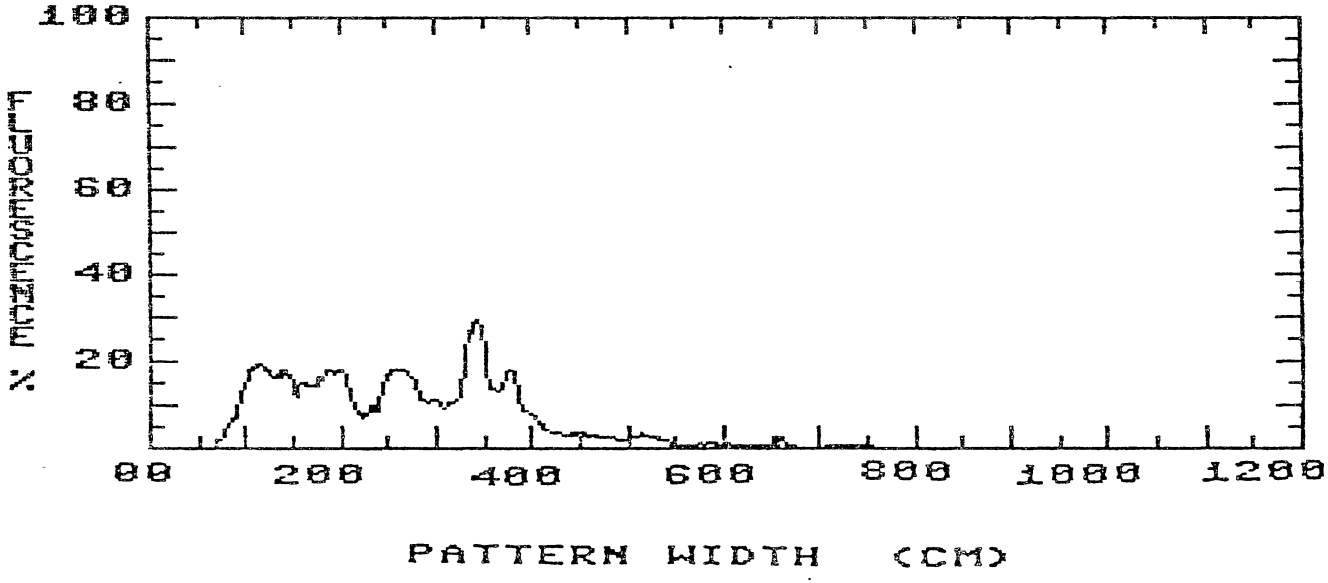

Figure 87. Average of Two Samples Pattern Distribution of 4-Flat Fan Nozzles Operated at 61 cm Nozzle Height, 42 L/ha, 2.235 m/s Sprayer Speed, 1.59 m/s Wind Speed, 0 Degrees Wind Direction, and Center of Nozzles located at 0.93, 1.69, 2.45, and 3.21 m

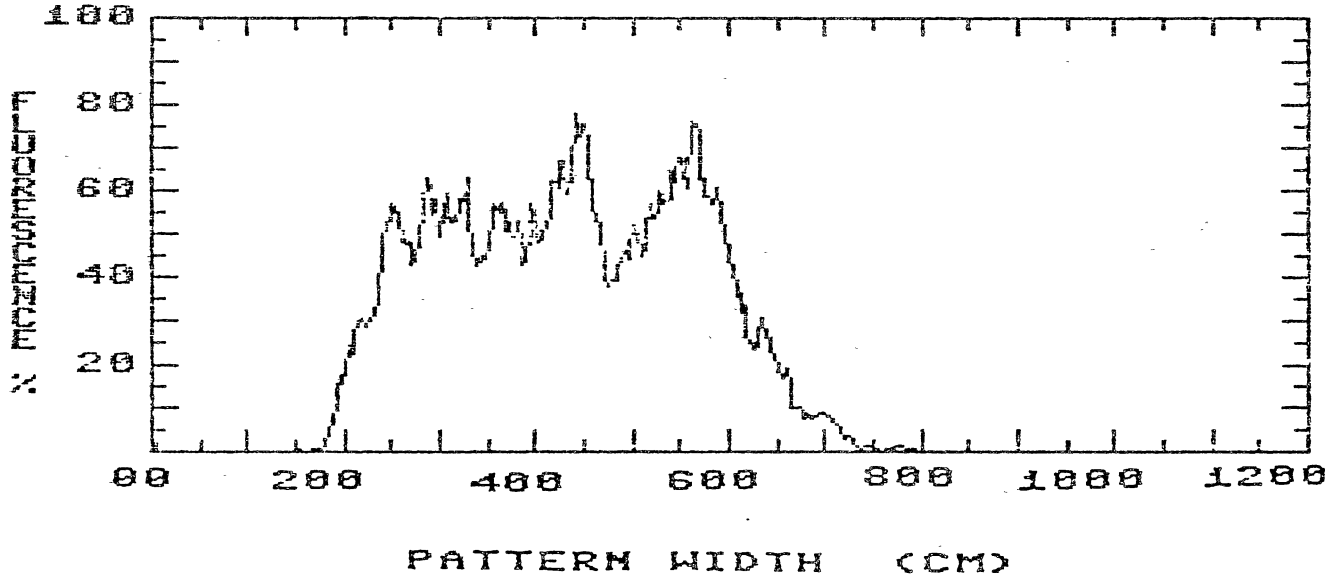

Figure 88. Average of Two Samples Pattern Distribution of 4-Girojet Nozzles Operated at 46 cm Nozzle Height, 42 L/ha, 2.235 m/s Sprayer Speed, 2200 rpm, 1.48 m/s Wind Speed, 10 Degrees Wind Direction, and Center of Nozzles located at 2.44, 3.48, 4.52. and 5.56 m

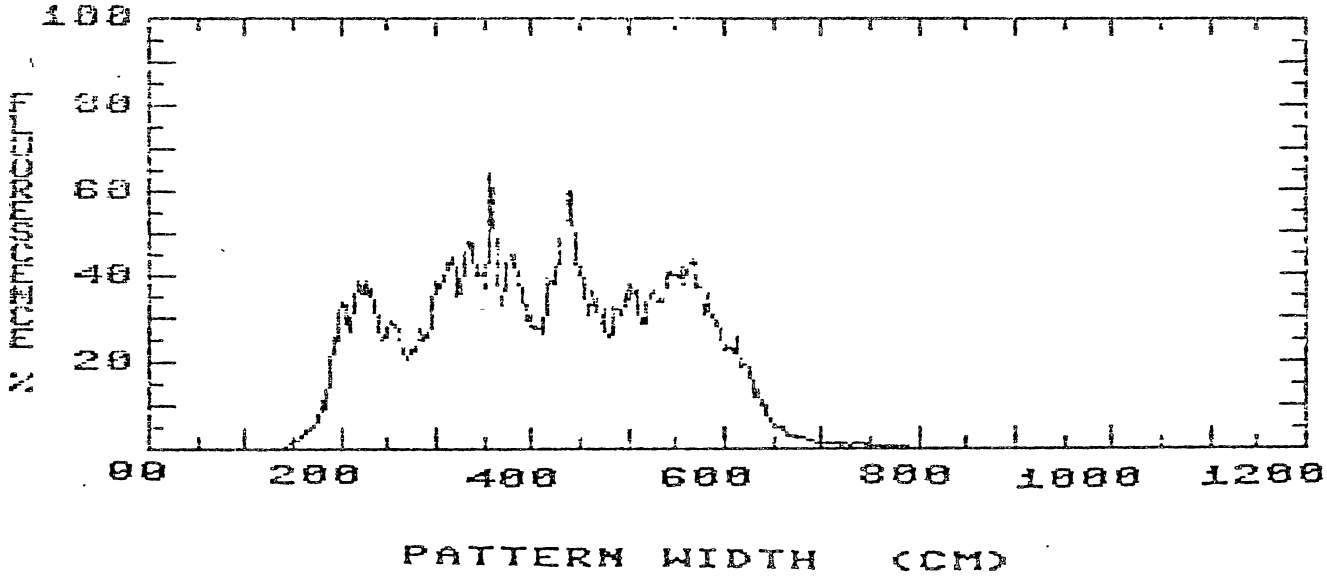

Figure 89. Average of Two Samples Pattern Distribution of 4-Girojet Nozzles Operated at 46 cm Nozzle Height, 42 L/ha, 2.235 m/s Sprayer Speed, 2200 rpm, 1.44 m/s Wind Speed, 28 Degrees Wind Direction, and Center of Nozzles located at 2.44, 3.48, 4.52. and 5.56 m

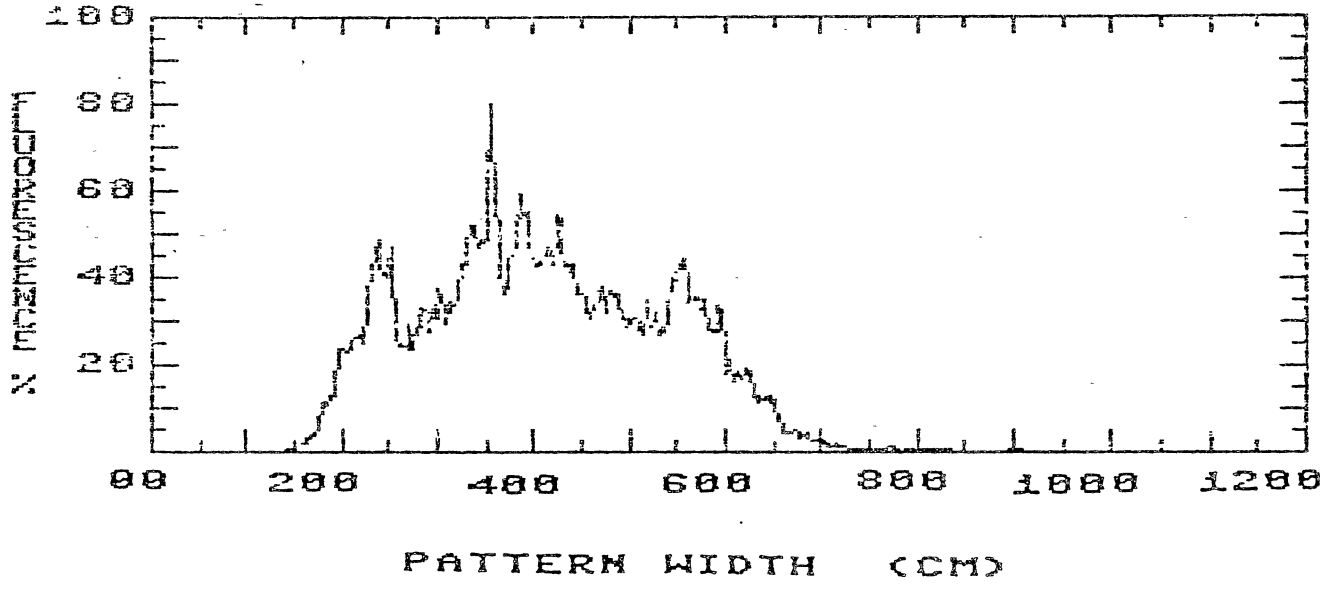

Figure 90. Average of Two Samples Pattern Distribution of 4-Girojet Nozzles Operated at 46 cm Nozzle Height, 42 L/ha, 2.235 m/s Sprayer Speed, 2200 rpm, 1.49 m/s Wind Speed, 7 Degrees Wind Direction, and Center of Nozzles located at 2.44, 3.48, 4.52. and 5.56 m

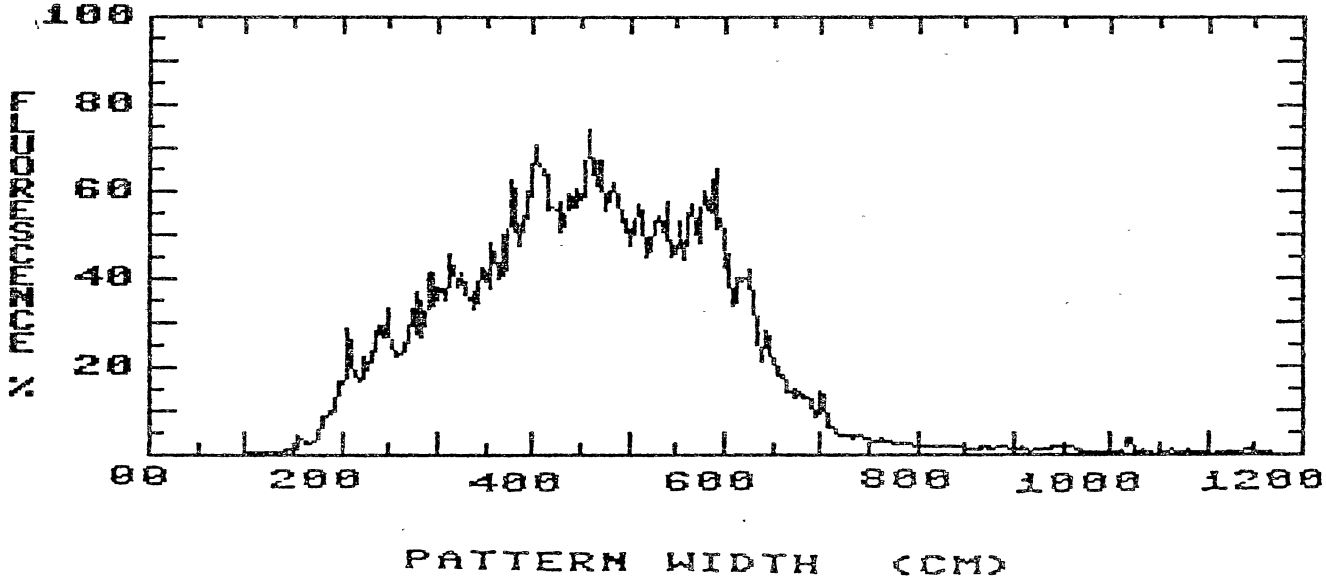

Figure 91. Average of Two Samples Pattern Distribution of 4-Girojet Nozzles Operated at 61 cm Nozzle Height, 42 L/ha, 2.235 m/s Sprayer Speed, 2200 rpm, 1.71 m/s Wind Speed, 7 Degrees Wind Direction, and Center of Nozzles located at 2.44, 3.48, 4.52. and 5.56 m

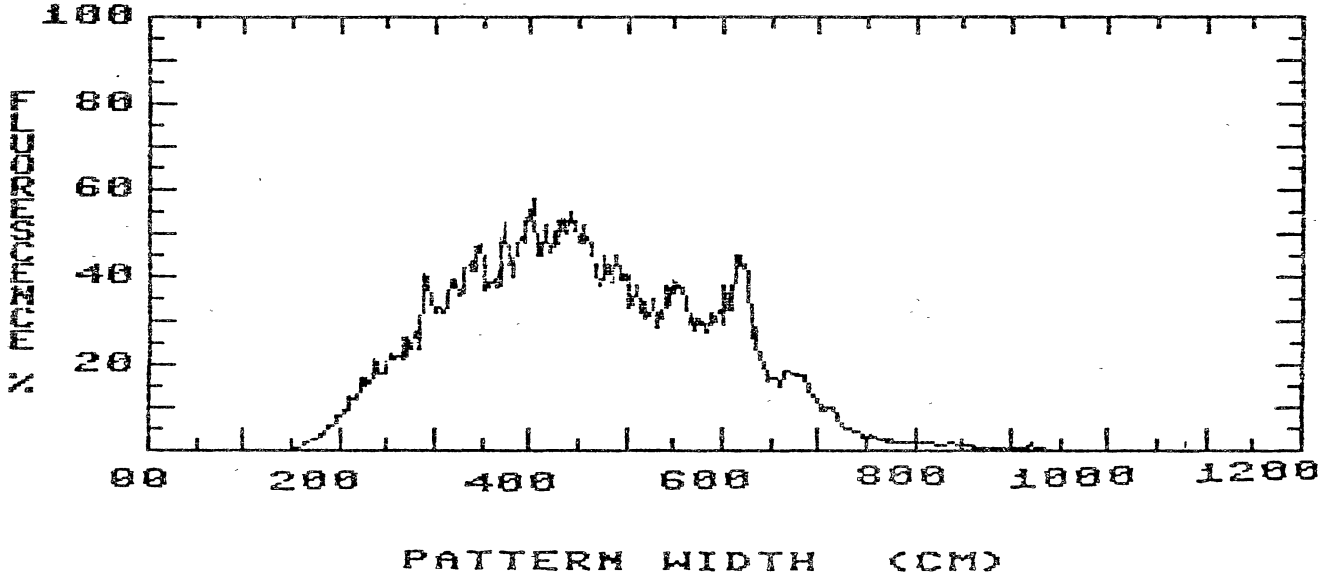

Figure 92. Average of Two Samples Pattern Distribution of 4-Girojet Nozzles Operated at 61 cm Nozzle Height, 42 L/ha, 2.235 m/s Sprayer Speed, 2200 rpm, 1.32 m/s Wind Speed, -6 Degrees Wind Direction, and Center of Nozzles located at 2.44, 3.48, 4.52. and 5.56 m

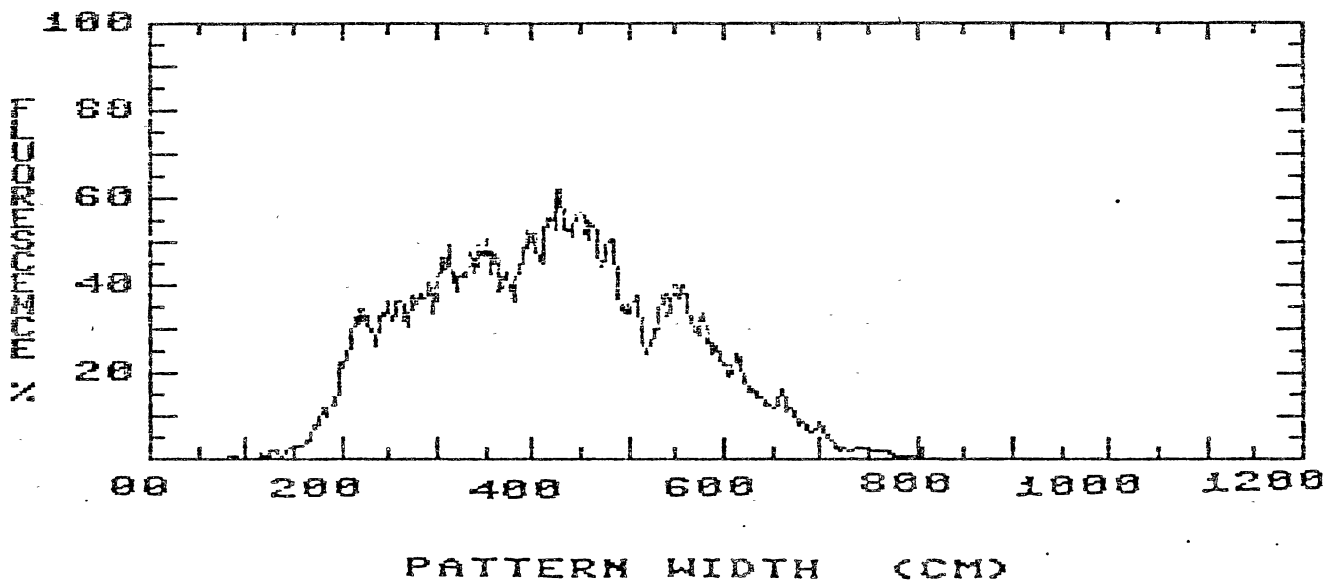

Figure 93. Average of Two Samples Pattern Distribution of 4-Girojet Nozzles Operated at 46 cm Nozzle Height, 42 L/ha, 2.235 m/s Sprayer Speed, 2200 rpm, 0.62 m/s Wind Speed, 16 Degrees Wind Direction, and Center of Nozzles located at 2.44, 3.48, 4.52. and 5.56 m

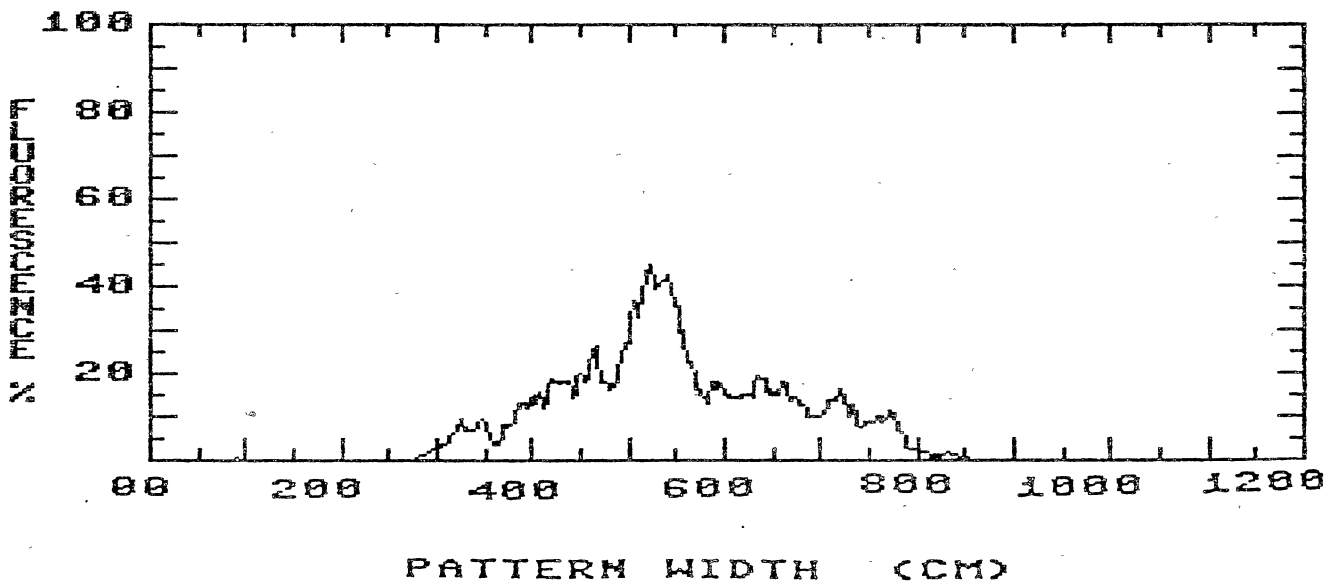

Figure 94. Average of Two Samples Pattern Distribution of 4-Micromax Nozzles Operated at 46 cm Nozzle Height, 42 L/ha, 2.235 m/s Sprayer Speed, 2500 rpm, 1.48 m/s Wind Speed, 24 Degrees Wind Direction, 15 Degrees Tilt Angle, and Center of Nozzles located at 2.44, 3.48, 4.52. and 5.56 m

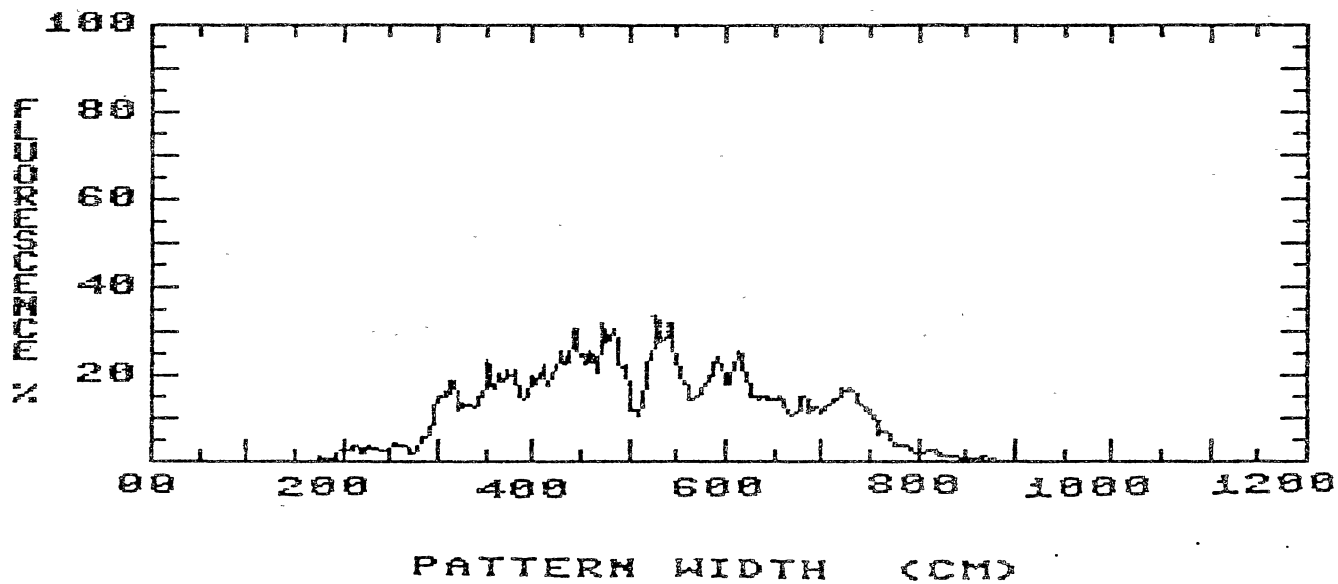

Figure 95. Average of Two Samples Pattern Distribution of 4-Micromax Nozzles Operated at 46 cm Nozzle Height, 42 L/ha, 2.235 m/s Sprayer Speed, 2500 rpm, 1.76 m/s Wind Speed, 18 Degrees Wind Direction, 15 Degrees Tilt Angle, and Center of Nozzles located at 2.44, 3.48, 4.52. and 5.56 m

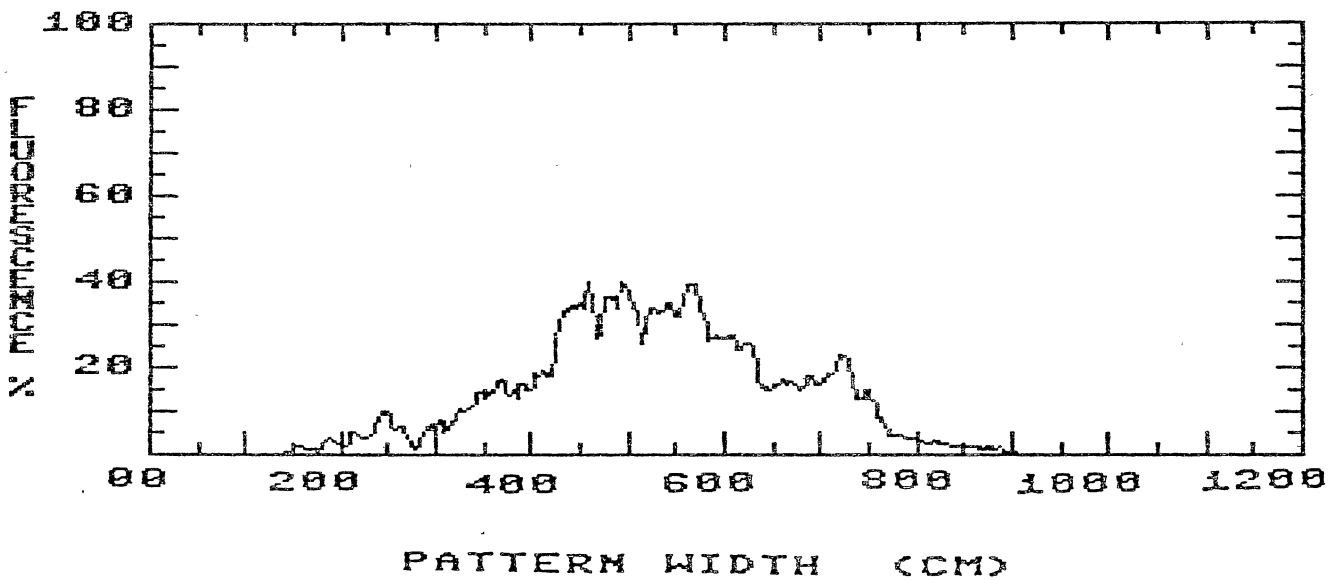

Figure 96. Average of Two Samples Pattern Distribution of 4-Micromax Nozzles Operated at 46 cm Nozzle Height, 42 L/ha, 2.235 m/s Sprayer Speed, 2500 rpm, 1.70 m/s Wind Speed, 27 Degrees Wind Direction, 15 Degrees Tilt Angle, and Center of Nozzles located at 2.44, 3.48, 4.52. and 5.56 m

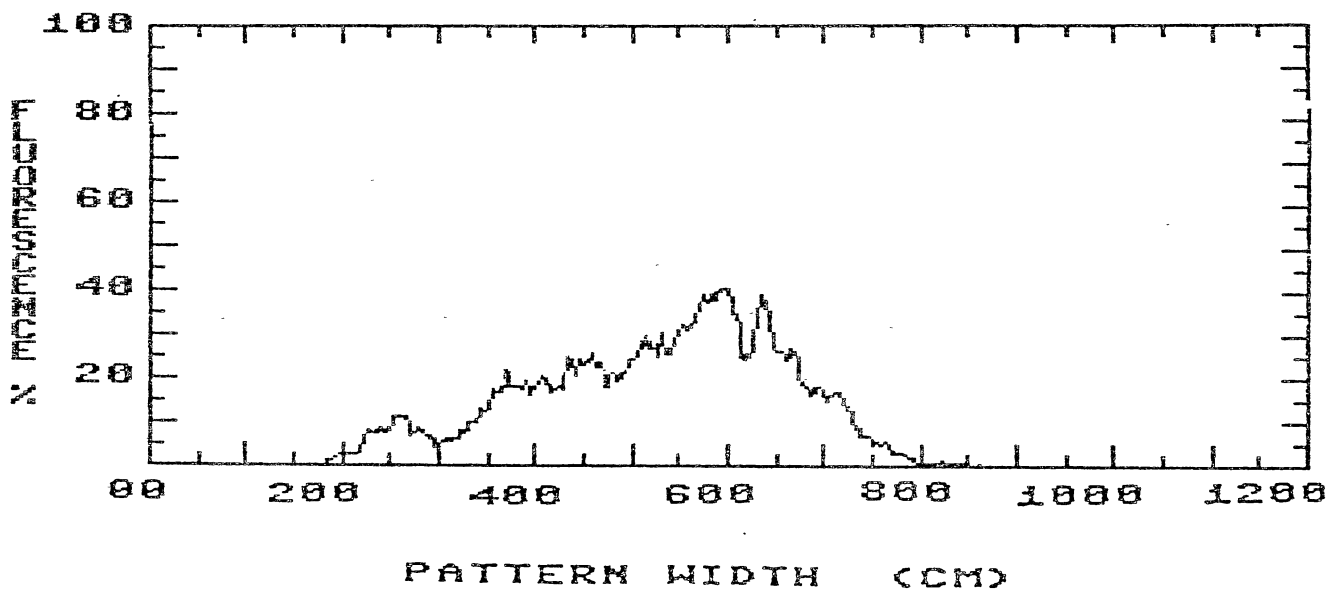

Figure 97. Average of Two Samples Pattern Distribution of 4-Micromax Nozzles Operated at 46 cm Nozzle Height, 42 L/ha, 2.235 m/s Sprayer Speed, 2500 rpm, 1.71 m/s Wind Speed, 25 Degrees Wind Direction, 15 Degrees Tilt Ange, and Center of Nozzles located at 2.44, 3.48, 4.52. and 5.56 m

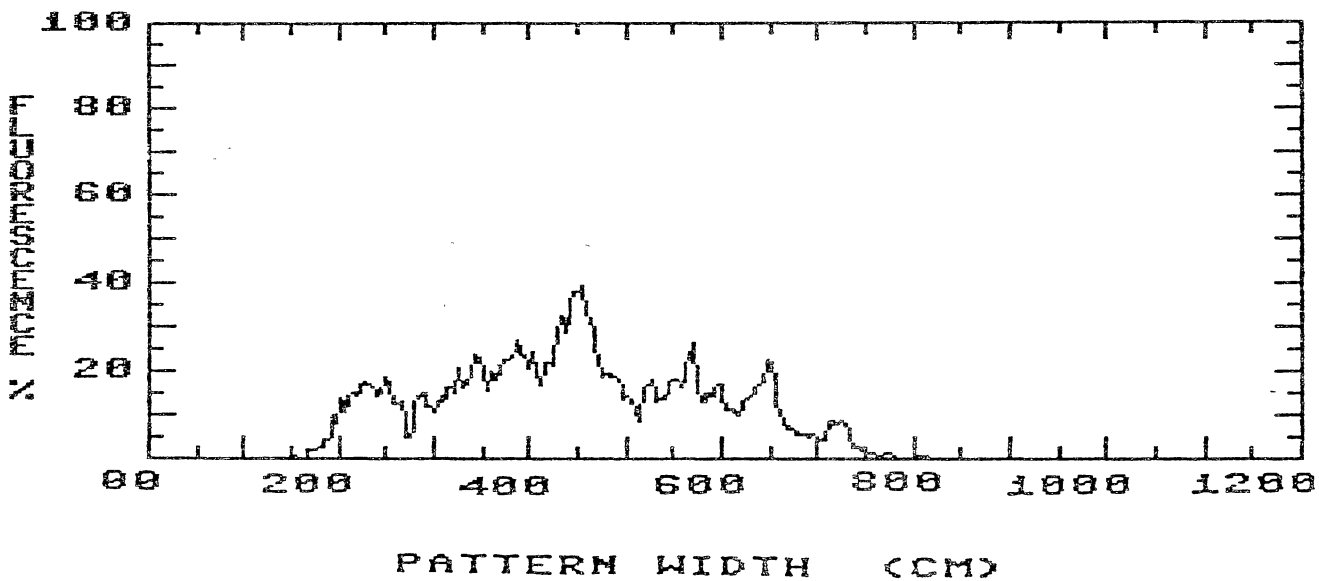

Figure 98. Average of Two Samples Pattern Distribution of 4-Micromax Nozzles Operated at 46 cm Nozzle Height, 42 L/ha, 2.235 m/s Sprayer Speed, 2500 rpm, 1.52 m/s Wind Speed, 27 Degrees Wind Direction, 30 Degrees Tilt Angle, and Center of Nozzles located at 2.44, 3.48, 4.52. and 5.56 m

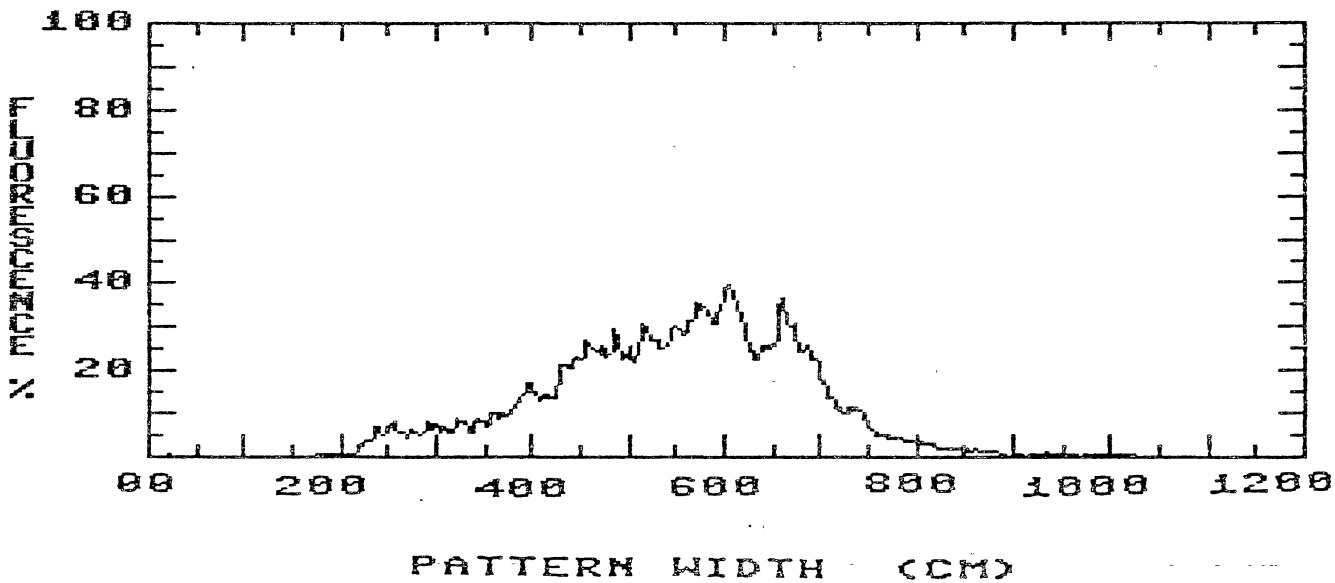

Figure 99. Average of Two Samples Pattern Distribution of 4-Micromax Nozzles Operated at 61 cm Nozzle Height, 42 L/ha, 2.235 m/s Sprayer Speed, 2500 rpm, 0.98 m/s Wind Speed, -7 Degrees Wind Direction, 15 Degrees Tilt Angle, and Center of Nozzles located at 2.44, 3.48, 4.52. and 5.56 m

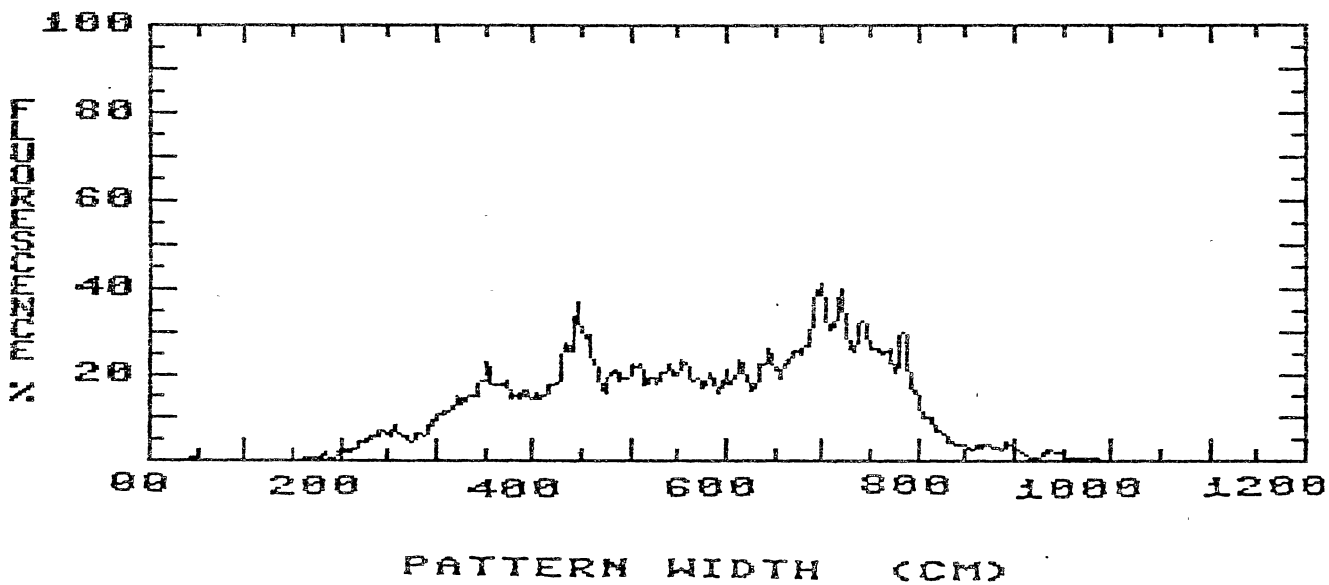

Figure 100. Average of Two Samples Pattern Distribution of 4-Micromax Nozzles Operated at 61 cm Nozzle Height, 42 L/ha, 2.235 m/s Sprayer Speed, 2500 rpm, 1.10 m/s Wind Speed, -24 Degrees Wind Direction, 15 Degrees Tilt Angle, and Center of

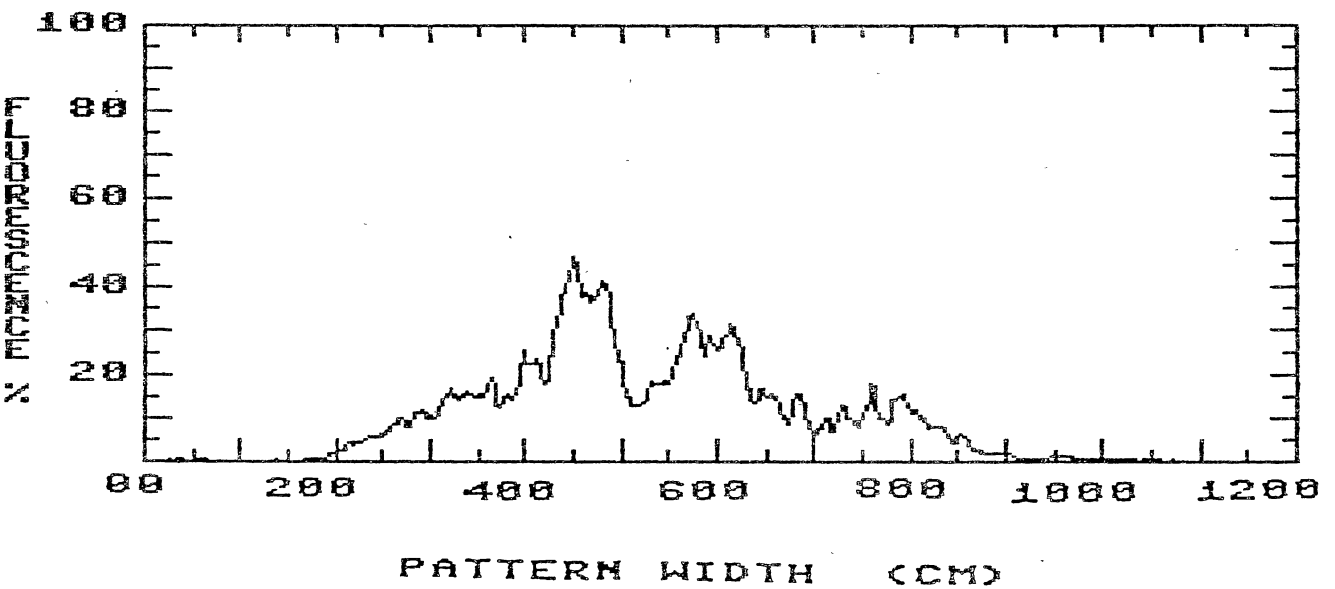

Figure 101. Average of Two Samples Pattern Distribution of 4-Micromax Nozzles Operated at 61 cm Nozzle Height, 42 L/ha, 2.235 m/s Sprayer Speed, 2500 rpm, 0.75 m/s Wind Speed, -27 Degrees Wind Direction, 15 Degrees Tilt Angle, and Center of Nozzles located at 2.44, 3.48, 4.52. and 5.56 m

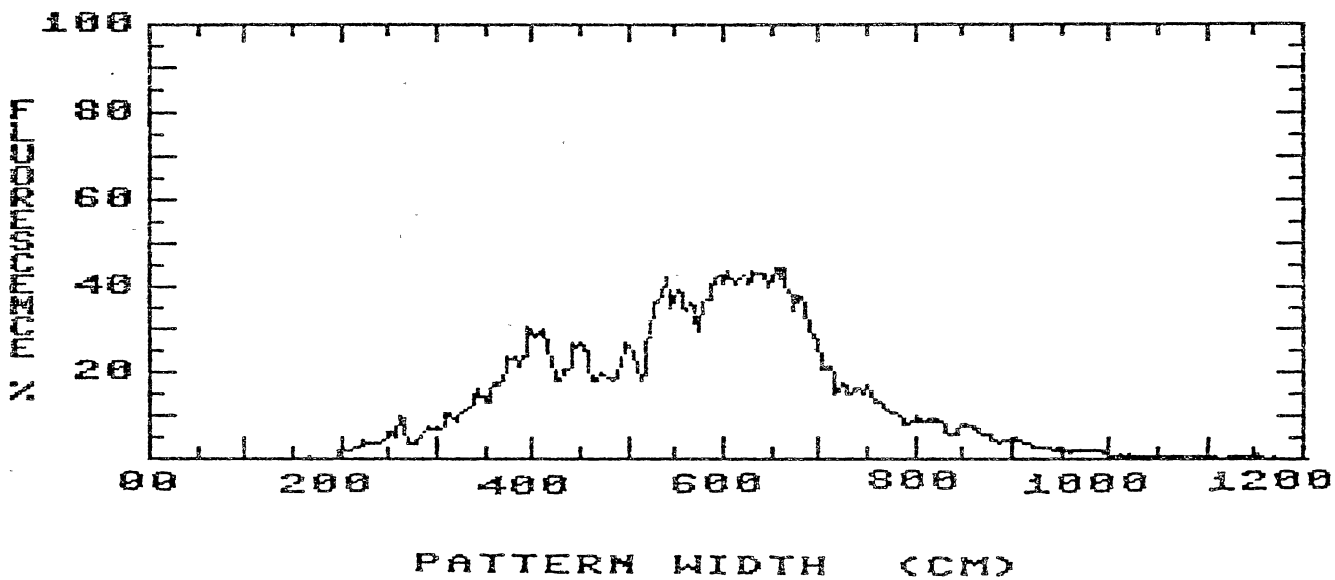

Figure 102. Average of Two Samples Pattern Distribution of 4-Micromax Nozzles Operated at 61 cm Nozzle Height, 42 L/ha, 2.235 m/s Sprayer Speed, 2500 rpm, 1.01 m/s Wind Speed, 24 Degrees Wind Direction, 30 Degrees Tilt Angle, and Center of Nozzles located at 2.44, 3.48, 4.52. and 5.56 m

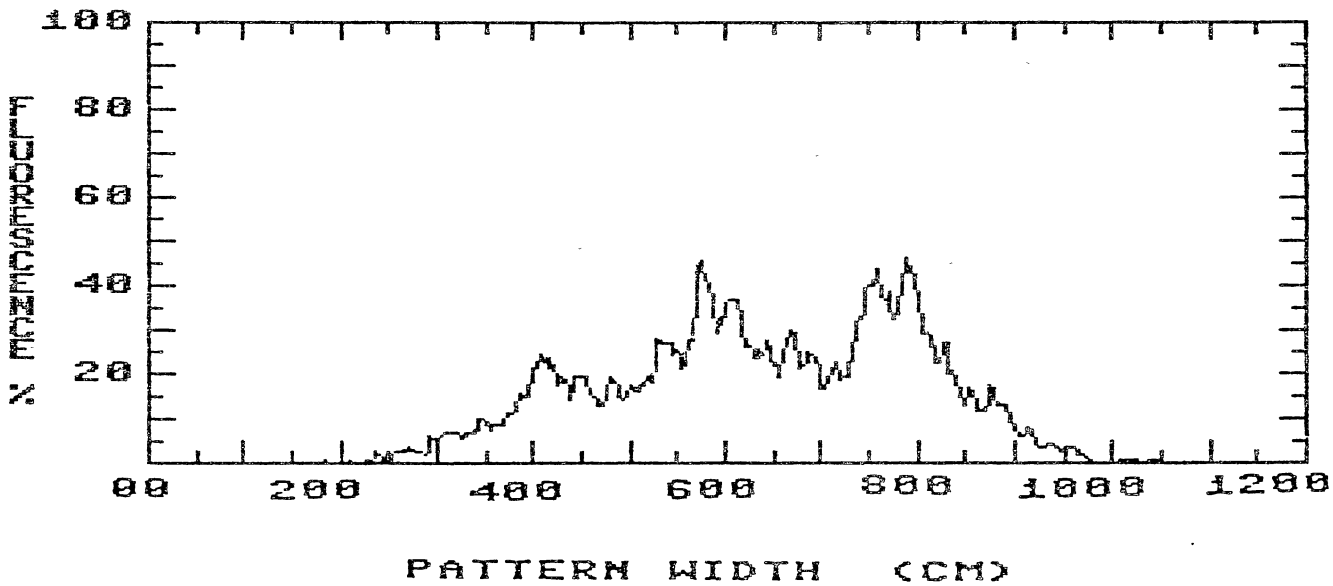

Figure 103. Average of Two Samples Pattern Distribution of 4-Micromax Nozzles Operated at 61 cm Nozzle Height, 42 L/ha, 2.235 m/s Sprayer Speed, 2500 rpm, 1.07 m/s Wind Speed, 3 Degrees Wind Direction, 30 Degrees Tilt Angle, and Center of Nozzles located at 2.44, 3.48, 4.52. and 5.56 m

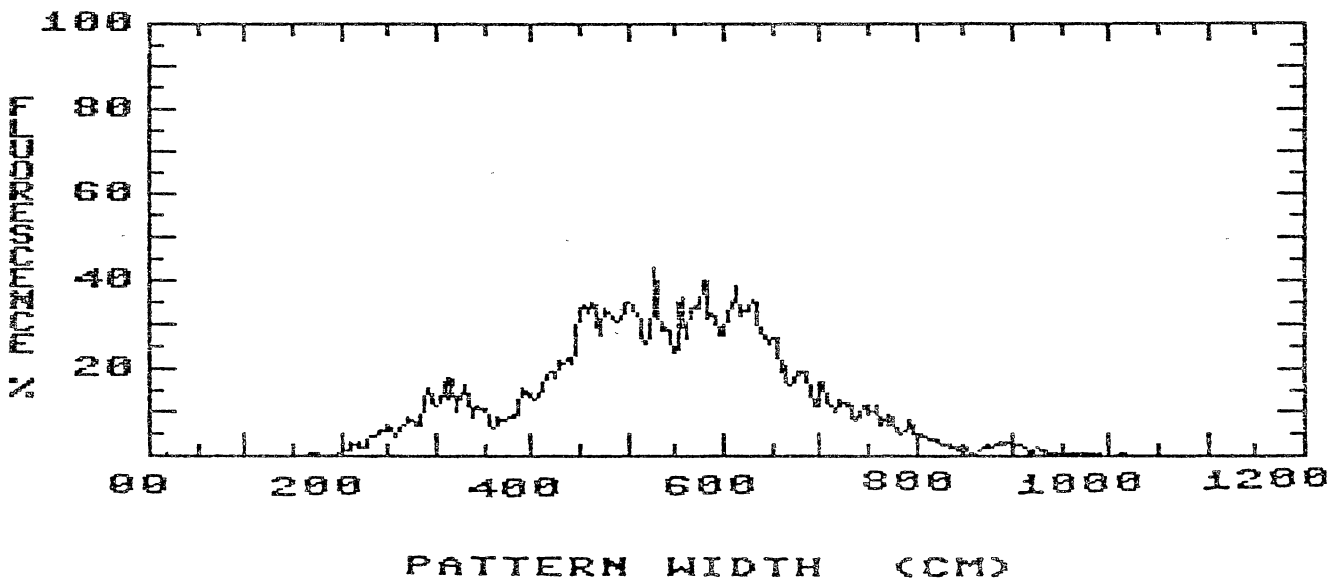

Figure 104. Average of Two Samples Pattern Distribution of 4-Rotojet Nozzles Operated at 46 cm Nozzle Height, 42 L/Ha, 2.235 m/s Sprayer Speed, 2500 rpm, 1.45 m/s Wind Speed, 3 Degrees Wind Direction, 15 Degrees Tilt Angle, and Center of Nozzles Located at 2.47, 3.49, 4.51, and 5.53 m

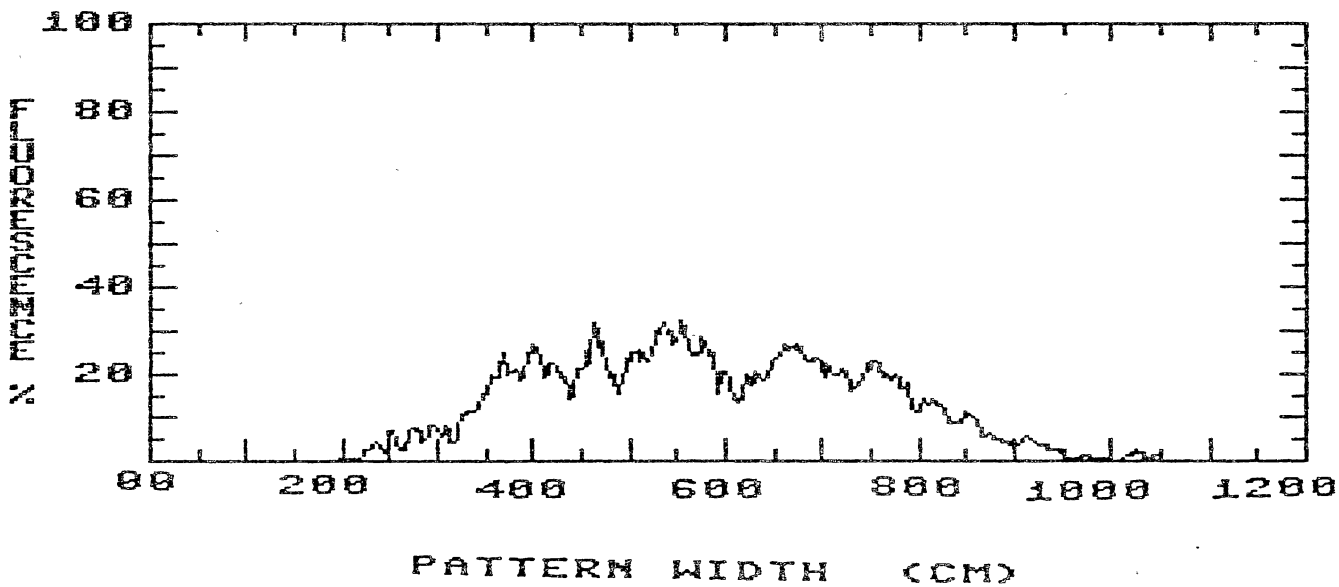

Figure 105. Average of Two Samples Pattern Distribution of 4-Rotojet Nozzles Operated at 46 cm Nozzle Height, 42 L/Ha, 2.235 m/s Sprayer Speed, 2500 rpm, 1.55 m/s Wind Speed, 16 Degrees Wind Direction, 15 Degrees Tilt Angle, and Center of Nozzles located at 2.47, 3.49, 4.51, and 5.53 m

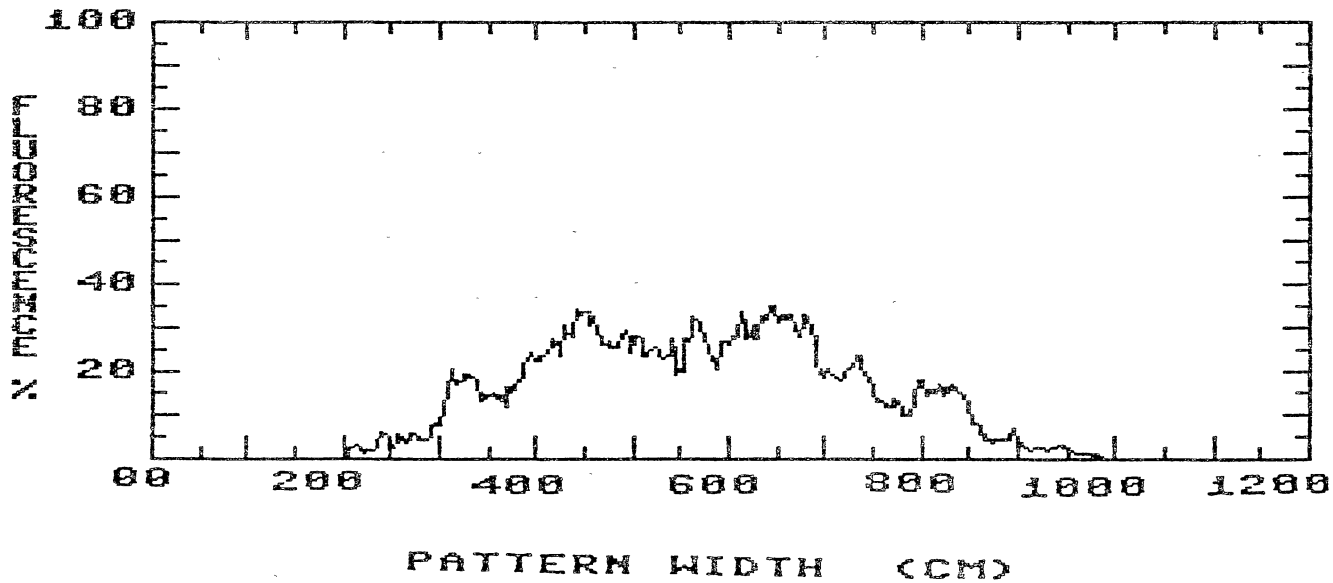

Figure 106. Average of Two Samples Pattern Distribution of 4-Rotojet Nozzles Operated at 46 cm Nozzle Height, 42 L/Ha, 2.235 m/s Sprayer Speed, 2500 rpm, 1.26 m/s Wind Speed, 13 Degrees Wind Direction, 15 Degrees Tilt Angle, and Center of Nozzles located at 2.47, 3.49, 4.51, and 5.53 m

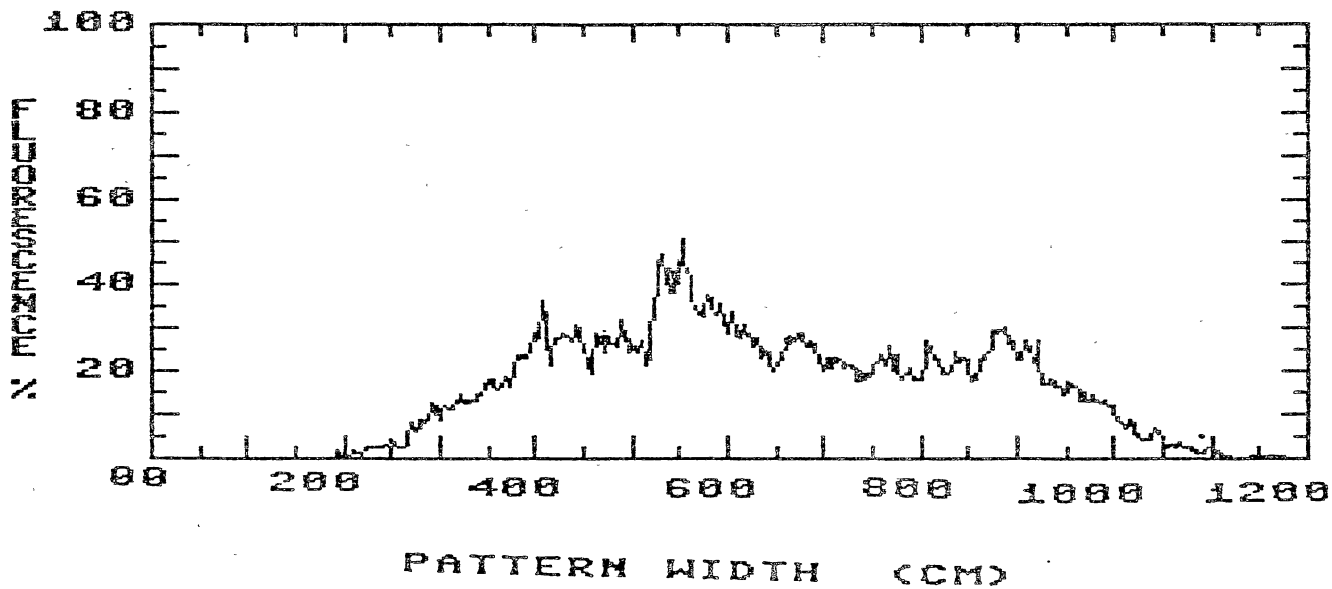

Figure 107. Average of Two Samples Pattern Distribution of 4-Rotojet Nozzles Operated at 46 cm Nozzle Height, 42 L/Ha, 2.235 m/s Sprayer Speed, 2500 rpm, 1.61 m/s Wind Speed, -7 Degrees Wind Direction, 30 Degrees Tilt Angle, and Center of Nozzles located at 2.47, 3.49, 4.51, and 5.53 m

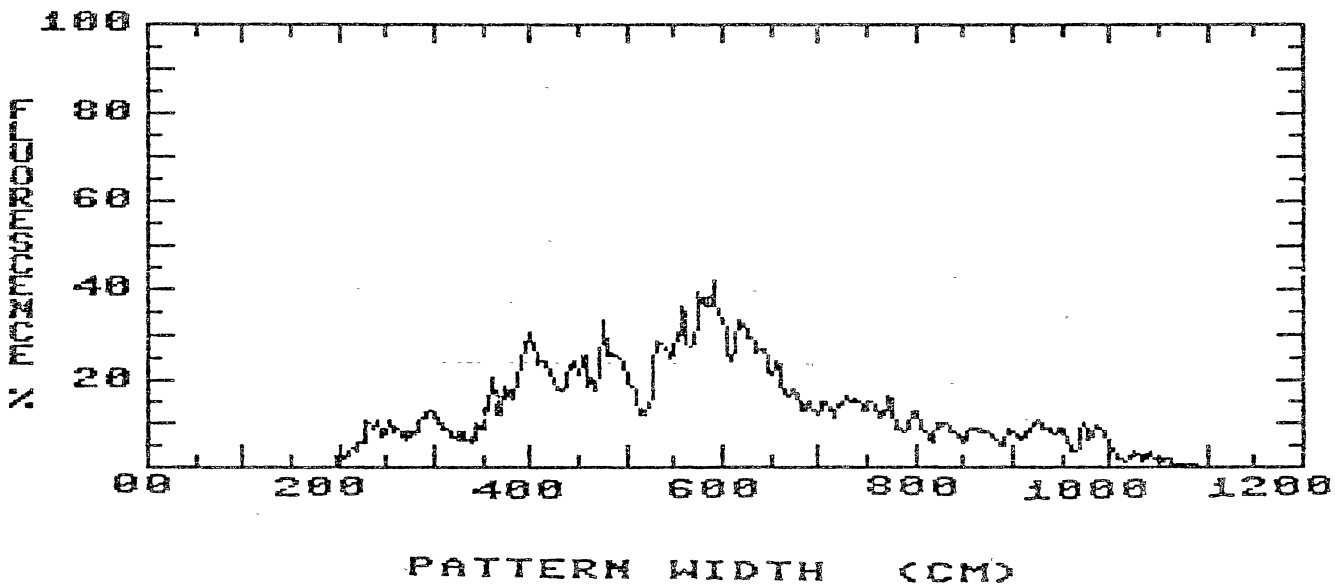

Figure 108. Average of Two Samples Pattern Distribution of 4-Rotojet Nozzles Operated at 46 cm Nozzle Height, 42 L/Ha, 2.235 m/s Sprayer Speed, 2500 rpm, 1.62 m/s Wind Speed, 13 Degrees Wind Direction, 30 Degrees Tilt Angle, and Center of

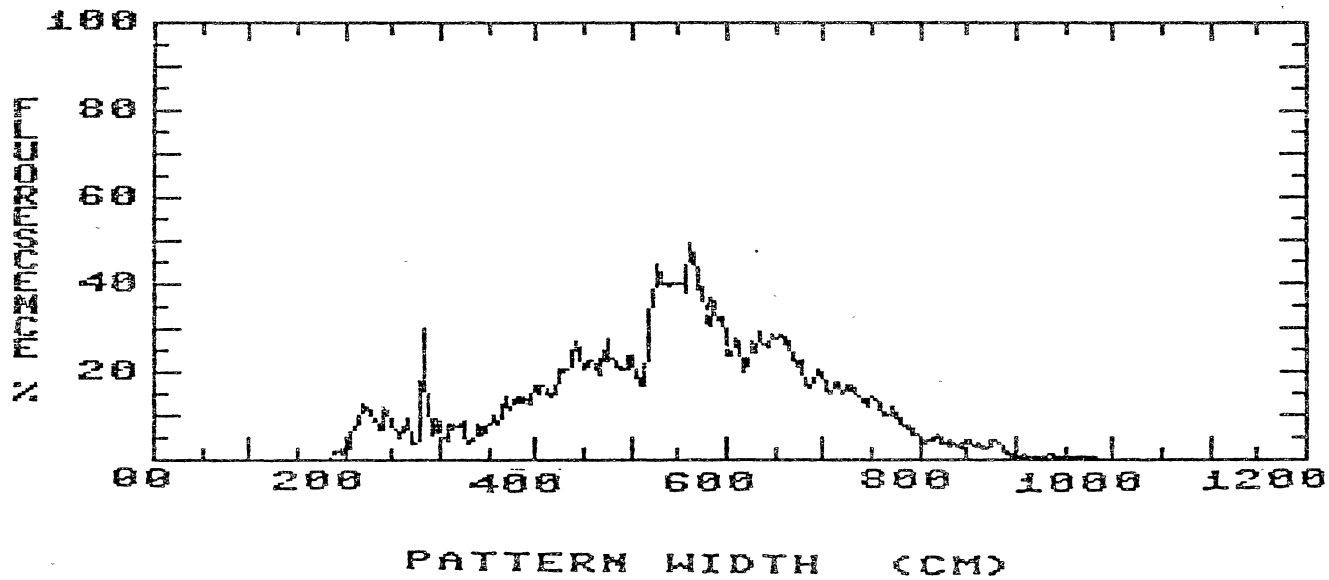

Figure 109. Average of Two Samples Pattern Distribution of 4-Rotojet Nozzles Operated at 61 cm Nozzle Height, 42 L/Ha, 2.235 m/s Sprayer Speed, 2500 rpm, 1.57 m/s Wind Speed, 21 Degrees Wind Direction, 15 Degrees Tilt Angle, and Center of Nozzles located at 2.47, 3.49, 4.51, and 5.53 m

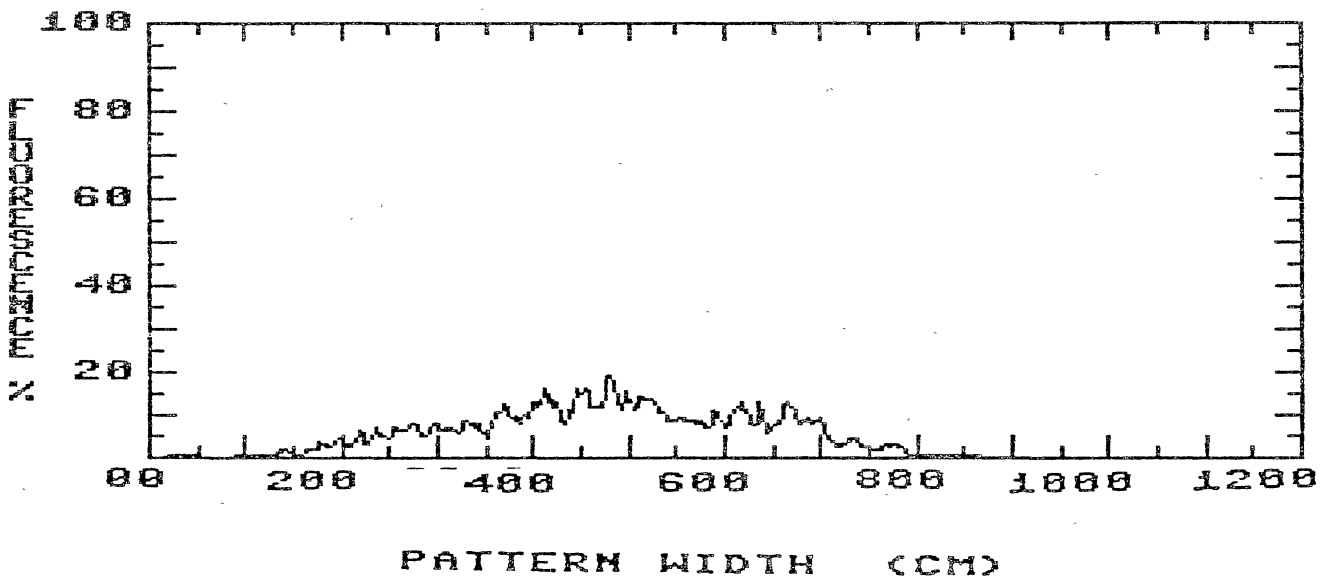

Figure 110. Average of Two Samples Pattern Distribution of 4-Rotojet Nozzles Operated at 61 cm Nozzle Height, 42 L/Ha, 2.235 m/s Sprayer Speed, 2500 rpm, 1.01 m/s Wind Speed, -1 Degrees Wind Direction, 30 Degrees Tilt Angle, and Center of Nozzles located at 2.47, 3.49, 4.51, and 5.53 m

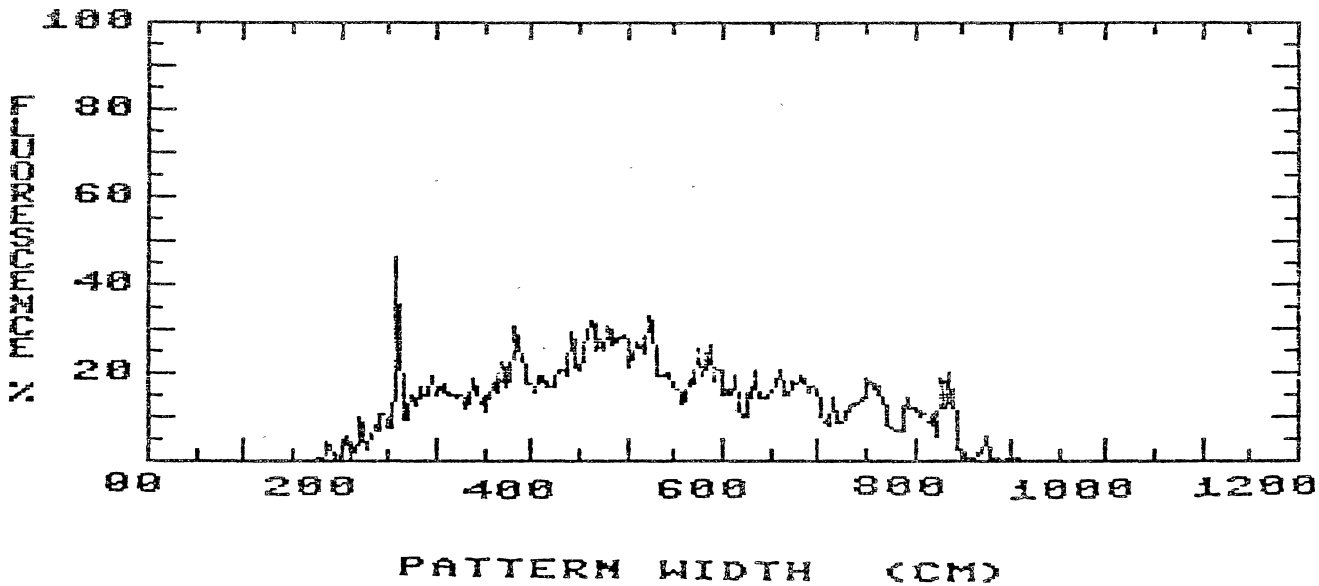

Figure 111. Average of Two Samples Pattern Distribution of 4-Rotojet Nozzles Operated at 61 cm Nozzle Height, 42 L/Ha, 2.235 m/s Sprayer Speed, 2500 rpm, 1.38 m/s Wind Speed, -15 Degrees Wind Direction, 30 Degrees Tilt Angle, and Center of Nozzles located at 2.47, 3.49, 4.51, and 5.53 m

APPENDIX G

CENTROID SHIFT COMPARISONS DATA

CENTROID SHIFT COMPARISONS OF THE SPRAY PATTERN DATA FOR SPINNING DISK NOZZLES VERSUS FLAT FAN NOZZLE[1]

Comparison	Nozzle Height (cm)	Disk Angle (cm)	Wind Speed (m/s)	Wind Dir. (deg)	CV (%)	Centroid Shift (cm)
8001 Flat Fan	46	--	1.48	20	30.45	19
Girojet	46	--	1.44	28	28.20	5
8001 Flat Fan	46	--	1.48	20	30.45	19
Girojet	46	--	1.48	10	19.20	28
8001 Flat Fan	46	--	1.48	20	30.45	19
Girojet	46	--	1.49	7	26.10	6
8001 Flat Fan	61	--	1.72	14	24.20	30
Girojet	61	--	1.71	7	18.60	50
8001 Flat Fan	61	--	1.37	24	31.65	95
Girojet	61	--	1.32	-6	16.95	17
8001 Flat Fan	61	--	0.56	10	20.24	46
Girejet	61	--	0.62	16	18.40	55
8001 Flat Fan	46	--	1.48	20	30.45	19
Micromax	46	15	1.48	24	46.65	145
8001 Flat Fan	46	--	1.72	6	28.35	12
Micromax	46	15	1.70	27	37.65	128
8001 Flat Fan	46	--	1.72	6	28.35	12
Micromax	46	15	1.71	25	21.65	113
8001 Flat Fan	46	--	1.54	4	23.30	18
Micromax	46	30	1.52	27	34.35	45
8001 Flat Fan	46	--	1.48	20	30.45	19
Micromax	46	30	1.52	27	34.35	45

(Continued)

Comparison	Nozzle height (cm)	Disk angle (cm)	Wind speed (m/s)	Wind dir. (deg)	CV (%)	Centroid Shift (cm)
8001 Flat Fan	61	--	0.76	-18	22.85	56
Micromax	61	15	0.75	-27	31.90	135
8001 Flat Fan	61	--	1.10	-28	24.20	30
Micromax	61	15	1.10	-24	17.50	201
8001 Flat Fan	61	--	1.04	-10	23.05	53
Micromax	61	15	0.98	-7	25.35	153
8001 Flat Fan	61	--	1.10	6	29.35	59
Micromax	61	30	1.07	3	24.30	188
8001 Flat Fan	61	--	0.98	7	25.15	48
Micromax	61	30	1.01	24	29.30	187
8001 Flat Fan	46	--	1.48	20	30.45	19
Rotojet	46	15	1.45	17	16.40	182
8001 Flat Fan	46	--	1.54	4	23.30	25
Rotojet	46	15	1.55	16	20.60	202
8001 Flat Fan	46	--	1.29	-4	25.95	40
Rotojet	46	15	1.26	-13	15.90	184
8001 Flat Fan	46	--	1.66	-20	30.25	25
Rotojet	46	30	1.61	-7	26.90	234
8001 Flat Fan	46	--	1.54	4	23.30	25
Rotojet	46	30	1.62	13	17.90	182
8001 Flat Fan	61	--	1.60	22	43.15	55
Rotojet	61	15	1.57	21	25.50	160

(Continued)

Comparison	Nozzle height (cm)	Disk angle (cm)	Wind speed (m/s)	Wind dir. (deg)	CV (%)	Centroid Shift (cm)
8001 Flat Fan	61	--	1.59	0	74.45	81
Rotojet	61	15	1.57	21	25.30	160
8001 Flat Fan	61	--	1.04	-10	23.05	53
Rotojet	61	30	1.01	-1	25.40	104
8001 Flat Fan	61	--	1.37	-24	31.65	95
Rotojet	61	30	1.38	-15	23.00	124

1) Flat fan nozzle was operated at 155 KPa and 51 cm nozzle spacing at 46 cm nozzle height, and at 289 KPa and 76 cm nozzle spacing at 61 cm nozzle height. Girojet was operated at 276 kPa and 2200 rpm, Micromax at 221 KPa and 2000 rpm, and Rotojet at 221 KPa and 2500 rpm at both 46 and 61 cm nozzle heights. The temperature and relative humidity were measured to be 36^{o}C and 64 %, respectively.

VITA 2

Reza Alimardani

Candidate for the Degree of

Master of Science

Thesis: PATTERN ANALYSIS OF A VERTIVAL SPINNING DISK NOZZLE

Major Field: Agricultural Engineering

Biographical:

Personal Data: Born in Tehran, Iran, October 10, 1959, the son of Mr. and mrs. Mohammad Ebrahim Alimardani

Education: Graduated from Azar No. 1 High School, Tehran, Iran, in August, 1976; recieved a Bachelor of Science degree in Agricultural Engineering from Oklahoma State University, Stillwater, Oklahoma, in May, 1983; Completed requirements for the Master of Science degree at Oklahoma State University in May, 1985.

Professional experience: Graduate Reaserch Assistant, OSU Agricultural Engineering Dept., Fall 1983 to Spring 1985.

Professional and Honorary Societies: Recieved Lew Wents Scholarship, OSU Agricultural Engineering Dept.; Student Member of American Society of Agricultural Engineers; Student Member of National Society of Professional Engineers; Member of Alfha Epsilon Honor Society.